

**ANGULAR DISTRIBUTION OF PROTONS  
FROM THE  $\text{Co}^{59}(\text{d}, \text{p})\text{Co}^{60}$  REACTION**

**Donald Lee Jarrell  
and  
Cornell Carpenter Angleman**

















ANGULAR DISTRIBUTION OF PROTONS  
FROM THE  $\text{Co}^{59}(\text{d},\text{p})\text{Co}^{60}$  REACTION

by

Donald Lee Jarrell  
B. S., United States Naval Academy  
(1950)

and

Cornell Carpenter Angleman  
B. S., United States Naval Academy  
(1950)

SUBMITTED IN PARTIAL FULFILLMENT OF  
THE REQUIREMENTS FOR THE DEGREE OF

MASTER OF SCIENCE

at the

MASSACHUSETTS INSTITUTE OF TECHNOLOGY

June 1957



ANGULAR DISTRIBUTIONS OF PROTONS FROM THE

$\text{Co}^{59}(\text{d},\text{p})\text{Co}^{60}$  REACTION

by

Donald Lee Jarrell  
Lieutenant, U. S. Navy

and

Cornell Carpenter Angleman  
Lieutenant, U. S. Navy

Submitted to the Department of Physics on May 20, 1957  
in partial fulfillment of the degree of

MASTER OF SCIENCE

ABSTRACT

The MIT-ONR electrostatic accelerator and broad-range magnetic spectrograph have been used to investigate the  $\text{Co}^{59}(\text{d},\text{p})\text{Co}^{60}$  reaction by bombarding a thin target of cobalt on Formvar with 6.0-Mev deuterons. An analysis of the proton groups for sixteen reaction angles between 10 and 110 degrees determined the angular distribution of the cross section and the Q-values for sixty levels of  $\text{Co}^{60}$  up to 3.7-Mev excitation. The ground-level Q-value was determined to be  $5.262 \pm 0.011$  Mev. Some of the levels observed have not been previously reported, and the Q-values of the other levels are in agreement with those previously observed by (d,p) and (n, $\gamma$ ) reactions. One previously reported level at a Q of 2.659 Mev was not observed. The present values remove some small discrepancies between those of the (d,p) and (n, $\gamma$ ) reactions.

From the angular distributions of this work, the reaction was observed to proceed predominantly by stripping. They have been compared with the predictions of Butler's stripping theory in order to assign values of  $\ell_n$ , the orbital angular momentum of the captured neutron, to thirty-seven levels. It was observed that most of the distributions required superposition of curves corresponding to two values of  $\ell_n$ . Results obtained endorse the recently assigned values of  $J = 5^+$  for the ground level and  $J = 2^+$  for the metastable state, instead of the previously reported values of  $4^+$  and  $1^+$ , respectively.

Thesis Supervisor: Harald A. Enge

Title: Assistant Professor of Physics

35887

DATE: 10/14/2009 10:10:10 AM

COPIES OF THE REPORT

3

Donald Lee Gortell  
Cincinnati, O. 45202

25.13

U.S. Navy  
Naval Air Station

[illegible]

06-5137 90 80104

## ΣΥΛΛΟΓΗ

[illegible]

From the angular distribution of this work, the reaction was observed to proceed predominantly by  $\sigma$ -attack. This has been confirmed by the prediction of Miller<sup>1</sup> according to which it is predicted that the reaction of  $\text{C}_2\text{H}_5\text{I}$  with  $\text{C}_2\text{H}_5\text{MgBr}$  will proceed by  $\sigma$ -attack. It was observed that out of the two distributions negative correlation of curves corresponding to two values of  $\theta$ . Results obtained indicate the reaction is  $\sigma$ -attack of  $\text{C}_2\text{H}_5\text{I}$  on the  $\text{C}_2\text{H}_5\text{MgBr}$  and  $\text{C}_2\text{H}_5\text{I}$  on the  $\text{C}_2\text{H}_5\text{MgBr}$  respectively. Instead of the previously reported values of  $\theta = 1^\circ$  and  $1^\circ$ , respectively.

Source: U.S. Census Bureau, *Marriage, Divorce, Remarriage in the 1990s*, Washington, D.C., 1995.

1110: constant modulus of torsion



## ACKNOWLEDGMENTS

The authors wish to express their appreciation and thanks to all of the members of the High Voltage Laboratory for their friendly assistance and cooperation, without which this work could not have been accomplished.

We are indebted to Professors W. W. Buechner and H. A. Enge for proposing this investigation. Professor Enge was a most patient and helpful adviser. We wish to express our thanks to Dr. C. H. Paris, Mr. A. Sperduto, and Mr. M. Mazari for their kind consideration of our many questions.

We should like to thank Mrs. Grace Rowe for the careful preparation of the numerous graphs in the thesis, Miss Estelle Freedman and Mr. W. A. Tripp for the tedious job of counting the tracks on the photographic plates, and Mr. E. W. Nickerson for his advice and assistance with mechanical problems.

Finally, we wish to thank Mrs. Mary E. White for her excellent preparation of the manuscript.

## MEMORANDUM

The subject is the request for information and data in  
all of the records of the High School Department for their  
relation and cooperation with the State and local  
educational authorities.

We are indebted to the Honorable E. V. Bennett and E. A. Tamm  
for preparing this information. The Honorable E. V. Bennett  
and Honorable Tamm. We wish to express our thanks to Mr. E. A. Tamm,  
Mr. A. Bennett, and Mr. E. Bennett for their kind consideration of our  
request.

We should like to thank Mr. Bennett for the careful review  
of the numerous records in the records of the High School Department and  
Mr. E. A. Tamm for the detailed list of records for the records on the  
Departmental files, and Mr. E. V. Bennett for his advice and assistance  
in this respect.

Finally, we wish to thank Mr. E. A. Tamm for his assistance  
in the preparation of this memorandum.

## TABLE OF CONTENTS

	Page Number
I. INTRODUCTION	1
II. APPARATUS	6
III. EXPERIMENTAL PROCEDURE	14
IV. RESULTS	24
PROBABLE ERRORS	24
DISCUSSION OF Q-VALUES AND COMPARISON WITH PREVIOUS WORK	28
STRIPPING THEORY	39
ANGULAR DISTRIBUTIONS	42
V. CONCLUSIONS	80
BIBLIOGRAPHY	

# TABLE OF CONTENTS

Page  
Number

i

I. INTRODUCTION

ii

II. STATEMENT

iii

III. EXPLANATION OF TERMS

iv

IV. SUMMARY

v

V. CONCLUSIONS

vi

VI. APPENDIX A - LIST OF REFERENCES  
AND OTHER MATERIALS

vii

VII. BIBLIOGRAPHY

viii

VIII. INDEX

ix

IX. SUMMARY

X. CONCLUSIONS



## I. INTRODUCTION

The MIT-ONR electrostatic accelerator is being used in a program of study of deuteron stripping reactions. This reaction is a valuable tool in nuclear spectroscopy as an aid in the determination of the angular momentum and parity of ground and excited levels of various nuclides.

The element cobalt has been the object of several studies of the beta-ray and gamma-ray decay of its isotopes. Charged-particle studies of  $\text{Co}^{59}$  by proton bombardment<sup>1</sup> and of  $\text{Co}^{60}$  through the  $\text{Co}^{59}(\text{d},\text{p})\text{Co}^{60}$  reaction<sup>2</sup> have been done at the High Voltage Laboratory of the Massachusetts Institute of Technology.

We have chosen the investigation of the angular distribution of protons from the  $\text{Co}^{59}(\text{d},\text{p})\text{Co}^{60}$  reaction in an effort to resolve an uncertainty in the Q-value for the ground level of  $\text{Co}^{60}$ , to determine more fully the excited levels of  $\text{Co}^{60}$ , and to furnish more information on the angular momentum and parity of these excited levels.

The work of Bartholomew and Kinsey<sup>3</sup> results in a Q-value for the ground level of  $5.260 \pm 0.007$  Mev, determined by subtracting the binding energy of the deuteron from their highest energy gamma ray. The  $\text{Co}^{59}(\text{d},\text{p})\text{Co}^{60}$  work of Foglesong and Foxwell<sup>2</sup> gave a Q-value of  $5.283 \pm 0.008$  Mev, a difference of 23 kev.

On the basis of the "shell model,"  ${}_{27}^{59}\text{Co}_{32}$  has a single "hole" in the proton  $1f_{7/2}$  shell, and the position of the four neutrons above the  $1f_{7/2}$  shell is somewhat in doubt. The states

# 1. INTRODUCTION

The fitting of a statistical model to a set of data is a process of trial and error. The model is chosen on the basis of a preliminary examination of the data. The model is then fitted to the data and the results are compared with the original data. If the model is not satisfactory, a new model is chosen and the process is repeated.

The first step in the fitting of a statistical model is the choice of a model. The model is chosen on the basis of a preliminary examination of the data. The model is then fitted to the data and the results are compared with the original data. If the model is not satisfactory, a new model is chosen and the process is repeated.

The second step in the fitting of a statistical model is the choice of a model. The model is chosen on the basis of a preliminary examination of the data. The model is then fitted to the data and the results are compared with the original data. If the model is not satisfactory, a new model is chosen and the process is repeated.

The third step in the fitting of a statistical model is the choice of a model. The model is chosen on the basis of a preliminary examination of the data. The model is then fitted to the data and the results are compared with the original data. If the model is not satisfactory, a new model is chosen and the process is repeated.

The fourth step in the fitting of a statistical model is the choice of a model. The model is chosen on the basis of a preliminary examination of the data. The model is then fitted to the data and the results are compared with the original data. If the model is not satisfactory, a new model is chosen and the process is repeated.

$2p_{3/2}$  and  $1f_{5/2}$  lie very close together.<sup>4</sup> Whether the addition of a neutron to an odd one in the  $2p_{3/2}$  state would cause the pair to jump from the  $2p_{3/2}$  state to the  $1f_{5/2}$  state depends on the magnitude of the difference of the pairing energies  $P_{f_{5/2}} - P_{p_{3/2}}$  relative to the level distance  $\epsilon_{f_{5/2}} - \epsilon_{p_{3/2}}$ . It is possible to show<sup>4</sup> that the order of filling these levels might proceed by three different schemes for configurations of 1, 2, 3, 4, 5, and 6 neutrons:

- a.  $(p_{3/2})^1; (f_{5/2})^2; (p_{3/2})^1(f_{5/2})^2; (f_{5/2})^4; (p_{3/2})^1(f_{5/2})^4; (f_{5/2})^6.$
- b.  $(p_{3/2})^1; (p_{3/2})^2; (p_{3/2})^3; (p_{3/2})^4; (p_{3/2})^3(f_{5/2})^2; (p_{3/2})^4(f_{5/2})^2.$
- c.  $(p_{3/2})^1; (p_{3/2})^2; (p_{3/2})^3; (p_{3/2})^4; (p_{3/2})^4(f_{5/2})^1; (p_{3/2})^4(f_{5/2})^2.$

The experimental evidence for the magnetic moments of  $\text{Co}^{58}$ <sup>5</sup> and  $\text{Co}^{60}$ <sup>6,7</sup> compared with the calculated magnetic moments<sup>4</sup> indicate the assignments of the thirty-first neutron in  $\text{Co}^{58}$  to the  $f_{5/2}$  state and the thirty-third neutron in  $\text{Co}^{60}$  to the  $p_{3/2}$  state, with three neutrons in the  $p_{3/2}$  state and two neutrons in the  $f_{5/2}$  state. Thus, it would seem that the neutrons fill in the following manner for three, four, and five neutrons:

$$(p_{3/2})^2(f_{5/2})^1; (p_{3/2})^2(f_{5/2})^2; (p_{3/2})^3(f_{5/2})^2.$$

This is not in accord with the schemes mentioned above but would seem to be a reasonable interpretation of data available.





A survey of present data on the angular momentum and parities of  $\text{Co}^{60}$  is presented in Figure 1. The 1.48-Mev beta ray from the ground level of  $\text{Co}^{60}$  to the 1.33-Mev level of  $\text{Ni}^{61}$  was first reported by Keister and Schmidt<sup>8</sup> to have a shape corresponding to  $\Delta J = 2$ , no, and hence led to the angular momentum and parity assignments of  $4^+$  and  $1^+$  to the ground and metastable levels, respectively, in contrast to the previously reported values of  $5^+$  and  $2^+$ .<sup>9</sup> More recent work by Dobrowolski et al<sup>6</sup>, using the method of paramagnetic resonance to measure the angular momentum and magnetic moment, and by Wolfson<sup>10</sup> on the 1.48-Mev beta ray, obtaining  $\Delta J = 3$ , no, leads to confirmation of the values of  $5^+$  and  $2^+$ .

The use of the deuteron stripping reaction as a means of assigning values of angular momentum to various energy levels of a nucleus is based on the pronounced maxima in a forward direction of the emergent particle. These maxima may be characterized by values of  $l_n$ , the orbital angular momentum of the captured nucleon. The angle at which a maximum occurs is a measure of the  $l_n$  value. Knowledge of the angular momentum and parity of the initial nucleus, together with the observed  $l_n$  value, will determine the parity of the residual nucleus and allowed values of the angular momentum.

Several theories accounting for the stripping maxima in the intermediate energy region have been published, notably by Butler<sup>11</sup>, Bhatia et al<sup>12</sup>, Daitch and French<sup>13</sup>, Friedman and Tobocman<sup>14</sup>, and others. In this investigation, an angular distribution formula from the noncoulomb stripping theory of Friedman and Tobocman<sup>14</sup> is used,

A survey of present data on the regular moment and the  
 line of  $CO_2$  is presented in figure 1. The 1.15-mv data for the  
 regular level of  $CO_2$  in the 1.15-mv level of  $CO_2$  are first re-  
 ported by Tolsted and Johnson<sup>11</sup> to have a value corresponding to  
 $\Delta E = 2.4$  ev, and have led to the regular moment and energy as dis-  
 cussed in 1<sup>st</sup> and 2<sup>nd</sup> to the present and subsequent levels, respectively.  
 In contrast to the previously reported value of 2<sup>nd</sup> and 3<sup>rd</sup>, these  
 recent work by Tolsted and Johnson<sup>11</sup>, using the method of spectroscopic  
 resonance to measure the regular moment and energy as discussed,  
 by Tolsted<sup>11</sup> on the 1.15-mv level, resulting in  $\Delta E = 3.0$  ev, leads  
 to confirmation of the value of 2<sup>nd</sup> and 3<sup>rd</sup>.

The use of the electron spin resonance as a means of  
 assigning values of regular moments to various energy levels of a  
 molecule is based on the fundamental nature of a forward direction of  
 the magnetic field. These values may be measured by values  
 of  $\Delta E$ , the optical regular moment of the regular moment. The  
 value at which a certain energy is a measure of the  $\Delta E$  value. From  
 edge of the regular moment and value of the initial moment, the  
 value also the observed  $\Delta E$  value, this indicates the parity of the  
 regular moment and allowed value of the regular moment.

Several specific examples in the regular moment in the  
 regular moment energy level have been published, notably by Tolsted<sup>11</sup>,  
 results of  $\Delta E$ , Tolsted and Johnson<sup>11</sup>, Tolsted and Johnson<sup>11</sup>, and  
 others. In this investigation, as regular distribution levels from  
 the regular moment energy of Tolsted and Johnson<sup>11</sup> is used.

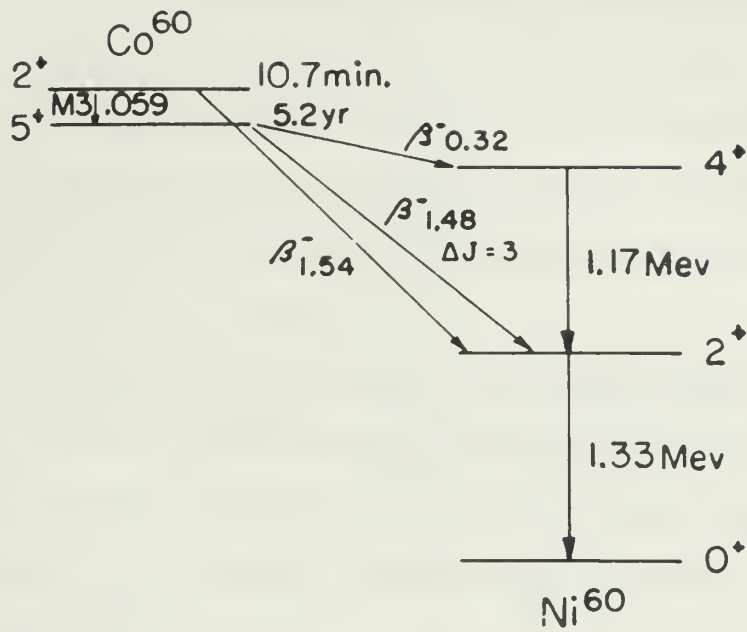


Figure 1

ENERGY LEVEL DIAGRAM SHOWING  
DECAY SCHEME OF  $\text{Co}^{60}$

(Ref. 6, 7, 9, 10)





together with tables and graphs prepared by Enge and Graue<sup>15</sup> for numerical calculations of the theoretical angular distribution curves.

The use of the MIT-ONR electrostatic generator and the broad-range magnetic spectrograph enabled us to investigate the Q-values and angular distributions of protons from the  $\text{Co}^{59}(\text{d},\text{p})\text{Co}^{60}$  reaction simultaneously. The investigation was carried out at energies of 6.01 and 6.18 Mev. The proton groups associated with the ground and excited levels were observed at seventeen angles between 5 and 110 degrees.

Sixty Q-values, corresponding to the ground level and fifty-nine excited levels of  $\text{Co}^{60}$ , were determined. Angular distribution curves and values of  $l_n$  for the ground level and twenty-five excited levels were calculated. Tentative assignments of  $l_n$  were given to eleven other levels.

calculated with tables and graphs prepared by W. G. and G. W. for  
numerical calculations of the theoretical angular distribution  
curves.

The use of the BETHE electronic energy formula and the  
present-day electronic energy tables as to investigate the  
g-values and angular distributions of various types of  
 $Co^{57}(4,7,10)$  excited states. The investigation was per-  
formed at energies of 4.02 and 4.18 MeV. The ground state was  
related with the ground and excited levels were observed at various  
angles between 2 and 110 degrees.

Eighty g-values, corresponding to the ground level and 115 g-  
values, nine excited levels of  $Co^{57}$ , were determined. Angular distribu-  
tion curves and values of  $g$  for the ground level and twenty-five  
excited levels were calculated. Tentative assignments of  $g$  were  
given to eleven other levels.

## II. APPARATUS

The major equipment used in this investigation consisted of the MIT-ONR electrostatic accelerator<sup>16</sup> and the associated deflecting magnet, a collimating slit system, target chamber, and the broad-range magnetic spectrograph<sup>17</sup>.

The major characteristic of a Van de Graaff generator used as a particle accelerator is the small energy spread possible (approximately 0.1 percent). The MIT-ONR generator has a range of normal operation of 5.0 to 7.5 Mev with a beam intensity upwards of 0.3 microamperes.

The physical features of the accelerator are shown in Figure 2. The energy of the particle beam is defined and controlled by the collimating slit system and the deflecting magnet. The particles are accelerated downward into the deflecting magnet and are then deflected through a 90-degree arc which has a radius of 60 centimeters by a given magnetic field which determines the momentum allowed to pass through the magnet.

By means of adjustable shims at the entrance and exit faces of the magnet, the beam was focused on a set of defining slits placed 185 centimeters from the exit face of the magnet<sup>16</sup>. The slit jaws are insulated, and the currents collected on them are used to control a corona current to the generator terminal, thus providing voltage control.

The particle beam then enters the target chamber (Figure 3) and provides a sharply defined beam impinging on a fixed position

# 1. INTRODUCTION

The main objective of this investigation is to study the effect of the concentration of the reactants on the rate of the reaction. The reaction studied is the reaction between hydrogen peroxide and potassium iodide in the presence of a catalyst.

The rate of reaction is measured by the volume of oxygen gas evolved in a given time. The reaction is carried out at different concentrations of the reactants and the rate of reaction is determined. The results are plotted on a graph of rate of reaction versus concentration of the reactants. The graph shows that the rate of reaction increases with the increase in the concentration of the reactants.

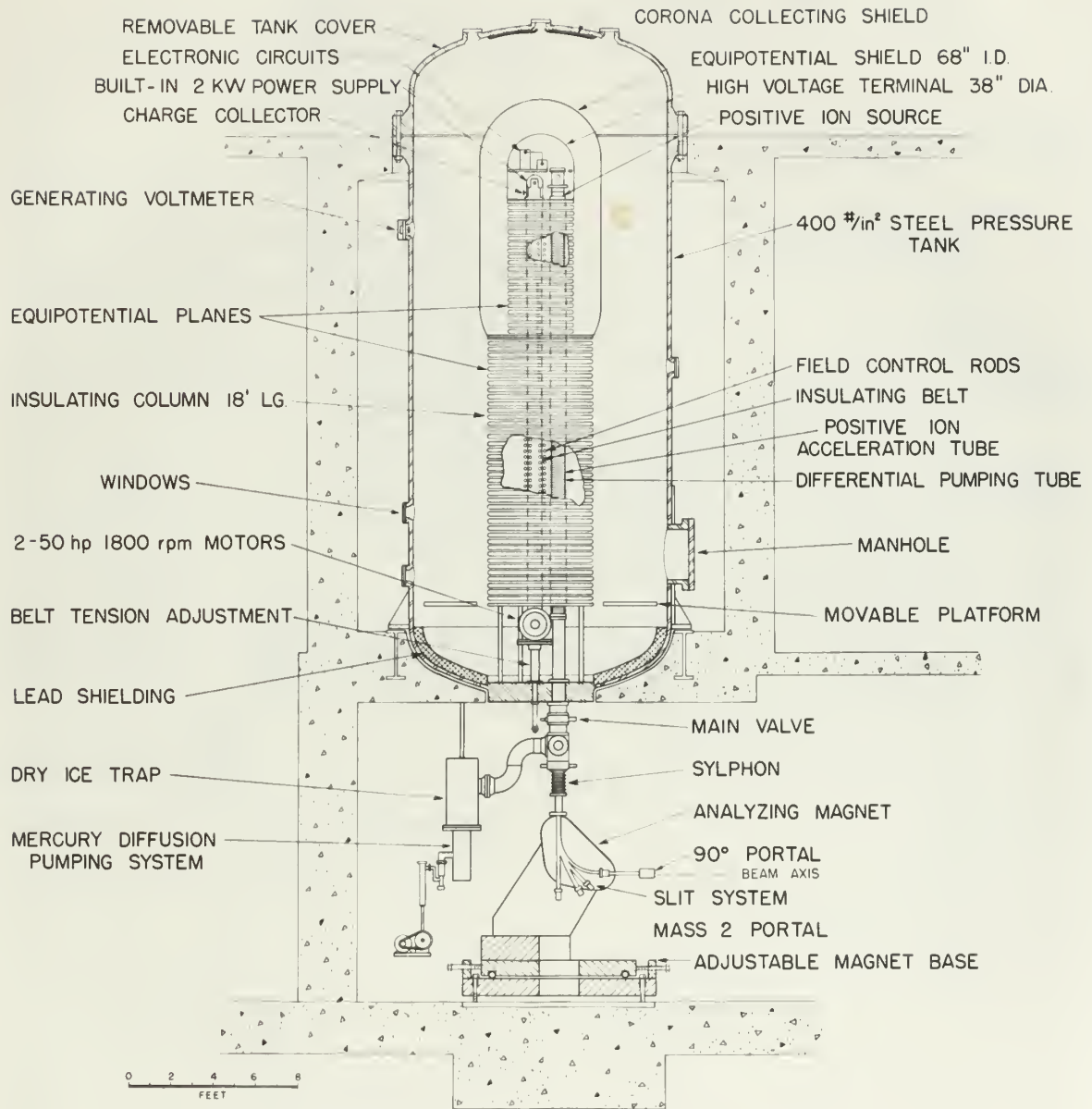
The overall order of the reaction is determined by the method of initial rates. The results are plotted on a graph of  $\log \text{rate}$  versus  $\log \text{concentration}$ . The slope of the line gives the order of the reaction. The results show that the reaction is first order with respect to hydrogen peroxide and first order with respect to potassium iodide. The overall order of the reaction is therefore 2.

The rate of reaction is also determined by the method of half-life. The results are plotted on a graph of  $\log t_{1/2}$  versus  $\log \text{concentration}$ . The slope of the line gives the order of the reaction. The results show that the reaction is first order with respect to hydrogen peroxide and first order with respect to potassium iodide. The overall order of the reaction is therefore 2.

The results of the investigation are summarized in the following table:

Concentration of $\text{H}_2\text{O}_2$ (M)	Concentration of $\text{KI}$ (M)	Rate of reaction (M/s)
0.1	0.1	0.01
0.2	0.1	0.02
0.1	0.2	0.02
0.2	0.2	0.04





POSITIVE ION ACCELERATOR FOR M.I.T.

Figure 2



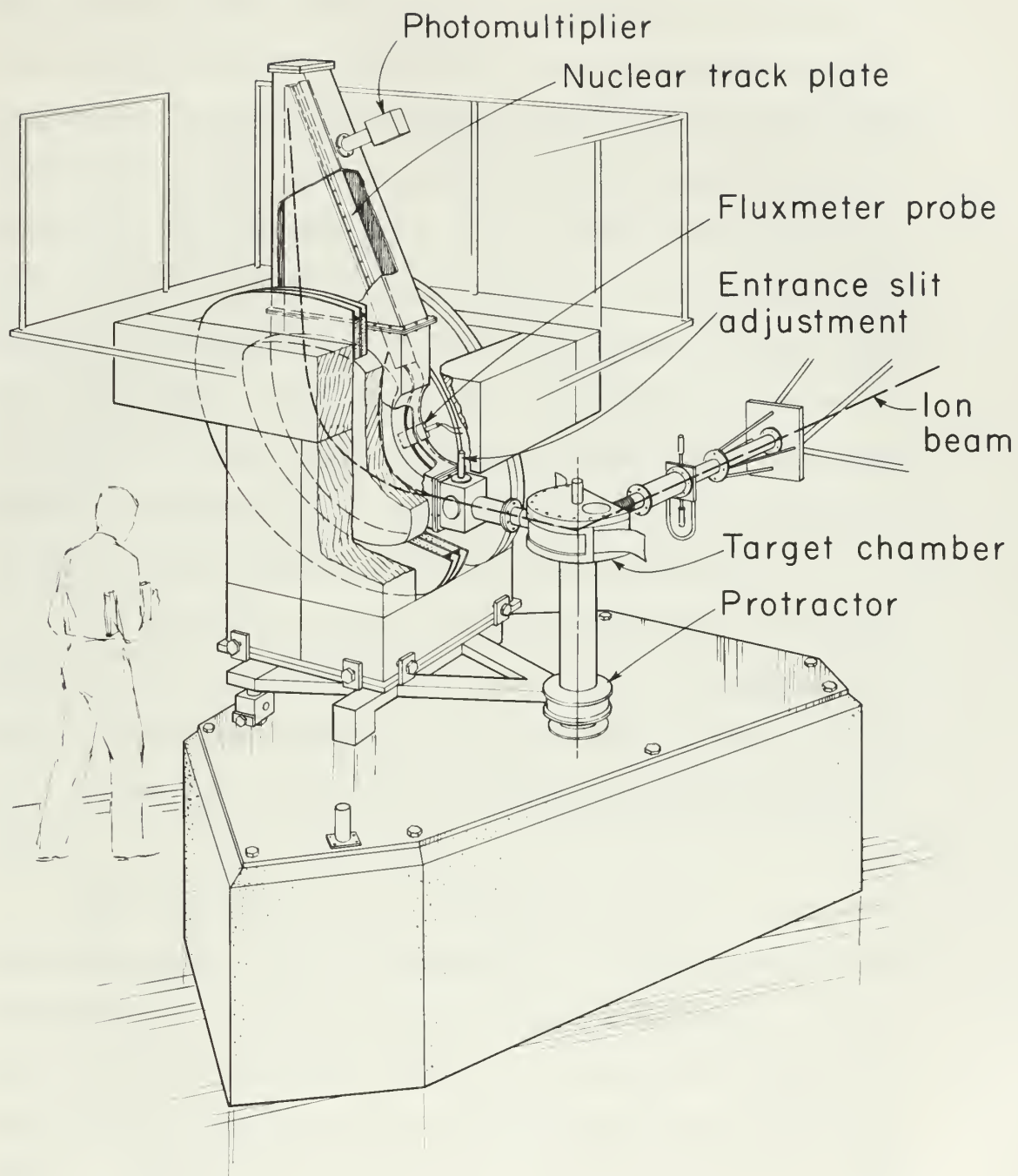


Figure 3





on the target. The particles from the target which emerge into the acceptance angle of the broad-range magnetic spectrograph are deflected with a radius proportional to their momentum. They are recorded on three ten-inch long Eastman NTA 25-micron photographic plates positioned at the top of the spectrograph, as shown in Figure 3. The photographic plates are contained in a plateholder and conform to a hyperbolic focal surface. They are indexed when in the plateholder by a set of razor-edged slits illuminated from below which give a set of sharp lines approximately 7 centimeters apart for the entire length of the photographic plate. These slits provide a reference for a measure of distance along the plates used when the particle tracks are counted after an exposure.

The magnetic spectrograph may be rotated about a vertical axis through the point at which the beam hits the target. Angles from 0 to 130 degrees with respect to the beam line from the accelerator may be used with a position error of less than 10 minutes of arc<sup>18</sup>.

The solid angle of the spectrograph has been shown to be independent of the angle of observation. It is defined by an entrance aperture to the spectrograph and by an 8-millimeter wide slit in front of the focal surface. The aperture angle may be varied, but is used for normal work with a half-angle of about  $2\frac{1}{2}$  degrees. The solid angle on the focal surface is about  $3.4 \times 10^{-4}$  steradian for a given peak at a distance along the plate of 52 centimeters. Since particles of different momenta are magnetically

[illegible][illegible]

with through the hole in which the door was located. The door was closed and the door was closed.

11/2/2005

[illegible]

deflected through different radii, they are recorded at different points on the focal surface. Since each position on the photographic plates corresponds to a different distance traveled by the particles, the solid angle varies with position on the plate. This variation is corrected for by using the experimental curve given by Browne and Buechner<sup>17</sup>.

The magnetic fields in the deflecting and spectrograph magnets are determined by a nuclear resonance technique, using the known gyromagnetic ratio of the  $\text{Li}^7$  nucleus. This consists of measuring the Larmor precession frequency using resonance induction of  $\text{Li}^7$  or of a proton in an aqueous solution of  $\text{LiCl}$ . The  $\text{LiCl}$  is contained in a small glass capsule positioned in the pole gap of the magnets. A secondary frequency standard is used for the frequency measurement and is calibrated against the broadcast frequency standard of the Bureau of Standards station WWV.

Thin targets are necessary in charged-particle work, since sharply defined groups of reaction particles result, thus taking advantage of the resolving power of the apparatus. The work of Fogleson and Foxwell<sup>2</sup> was done at 90 degrees on a comparatively thick cobalt layer evaporated onto platinum sheet. The present work, using transmission through the target for all angles less than 90 degrees, required the use of a thin cobalt layer on thin Formvar film.

Circular (about 1-inch diameter) target frames were covered with four double layers of Formvar. The thickness of the Formvar was measured by means of an alpha-particle thickness gauge developed





by Enge, Wahlig, and Aanderaa<sup>19</sup>. The average thickness was found to be about 13 mils air equivalent.

Co<sup>59</sup> in the form of cobalt sponge obtained from Johnson, Matthey and Company, London, was evaporated under vacuum in a steel tank using a tungsten crucible. The tungsten was in strip form one-quarter inch wide and 20 mils in thickness; the strip was ground down in a small area to about 10-mils thickness to form a "boat." By passing a current through the tungsten strip, the cobalt was heated to a temperature above the melting point and allowed to evaporate. The evaporation was allowed to proceed until no cobalt remained in the boat. The temperature had to be controlled to within quite narrow limits in order to achieve evaporation but yet not destroy the Formvar backing by excessive heat. Some fifteen evaporation attempts were made before securing the necessary number of targets. After evaporation, the thickness of the cobalt was measured by measuring the thickness of the cobalt plus Formvar and subtracting the thickness of the Formvar.

The targets were placed in the target chamber shown in Figure 3. This chamber is insulated from ground and has small apertures for the entrance of the particle beam and for the exit of emergent particles into the spectrograph. The secondary electrons from nearby energy-analyzing slits are prevented from entering by insulating the entrance aperture from the target chamber and biasing to -300 volts. The amount of particle charge collected





in the target chamber is measured by a combined current integrator and sensitive microammeter<sup>20</sup>, with an accuracy better than 1 percent for the beam currents used.

In order to reduce the surface contamination buildup and to insure better heat removal, the targets were placed in a rotating target mount<sup>21</sup>. This consists of a geared target holder driven with a flexible shaft by a D. C. motor. Magnetic coupling is used to transmit drive power through the lid of the target chamber. Speed of rotation is approximately one revolution per second.

After the photographic plates are exposed and developed, they are counted by mounting them on an accurate traveling stage and observing the tracks by use of a binocular microscope, with a Leitz dark-field illuminator source. For normal track size and intensity, a 20X objective is used, defining a one-half millimeter square. For very dense peaks or short tracks, a 43X objective is used which defines a field of view of about one-quarter millimeter square. The number of particle tracks across the exposed strip is plotted against distance along the plates. The position of the point at one-third the peak height on the high-energy side of the peak has been used as a measure of the position of a group<sup>22</sup>. The distance is measured to an accuracy of  $\pm 0.1$  millimeter or better. With the distance known, the corresponding value of  $\rho$ , the radius of curvature of a given peak, is found from the calibration curve. This is multiplied by B, the known magnetic field of the spectrograph. This gives the value  $B\rho$ , the momentum of the particle, and, since the type of particle is

the first of these is the fact that the system is not a simple one, and the second is the fact that the system is not a simple one.

[illegible]

Under of certain facts stated the records were in official custody  
 since a field of view at least one-quarter million square feet  
 very dense forest to about twenty miles. The objective is that the  
 a box objective is used, containing a one-half million square feet  
 two-third thousand square feet. The forest was also the  
 are bounded by several lines to the north and south and the  
 after the development of the area and beyond the boundary, they

an amount of  $\pm 0.1$  millimeter or more. With the following values  
a measure of the position of  $\pm 1$  mm<sup>2</sup>. The distance is measured in  
the peak height on the right-hand side of the wave and used as  
distance along the axis. The position of the point on the wave

the corresponding value of  $\alpha$ , the radius of curvature of a given curve, is found from the following curve. This is indicated by 2, the lower curve of the stereograph. This gives the value of the radius of the circle, and gives the time of arrival at the summit of the circle, and gives the time of arrival at the summit of the circle.



known, use may be made of tables of  $B\rho$  versus energy<sup>23</sup> to find the energy of the emergent particles.

Calibration of the magnetic spectrograph<sup>17</sup> is based on the accurately known momentum of polonium alpha particles. A polonium-coated silver wire is placed accurately in the target chamber in the same position as the beam spot on the target. Then exposures are made at various values of field strength of the spectrograph. This places the alpha particles at different positions along the photographic plate and provides the relation between distance along the plate versus radius of curvature. The value of 331.59 kilogauss centimeters for polonium alpha particles is used. The calibration error is found to be about  $\pm 0.04$  percent in particle energy.

known, and we are sure of finding it in every case.

Copyright 1999 by the American Psychological Association or one of its allied publishers. This article is intended solely for the personal use of the individual user and is not to be disseminated broadly.

add the number of  $\gamma$ -rays per second to the total

1. The first group of people who are interested in the results of the study are the researchers themselves. They want to know if the study was successful in achieving its objectives and if the results are consistent with their expectations.

collected eleven years in a row and averaged 10.44 percent.

THE above positions are not based upon the theory of evolution.

Advertisement will be accepted until 15 days before departure of each cruise.

This picture was taken yesterday at 10:00 AM.

bioRxiv preprint doi: <https://doi.org/10.1101/000000>; this version posted January 1, 2016. The copyright holder for this preprint (which was not certified by peer review) is the author/funder, who has granted bioRxiv a license to display the preprint in perpetuity. It is made available under aCC-BY-NC-ND 4.0 International license.

the glass between columns is approximately 10 cm.

cost estimates for jobs are based on the

Overall error is  $\sqrt{0.0001 + 0.0001} = 0.0002$  percent in power.

1999

### III. EXPERIMENTAL PROCEDURE

The first step in the investigation after the targets were made consisted of bombarding a target with 6.5-Mev protons and analyzing the elastically scattered proton groups to determine the contaminants contained in the target and to measure the effective thickness of the cobalt coating. Elastic runs were made at 90 degrees, as shown in Table I. The results from one such bombardment are shown in Figure 4 and in Table I. For scattering at 90 degrees from a target initially at rest, nonrelativistically we use the following

$$m = \frac{E_{in} m_p + E_o m_p}{E_{in} - E_o}, \quad \begin{array}{l} \text{(where } m_p \text{ is the} \\ \text{mass of a proton)} \end{array}$$

to determine the mass of the scattering nuclei.

According to the manufacturer<sup>23</sup>, Formvar contains 33 percent oxygen, 59.1 percent carbon, and 7.8 percent hydrogen (by weight) plus traces of sulfur and nitrogen. For use, Formvar is diluted with ethylene dichloride, which adds only chlorine to the list of contaminants contained in the backing. The calcium could possibly be present in the distilled water used in floating the Formvar films onto the target frame. The arsenic and silver are believed to be due to previous evaporated materials which were not completely removed from the evaporator.

It is noted that the analysis of contamination on one of a different group of targets showed less sodium and chlorine than in the first run, which may be due to better cleaning of the evaporator before making new targets, or may be a case of "sweat physics."





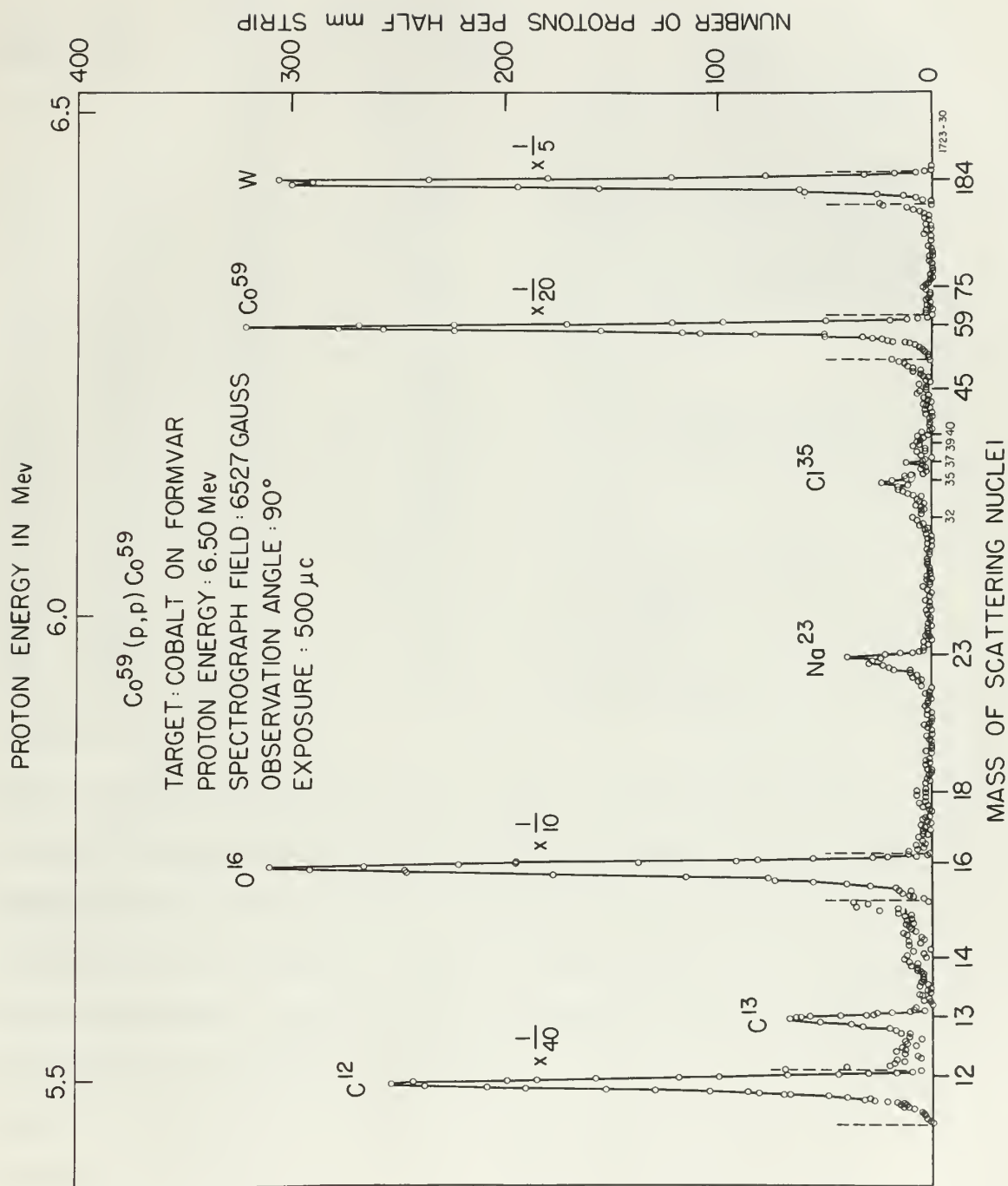


Figure 4





Table I. Mass Analysis of Cobalt Target on Formvar Backing

Element	Number Z	Significant Isotope A	No. Tracks in Peak $\div Z^2$ Rel. to Co <sup>59</sup>	Origin
C	6	12	3500.0	Backing and vacuum system
C	6	13	34.5	Backing and vacuum system
N	7	14	1.67	Backing and vacuum system
O	8	16	638.0	Backing and vacuum system
O	8	18	0.57	Backing and vacuum system
Na	11	23	4.7	Sweat Physics
S	16	32	1.58	Backing
Cl	17	35	0.57	Backing, Sweat Physics
Cl	17	37	0.23	Backing, Sweat Physics
K	19	39	0.14	?
Ca	20	40	0.11	Backing
Co	27	59	100.0	Evaporated material
As	33	75	0.03	Evaporator
Ag	47	107	0.3	Evaporator
W	74	184	4.0	Tungsten boat

Note: An estimate of the relative amount of each element present has been made by assuming (very incorrectly in general) Rutherford scattering. The number of tracks assigned to each element was divided by  $Z^2$  and is given in the fourth column of Table I relative to the cobalt peak. Column 5 gives the assigned origin of these contaminants, as a matter of interest.

Table 1. Mass analysis of cobalt target on various binding

Element	Mass- number	Relative intensity A	Relative intensity B	Relative intensity C
Hydrogen	1	100	100	100
Helium	4	10	10	10
Lithium	7	10	10	10
Boron	11	10	10	10
Carbon	12	10	10	10
Nitrogen	14	10	10	10
Oxygen	16	10	10	10
Fluorine	19	10	10	10
Neon	20	10	10	10
Sodium	23	10	10	10
Magnesium	24	10	10	10
Aluminum	27	10	10	10
Silicon	28	10	10	10
Phosphorus	31	10	10	10
Sulfur	32	10	10	10
Chlorine	35	10	10	10
Argon	36	10	10	10
Potassium	39	10	10	10
Calcium	40	10	10	10
Scandium	45	10	10	10
Titanium	48	10	10	10
Vanadium	51	10	10	10
Chromium	52	10	10	10
Manganese	55	10	10	10
Iron	56	10	10	10
Cobalt	59	10	10	10
Nickel	60	10	10	10
Copper	63	10	10	10
Zinc	65	10	10	10
Gallium	69	10	10	10
Germanium	72	10	10	10
Arsenic	75	10	10	10
Selenium	78	10	10	10
Bromine	80	10	10	10
Krypton	84	10	10	10
Rubidium	85	10	10	10
Strontium	88	10	10	10
Yttrium	89	10	10	10
Zirconium	90	10	10	10
Niobium	93	10	10	10
Molybdenum	96	10	10	10
Technetium	98	10	10	10
Ruthenium	101	10	10	10
Rhodium	103	10	10	10
Palladium	106	10	10	10
Silver	108	10	10	10
Cadmium	112	10	10	10
Indium	115	10	10	10
Thallium	120	10	10	10
Lead	124	10	10	10
Bismuth	126	10	10	10
Polonium	128	10	10	10
Astatine	130	10	10	10
Radium	132	10	10	10
Actinium	133	10	10	10
Thorium	138	10	10	10
Protactinium	140	10	10	10
Uranium	144	10	10	10
Neptunium	146	10	10	10
Plutonium	150	10	10	10
Americium	151	10	10	10
Cerium	140	10	10	10
Lanthanum	139	10	10	10
Praseodymium	141	10	10	10
Samarium	150	10	10	10
Europium	152	10	10	10
Gadolinium	157	10	10	10
Terbium	159	10	10	10
Dysprosium	163	10	10	10
Ytterbium	173	10	10	10
Lutetium	175	10	10	10
Hafnium	178	10	10	10
Tantalum	181	10	10	10
Tungsten	184	10	10	10
Rhenium	187	10	10	10
Osmium	192	10	10	10
Iridium	193	10	10	10
Ptassium	195	10	10	10
Gold	197	10	10	10
Mercury	200	10	10	10
Thallium	205	10	10	10
Lead	208	10	10	10
Bismuth	209	10	10	10
Polonium	210	10	10	10
Astatine	211	10	10	10
Radium	226	10	10	10
Actinium	227	10	10	10
Thorium	232	10	10	10
Protactinium	231	10	10	10
Uranium	238	10	10	10
Neptunium	237	10	10	10
Plutonium	244	10	10	10
Americium	243	10	10	10
Cerium	140	10	10	10
Lanthanum	139	10	10	10
Praseodymium	141	10	10	10
Samarium	150	10	10	10
Europium	152	10	10	10
Gadolinium	157	10	10	10
Terbium	159	10	10	10
Dysprosium	163	10	10	10
Ytterbium	173	10	10	10
Lutetium	175	10	10	10
Hafnium	178	10	10	10
Tantalum	181	10	10	10
Tungsten	184	10	10	10
Rhenium	187	10	10	10
Osmium	192	10	10	10
Iridium	193	10	10	10
Ptassium	195	10	10	10
Gold	197	10	10	10
Mercury	200	10	10	10
Thallium	205	10	10	10
Lead	208	10	10	10
Bismuth	209	10	10	10
Polonium	210	10	10	10
Astatine	211	10	10	10
Radium	226	10	10	10
Actinium	227	10	10	10
Thorium	232	10	10	10
Protactinium	231	10	10	10
Uranium	238	10	10	10
Neptunium	237	10	10	10
Plutonium	244	10	10	10
Americium	243	10	10	10

Note: In column 1 the relative mass of each element is given. The mass number of the element is given in the first column of Table 1 relative to the cobalt peak. Column 2 gives the relative mass of each element. The mass number of the element is given in the first column of Table 1 relative to the cobalt peak. Column 3 gives the relative mass of each element. The mass number of the element is given in the first column of Table 1 relative to the cobalt peak. Column 4 gives the relative mass of each element. The mass number of the element is given in the first column of Table 1 relative to the cobalt peak. Column 5 gives the relative mass of each element. The mass number of the element is given in the first column of Table 1 relative to the cobalt peak.

In other words, prior to evaporating perspiration was left on the crucible, electrodes, and target frame supports because of handling. The greater apparent abundance of Na versus Cl may be caused by the effects of high deuteron bombarding energy.

Since the targets were quite fragile, we had to use a total of five targets from two different evaporations. The contaminants were checked for each group. Normalization of the different runs is described later.

The following procedure was employed in the angular distribution runs: We first determined the approximate barrier height of  $\text{Co}^{59}$  from the equation<sup>24</sup>  $B \approx 0.76 \text{ } zZ^{2/3} \text{ Mev}$ , and found it to be  $\approx 6.8 \text{ Mev}$  for deuterons on cobalt. It was desirable to use a bombarding energy of roughly this value to minimize exposure time, but a value of  $6.0 \text{ Mev}$  was chosen because the accelerator was better stabilized at this energy; an important factor in long runs, such as were made.

The energy of the bombarding deuterons was established by setting up the desired magnetic field in the deflecting magnet. This energy was a constant throughout a set of angular runs, but the setting of the magnetic spectrograph field was changed every few angles to maintain an approximately constant position of the ground level proton peaks from  $\text{Co}^{59}$  on the photographic plate. This insured that the peaks had a constant solid angle throughout the run and thus removed the need for solid-angle correction in comparing the intensities of peaks at different angles. The exact



in other words, prior to evaporating completely and left on the  
residue, condensed, and before being exposed to heating.  
The greater amount of residue at 100°C than at 150°C was due to the  
effects of this residue containing energy.

Since the residue was quite small, it was not a solid  
of the residue from two different experiments. The experiments  
were checked the same way. Residue of the different runs  
is described later.

The following procedure was followed in the analysis of the  
residue runs: The first detailed analysis was made of the residue  
of 100°C from the experiment of 100°C at 100°C, and found it to  
be 0.6 for the residue as usual. It was therefore used as a  
reference energy of weight; this value to compare against the  
the value of 0.6 for the residue from the experiment was taken  
as the energy of the residue; in the residue from 100°C, and as  
the energy of the residue.

The energy of the residue from the experiment was calculated by  
using up the residue amount 100°C in the residue amount.  
This energy was a constant throughout a set of residue runs, and  
the residue of the residue from 100°C was found to be  
the same as the residue of the residue from 100°C. The residue of the  
residue from 100°C was found to be the same as the residue from 100°C.  
The residue from the residue was a constant with the residue from 100°C.  
The residue from the residue was found to be the same as the residue from 100°C.  
The residue from the residue was found to be the same as the residue from 100°C.

energy of the deuteron beam was determined by an elastic deuteron exposure and by using the accurately known Q-value<sup>25</sup> ( $2.717 \pm 0.007$  Mev) for the  $C^{12}(d,p)C^{13}$  reaction which appeared in all exposures.

The first series of angular distributions was made at an average deuteron energy of 6.009 Mev, and the exposures were 500 microcoulombs. The second series was made, through an error in setting up the deflecting magnet, at an average energy of 6.187 Mev, and with varied exposures. Table II summarizes these runs. The longer runs of the second series were designed to resolve better several weak peaks seen in the first series in order to determine their energy with greater accuracy. The higher energy of the second series shifted the position of the proton peaks a distance approximately two centimeters toward the high-energy end of the plates. The average deuteron current input to the target chamber was about 0.10 microamperes.

When making the (d,p) distribution runs, the photographic plates were covered with two layers of 1.5-mil aluminum foil to screen out alpha particles and deuterons. After exposure, the plates were developed and counted, as described previously. We plotted the number of protons per one-half millimeter strip versus distance along the plate, as shown by the example in Figure 5. The proton groups from cobalt were identified by observing the shift in position on the plate from one angle to another. The expected drift was calculated as an aid in identification. In each run, one or more of the proton groups were obscured by the large ground level



The first two of these experiments were carried out in the laboratory of the author, and the results are given in Table I. The third experiment was carried out in the laboratory of the author, and the results are given in Table II. The fourth experiment was carried out in the laboratory of the author, and the results are given in Table III. The fifth experiment was carried out in the laboratory of the author, and the results are given in Table IV. The sixth experiment was carried out in the laboratory of the author, and the results are given in Table V. The seventh experiment was carried out in the laboratory of the author, and the results are given in Table VI. The eighth experiment was carried out in the laboratory of the author, and the results are given in Table VII. The ninth experiment was carried out in the laboratory of the author, and the results are given in Table VIII. The tenth experiment was carried out in the laboratory of the author, and the results are given in Table IX.

TABLE II. Summary of Targets and Exposure for Angular Distribution

<u>Angle</u>	<u>Exposure (<math>\mu</math>coul.)</u>	<u>Target</u>	<u>Remarks</u>
10°	500	B 3	
15	500	B 3	
20	500	B 3	
25	500	B 3	
30	500	B 3	
35	500	B 3	
40	500	B 3	
45	500	B 3	
50	500	B 3	
55	500	B 3	
60	500	B 3	
70	500	B 3	
80	500	B 8	
90	500	B 8	
5	1000	A 3	Unusable-deuterons
15	1000	A 3	
25	1427	A 3	
30	1000	A 4	
45	1000	A 4	
90	1250	A 3	
100	1250	A 3	
110	1250	A 3	
15	500	B 6	First test run
45	250	A 4	Second test run

TABLE II. Trends of freight and volume by loading destination

Year	Volume (10,000 tons)	Freight (10,000 tons)	Destination
1960	200	1.5	
1961	200	1.5	
1962	200	1.5	
1963	200	1.5	
1964	200	1.5	
1965	200	1.5	
1966	200	1.5	
1967	200	1.5	
1968	200	1.5	
1969	200	1.5	
1970	200	1.5	
1971	200	1.5	
1972	200	1.5	
1973	200	1.5	
1974	200	1.5	
1975	200	1.5	
1976	200	1.5	
1977	200	1.5	
1978	200	1.5	
1979	200	1.5	
1980	200	1.5	
1981	200	1.5	
1982	200	1.5	
1983	200	1.5	
1984	200	1.5	
1985	200	1.5	
1986	200	1.5	
1987	200	1.5	
1988	200	1.5	
1989	200	1.5	
1990	200	1.5	
1991	200	1.5	
1992	200	1.5	
1993	200	1.5	
1994	200	1.5	
1995	200	1.5	
1996	200	1.5	
1997	200	1.5	
1998	200	1.5	
1999	200	1.5	
2000	200	1.5	
2001	200	1.5	
2002	200	1.5	
2003	200	1.5	
2004	200	1.5	
2005	200	1.5	
2006	200	1.5	
2007	200	1.5	
2008	200	1.5	
2009	200	1.5	
2010	200	1.5	
2011	200	1.5	
2012	200	1.5	
2013	200	1.5	
2014	200	1.5	
2015	200	1.5	
2016	200	1.5	
2017	200	1.5	
2018	200	1.5	
2019	200	1.5	
2020	200	1.5	
2021	200	1.5	
2022	200	1.5	
2023	200	1.5	
2024	200	1.5	
2025	200	1.5	
2026	200	1.5	
2027	200	1.5	
2028	200	1.5	
2029	200	1.5	
2030	200	1.5	

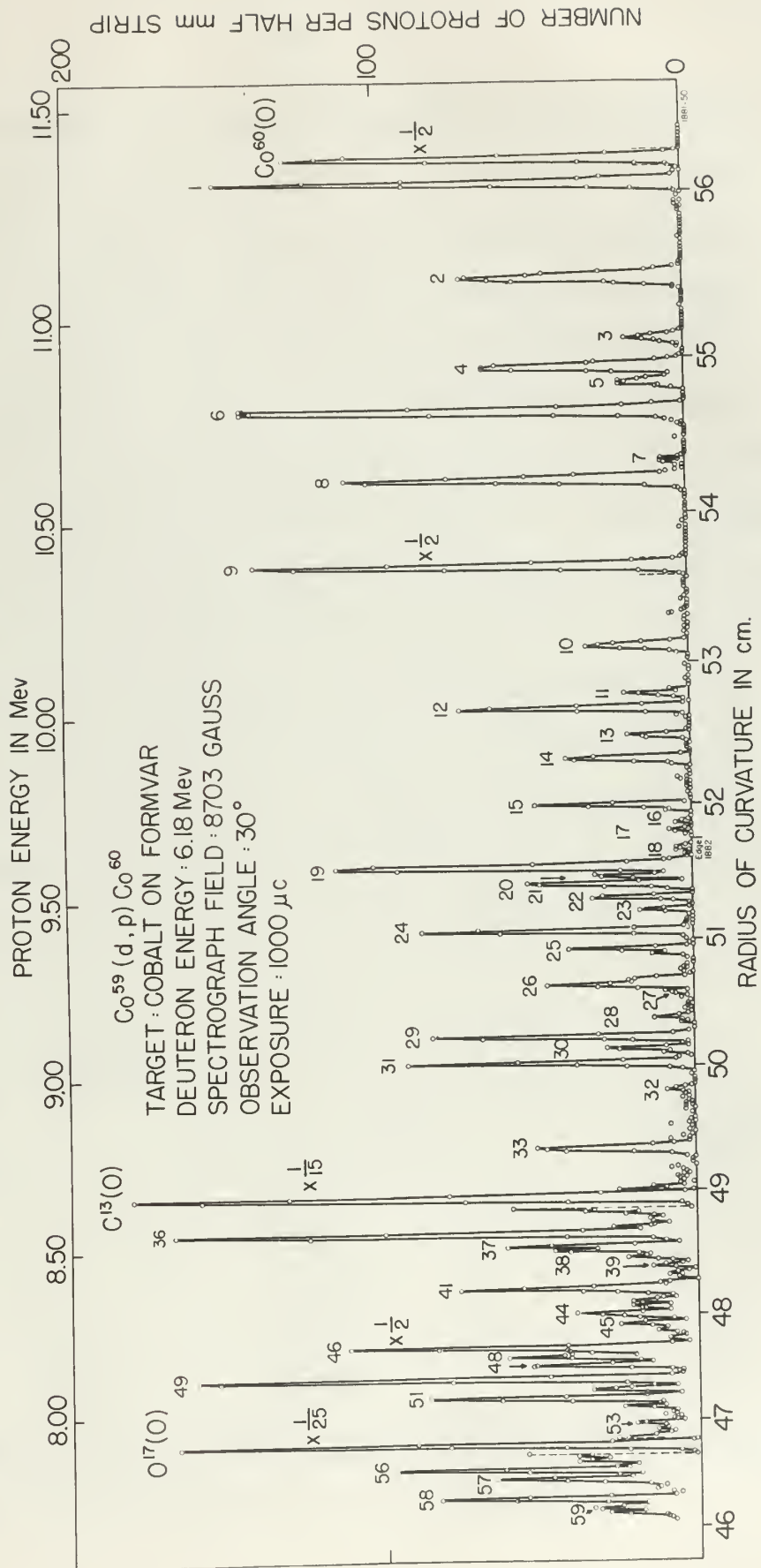


Figure 5





and first excited levels of the  $O^{16}(d,p)O^{17}$  and  $C^{12}(d,p)C^{13}$  reactions. Since these latter are light nuclei, the shift of peak position versus angle is greater for them than for the cobalt peaks. Hence, the cobalt peaks which had been obscured at one angle by carbon and oxygen could be seen at a different angle.

The data from the different runs were normalized in order to correct for the various thicknesses of cobalt and for the different amounts of exposure used. For the latter, the number of proton tracks in a peak was corrected to a 500 microcoulomb exposure by multiplying by the ratio of 500 over the actual exposure for the run. To determine the target thicknesses relative to the original one (B 3), the total number of proton tracks on the first plate (up to excited level No. 14) was corrected for the amount of exposure and then compared with the first plate of target B 3 at a common angle of exposure. The results are summarized in Table III:

TABLE III

Target Thickness Relative to Target B 3

<u>Target</u>	<u>Relative Thickness</u>	<u>Angle of Comparison</u>
A 3	0.9362	15°
A 4	0.7300	30° + 45°
B 6	0.7746	15
B 8	0.7203	90°

The reciprocal of the relative thickness was multiplied with the peak counts after normalization for exposure amount.

and first excited levels of the  $^{235}\text{U}$  and  $^{238}\text{U}$  isotopes. Since these levels are in the region of the first excited level, the width of the position versus angle is greater for them than for the other peaks. Hence, the relative peak widths had been observed to be large by angles and regions could be seen to be different angles. The data from the different runs were corrected in order to correct for the various thicknesses of material and for the different amounts of exposure used. For the latter, the number of photons tracks in a peak was corrected to a 500 micron-thickness exposure by multiplying by the ratio of 500 over the actual exposure for the run. To determine the relative thicknesses relative to the original one (U 3), the total number of photon tracks on the first plate (no 10 excited level in U) was corrected for the number of photons and then compared with the first plate of Figure 2.3 as a common angle of exposure. The results are presented in Table III.

TABLE III

Relative thickness relative to Figure 2.3

Figure of Exposure	Relative thickness	Figure
12	0.135	3
100 + 12	0.135	4
12	0.135	5
100	0.135	6

The thickness of the relative thickness was calculated with the same method after correction for exposure amount.

It was noted by comparison of corresponding peaks at the same angle on two different targets that random fluctuations of the proton counts were relatively high; that is, several peaks out of fifteen on the first plate would be two or three standard deviations off with respect to two guides: the same peak obtained from the other target and the expected value obtained by approximating a smooth angular distribution through the peak counts of adjacent angles. In normalizing to minimize this effect where more than one exposure had been made at the same angle (Table III), a weighted mean count was determined for each such angle.

The first step was to multiply the amount of exposure for a given target and angle by the relative target thickness to obtain a standardized exposure which would have produced the same number of proton tracks within the limits of fluctuation had the standard target been used. Then, for each angle a factor of 500, the standard exposure, was divided by the sum of all standardized exposures, including the standard one. This was then multiplied by the sum of all protons counted in the peak on all exposures regardless of target to give the mean count. Example:

<u>Target</u>	<u>No. Counts 1 Peak</u>	<u>Exposure</u>	<u>Relative Thickness</u>
Standard	1000	500	1
Other	600	500	0.50

The standardized exposure of the other target is 250 and the mean count =  $(\frac{500}{500 + 250})(1000 + 600) = 1067$ . The advantage of this





procedure over others which might produce the same result is the simplicity of using the unweighted summation of all counts at the same angle for each peak. It was felt that the error in the mean value due to the error in determining the relative target thickness would be much less than the random fluctuations seen in single counts.



provision was made about the time the war broke out in 1914. The importance of having the necessary amount of all kinds of food was made for each food. It was this that was the first step. The value of the food is determined by the relative value of the food. It was this that was the first step.

It was this that was the first step.

It was this that was the first step.

It was this that was the first step.

It was this that was the first step.

It was this that was the first step.

It was this that was the first step.

It was this that was the first step.

It was this that was the first step.

It was this that was the first step.

It was this that was the first step.

It was this that was the first step.

It was this that was the first step.

It was this that was the first step.

It was this that was the first step.

It was this that was the first step.

It was this that was the first step.

It was this that was the first step.

It was this that was the first step.

It was this that was the first step.

It was this that was the first step.

It was this that was the first step.

It was this that was the first step.

It was this that was the first step.

#### IV. RESULTS

##### PROBABLE ERRORS

The probable error quoted for the  $Q$ -values and excitation energies is, strictly speaking, not probable error but uncertainty in energy. This difference in meaning is mentioned because the term "probable error" has a particular definition in the field of statistics which is not the meaning used in this paper. The statistically determined standard error is not the major consideration involved in the quoted error, but is rather the question of the accuracy of our values compared to the "true" values. This is then basically a question of how accurate a calibration has been made against the standard polonium alpha particle. The uncertainty consists of two types of errors, one random in nature and the other systematic. A detailed examination of the uncertainty of each level has not been made, but the general effects have been determined, and it is felt that the uncertainty quoted is reasonable.

The factors which may contribute to the random error are:

1. The spread in energy of the incident particles resulting from finite slit widths;
2. The finite width of the beam which illuminates a finite area on the target, not a point source;
3. The spread in energy of the emergent particles because of variations in target thickness; and
4. Small adjustments of the magnet current to compensate for drift.

IV. SUMMARY

PROBABLE ERROR

The probable error quoted for the 4-values and estimated  
emphasizes its statistical meaning, not probable error and uncertainty  
in energy. This difference in meaning is pointed out in the paper.  
"probable error" has a particular definition in the table of statis-  
tics which is not the meaning used in this paper. The statistically  
determined statistical error is not the same as the error involved in  
the quoted error, but in rather the question of the accuracy of our  
values compared to the "true" values. This is then actually a ques-  
tion of how accurate a calibration has been made against the stan-  
dard potential alpha particles. The uncertainty consists of two types  
of error, one random in nature and the other systematic. A de-  
tailed examination of the uncertainty of each level has not been  
made, but the general effects have been determined, and it is felt  
that the uncertainty quoted is reasonable.

The factors which may contribute to the random error are:

1. The spread in energy of the incident particles

resulting from finite slit widths;

2. The finite width of the beam when it strikes a

thinness near the target, not a point source;

3. The spread in energy of the emitted particles

because of variations in target thickness; and

4. Small adjustments of the magnet current to obtain

data for each.

Since each Q-value is the mean of three or four measurements (with one exception), it is possible to obtain an estimate of the random error by examination of the standard error of the mean values. The mean value is determined from

$$\bar{x} = \frac{1}{n} \sum_{i=1}^n x_i$$

where n is the number of observations. The standard error is then:

$$\sigma_{\bar{x}} = \left[ \frac{\sum_{i=1}^n (x_i - \bar{x})^2}{n(n-1)} \right]^{\frac{1}{2}} .$$

This procedure resulted in an average standard error throughout the range of Q-values reported of about 1.2 kev.

The systematic errors are of greater consequence and are in general a function of the energy of the emergent protons. These errors include the following:

1. The calibration error of the magnetic spectrograph, which includes the uncertainty in the Bp value of the polonium alpha particles;
2. Peak position and validity of the use of the one-third height position;
3. Since the energies of the protons and deuterons were measured after these particles had passed through the target, there is an error caused by the different energy losses suffered by protons and deuterons in the target. This difference in energy loss is partially



Since each observation is the sum of three or four measurements

(with one exception), it is possible to obtain an estimate of the random error by examination of the standard error of the mean values.

The mean value is determined from

$$\bar{x} = \frac{1}{n} \sum_{i=1}^n x_i$$

where  $n$  is the number of observations. The standard error is found

$$s = \sqrt{\frac{\sum_{i=1}^n (x_i - \bar{x})^2}{n(n-1)}}$$

This procedure resulted in an average standard error throughout the

study of 0.00015, repeated at about 1.5 per cent.

The standard error of the mean is found by dividing the standard error

by the square root of the number of observations. Thus

errors are the following:

1. The standard error of the magnetic measurement,

which includes the standard error of the value of the magnetic field

particles;

2. The standard error of the value of the magnetic field

which includes the standard error of the value of the magnetic field

particles. Since the standard error of the magnetic field is

measured after each particle has passed through the system, there is

an error caused by the different energy losses suffered by particles and

particles in the system. This difference is enough that it is relatively

canceled in the Q-equation. However, even though a small correction was made to compensate for the thickness of the cobalt when finding the deuteron energy, these losses cannot be accurately determined, since the exact path of each and every particle is not known; and

4. The effect of temperature on the fluxmeter circuits, which is random in part.

The targets used were continuously rotating and hence the effect of surface contamination was felt to be negligible in comparison with the above effects. The values assigned to each of these terms are shown in Table IV.

TABLE IV

Systematic Errors for Q-values

Errors given in percent of particle energy

1. Calibration error	0.04
2. Error caused by position of carbon and cobalt in target	0.02
3. Peak position and one-third height	0.03
4. Temperature coefficients in fluxmeter	<u>0.03</u>
Root of sum of squares	~ 0.06

The total uncertainty for a given Q-value was determined by first combining the random and systematic errors for one measurement of particle energy and then combining the various uncertainties in the Q-equation to obtain the total uncertainty in Q-value. This results in a very generous estimate of the total uncertainty in Q-value,

concerning the  $\beta$ -transition, however, even though a small correction may be made to compensate for the decrease of the kinetic energy during the transition itself, these values cannot be considered as exact since the exact value of each of these quantities is not known; and

4. The effect of the transition on the electron spin

which is treated in part.

The various data were continuously checked and under the effect of various considerations was left to no negligible in comparison with the above effects. The values obtained on each of these points are shown in Table IV.

TABLE IV

Gamma-ray energy for  $^{60}\text{Co}$

Energy given in terms of relative energy

1. Calculated value 0.98
  2. Value based on position of carbon and oxygen in target 0.98
  3. Peak position and one-third width 0.98
  4. Temperature fluctuations in detector 0.98
- Root of sum of squares 0.00

The total uncertainty for a given value was obtained by first combining the random and systematic errors for the measurement of particle energy and then combining the various uncertainties in the  $\beta$ -transition to obtain the total uncertainty in value. This is done in a very general sense of the total uncertainty in value.



since some of the systematic errors in the determination of the energies of the incident and emergent particles tend to cancel out. This particularly applies to the calibration error.

As an example, for the ground-state Q-value, the proton energy is about 11.4 Mev. This is found to have an error of  $\pm 7$  kev. The uncertainty in the deuteron energy required more calculation, since most of the deuteron energies were determined from the  $C^{12}(d,p)C^{13}$  reaction, which has an uncertainty of  $\pm 7$  kev. The energy uncertainty of the deuteron is thus about  $\pm 9$  kev, which, combined with the proton uncertainty, gives an uncertainty in the Q-value of the ground level of about  $\pm 11$  kev.

The uncertainty in Q-value is given in the results as a constant  $\pm 11$  kev. This is due primarily to the larger expected error in peak position at lower proton energies where the peaks are closely spaced. This is an arbitrary assignment, but it is possible to make larger errors in peak position under these conditions.

The errors or uncertainties of the excitation energies are due to similar causes. The random error was determined by an examination of the standard errors of the mean values and was found to be about  $\pm 4$  kev. The systematic errors are approximately proportional to the excitation energy. In the calculation of the excitation energies, the results depend on the energy differences between groups recorded on the same plate and the systematic errors tend to cancel out. This has led to the assignment of a systematic error of  $\pm 0.1$  percent of the excitation energy. The total uncertainty is then the square root of the sums of the squares of the random and systematic errors.



some sort of the systematic errors in the determination of the value of the constants and systematic errors in the calculation of the constants. This is especially true for the calculation of the constants.

As an example, let the ground-state energy, the energy of the

is about 11.5 eV. This is found to have an error of  $\pm 1$  eV. The

uncertainty in the ground-state energy is about 1 eV. This is

most of the ground-state energy is determined from the  $\psi(0, \psi(0))$

function, which has an uncertainty of  $\pm 1$  eV. The energy of the

of the function is about  $\pm 1$  eV, which, combined with the error

uncertainty, gives an uncertainty in the value of the ground-state

of about  $\pm 1$  eV.

The uncertainty in the value of the function is about  $\pm 1$  eV.

about  $\pm 1$  eV. This is the uncertainty in the larger ground-state

in the value of the function. The uncertainty in the value of the

function. This is an arbitrary assumption, but it is possible to

larger errors in the calculation of the function.

The error in the calculation of the function is about  $\pm 1$  eV.

so that the error in the calculation of the function is about  $\pm 1$  eV.

of the ground-state energy of the function and the error in the

$\pm 1$  eV. The uncertainty in the value of the function is about  $\pm 1$  eV.

uncertainty in the value of the function. In the calculation of the

function, the error in the calculation of the function is about  $\pm 1$  eV.

the error in the calculation of the function is about  $\pm 1$  eV.

the error in the calculation of the function is about  $\pm 1$  eV.

uncertainty in the value of the function. The total uncertainty in the

sum of the errors in the calculation of the function is about  $\pm 1$  eV.

# DISCUSSION OF Q-VALUES AND COMPARISON WITH PREVIOUS WORK

The determination of the energy of a given particle group is done in the following manner. The calibration table is used to convert the third-height distance into  $\rho$ , the trajectory radius of the particle in the magnetic spectrograph. Knowing the value of the magnetic field  $B$  in kilogauss, we next find the "magnetic rigidity" of the particle,  $B\rho$ , and enter the tables calculated by Enge<sup>23</sup>, where the following equation relating energy of a particle to its momentum has been solved for protons, deuterons, tritons, and alpha particles, for values of  $B\rho$  from  $10^5$  to  $6.5 \times 10^5$  gauss centimeters.

$$E_0 = m_0 c^2 \left[ \left( 1 + \left( \frac{ZeB\rho}{m_0 c} \right)^2 \right)^{\frac{1}{2}} - 1 \right]$$

where  $m_0$  = rest mass of the particle.

The equation for the  $Q$ -value of a given reaction can be expressed in the following form:

$$Q = \frac{M_R + M_0}{M_R} E_0 - \frac{M_R - M_I}{M_R} E_I - 2 \cos \theta \frac{(M_I M_0 E_I E_0)^{\frac{1}{2}}}{M_R} + \delta_{rel}$$

where  $M_R$  = mass of residual nucleus

$M_0$  = mass of emitted particle

$E_0$  = energy of emitted particle

$M_I$  = mass of incident particle

$E_I$  = energy of incident particle

$\theta$  = reaction angle in laboratory coordinate.

# DISCUSSION OF RESULTS

## OVERALL AND PARTIAL RESULTS

The definition of the energy of a given particle group is given in the following manner. The definition is used to convert the third-order distance into a two-body distance of the particle in the magnetic spectrum. Knowing the value of the magnetic field  $H$  in kilogauss, we can find the magnetic rigidity of the particle,  $B\rho$ , and then the value calculated by (10), where the following equation relating energy of a particle to its momentum has been solved for  $p$ ,  $m_0$ ,  $c$ ,  $\beta$ , and  $\gamma$ , and also  $\beta^2$ . For values of  $\beta$  from  $10^{-2}$  to  $0.5 \times 10^2$  gauss centimeters.

$$\left[ 1 - \left( \frac{m_0 c}{B\rho} \right)^2 \right]^{1/2} = \beta$$

where  $B\rho$  = total mass of the particle.

The equation for the  $\beta$ -value of a given reaction can be written in the following form:

$$\beta = \frac{H_0 + H_1}{H_0} \left( \frac{H_0}{H_1} - 1 \right)^{-1/2} = \frac{H_0}{H_1} \left( \frac{H_1}{H_0} - 1 \right)^{-1/2}$$

where  $H_0$  = mass of incident particle

$H_1$  = mass of emitted particle

$H_2$  = energy of emitted particle

$H_3$  = mass of incident particle

$H_4$  = energy of incident particle

$\beta$  = reaction angle in laboratory coordinates.



The term  $\delta_{\text{rel}}$  is a small relativistic correction term and is approximately:

$$\delta_{\text{rel}} \approx \frac{1}{2M_R c^2} \left[ E_I^2 + E_O^2 - E_R^2 - \cos \theta (M_I M_O E_I E_O)^{\frac{1}{2}} \left( \frac{E_I}{M_I} + \frac{E_O}{M_O} \right) \right]$$

where  $E_R$ , the energy of the residual nucleus, is found from

$$E_R = \frac{M_I}{M_R} E_I + \frac{M_O}{M_R} E_O - 2 \cos \theta \frac{(M_I M_O E_I E_O)^{\frac{1}{2}}}{M_R}.$$

To find the bombarding energy of a particle using elastic scattering, we set  $Q$  equal to zero and have

$$E_I = \frac{M_R + M_O}{M_R - M_I} E_O - 2 \cos \theta (M_I M_O E_I E_O)^{\frac{1}{2}} + \delta_{\text{rel}} \frac{M_R}{M_R - M_I}$$

Unless  $\theta$  is equal to 90 degrees, we have a second-order equation; therefore, the method of successive approximations was employed in the solution of this equation. This technique was also employed when the deuteron energy was obtained from the  $C^{12}(d,p)C^{13}$  reaction leading to the ground level of  $C^{13}$ .

The  $Q$ -values were computed from four exposures, the 45- and 60-degree exposures of the 6.009-Mev series, and the 25- and 30-degree exposures of the 6.187-Mev series. The exposures at 45 and 60 degrees were 500  $\mu$ coulomb and, in examining the results, we found several small peaks identified with  $Co^{60}$  were observed besides the large ones. The second set of exposures was given longer bombardment in order to obtain better counting statistics for small proton groups.



The term  $\delta$  is a small correction to the main term  $\epsilon$

approximate

$$\left[ \frac{1}{2} \frac{d^2}{dt^2} + \frac{1}{2} \frac{d^2}{dx^2} \right] \psi = \epsilon \psi$$

where  $\epsilon$  is the energy of the system, known to be zero

$$\frac{1}{2} \frac{d^2}{dt^2} + \frac{1}{2} \frac{d^2}{dx^2} = \epsilon$$

to find the potential energy of a particle with mass

unitary, we set  $\epsilon$  equal to zero and have

$$\frac{1}{2} \frac{d^2}{dt^2} + \frac{1}{2} \frac{d^2}{dx^2} = 0$$

where  $\epsilon$  is equal to 0, we have a second-order equation

that, therefore, has a set of two linearly independent solutions

in the vicinity of the origin. This solution is also unique

when the boundary conditions are satisfied, the  $\psi(x)$  solution

is the only one that is bounded at the origin.

The solution is unique for the boundary conditions, the  $\psi(x)$  solution

is the only one that is bounded at the origin, the  $\psi(x)$  solution

is the only one that is bounded at the origin, the  $\psi(x)$  solution

is the only one that is bounded at the origin, the  $\psi(x)$  solution

is the only one that is bounded at the origin, the  $\psi(x)$  solution

is the only one that is bounded at the origin, the  $\psi(x)$  solution

is the only one that is bounded at the origin, the  $\psi(x)$  solution

The 25- and 30-degree exposures were selected for computation to give the highest average intensity of all the peaks regardless of the shape of their angular distribution. The use of four separate exposures at different angles insured at least three separate determinations of the Q-value for each level, with but one exception. The average Q-value and excitation energy for the ground level and fifty-nine excited levels are given in Table V. Level number 54 is inclosed in parentheses to indicate that it is the mean of only two measurements and has a larger random error. This peak was consistently observed at other angles but was obscured by the  $O^{17}$  ground level on two of the four exposures used in determining Q-values.

In the computations for the Q-values, the relativity correction was less than 0.5 kev for the 25, 30, and 45-degree exposures, and was less than 0.8 kev for the 60-degree exposure. It has been included in the results for the 60-degree exposure.

A separate series of computations for the Q-value of the ground level at twelve different angles gave a Q of  $5.262 \pm 0.011$  Mev. The maximum spread in these Q-values was 7 kev, with a standard random error of less than 2 kev.

The agreement for the Q-values of the excited levels was good on all exposures. The standard random error was found to be less than 4 kev for any level, and for most levels, it was less than 3 kev.

The 25- and 30-degree experiments were arranged in comparison to give the highest average intensity of all the pairs registered at the same at least within the experiment. The use of four separate exposures at different angles insured on each plate separate distributions of the particles for each level, and no overlapping. The average particle and scattering energy for the ground level and fifty-degree scattered levels are given in Table V. Total number of particles in parentheses is indicated that it is the sum of only two measurements and has a larger relative error. This sum has been already observed at other angles and has been reported by the 25-degree level as for all the four exposures and in determining the values.

In the comparison for the particles, the relatively narrow lines were seen from 25 to 30 for the 25, 30, and 35-degree exposures, and were less than 0.1 for the 30-degree exposure. It was then included in the results for the 30-degree exposure. A separate series of experiments for the particles of the ground level at twenty different angles gave a  $\sigma$  of  $2.50 \pm 0.11$  for. The various spread in these figures was 7 per cent, with a standard error of less than 1 per cent. The agreement for the values of the scattered levels was good on all exposures. The standard error for each level is less than 1 per cent for each level, and for each level, it was less than 1 per cent.

TABLE V

Q-values for  $\text{Co}^{59}(\text{d},\text{p})\text{Co}^{60}$  and Excitation Energies of  $\text{Co}^{60}$ 

<u>Level</u>	<u>Q-value in Mev + 0.011</u>	<u>Excitation Energy in Mev</u>
Ground State	5.262	0
1	5.204	0.058 $\pm$ 0.004
2	4.980	0.282 $\pm$ 0.004
3	4.830	0.432 $\pm$ 0.004
4	4.761	0.501 $\pm$ 0.004
5	4.721	0.541 $\pm$ 0.004
6	4.650	0.612 $\pm$ 0.004
7	4.524	0.738 $\pm$ 0.004
8	4.479	0.783 $\pm$ 0.004
9	4.256	1.006 $\pm$ 0.004
10	4.055	1.207 $\pm$ 0.004
11	3.925	1.337 $\pm$ 0.004
12	3.885	1.377 $\pm$ 0.004
13	3.815	1.447 $\pm$ 0.004
14	3.750	1.512 $\pm$ 0.004
15	3.624	1.638 $\pm$ 0.004
16	3.578	1.684 $\pm$ 0.004
17	3.555	1.707 $\pm$ 0.004
18	3.514	1.748 $\pm$ 0.004
19	3.463	1.799 $\pm$ 0.004
20	3.433	1.829 $\pm$ 0.004



TABLE V

Calculated for  $\alpha = 0.05$  and  $\beta = 0.80$  for various values of  $\rho$

Level	Calculated for $\alpha = 0.05$ and $\beta = 0.80$	Calculated for $\alpha = 0.05$ and $\beta = 0.80$
0	0.000	0.000
1	0.000	0.000
2	0.000	0.000
3	0.000	0.000
4	0.000	0.000
5	0.000	0.000
6	0.000	0.000
7	0.000	0.000
8	0.000	0.000
9	0.000	0.000
10	0.000	0.000
11	0.000	0.000
12	0.000	0.000
13	0.000	0.000
14	0.000	0.000
15	0.000	0.000
16	0.000	0.000
17	0.000	0.000
18	0.000	0.000
19	0.000	0.000
20	0.000	0.000

<u>Level</u>	<u>Q-value</u>	<u>Ex (Mev)</u>
21	3.412	1.850 $\pm$ 0.004
22	3.375	1.887 $\pm$ 0.004
23	3.339	1.923 $\pm$ 0.004
24	3.283	1.979 $\pm$ 0.004
25	3.231	2.031 $\pm$ 0.005
26	3.131	2.131 $\pm$ 0.005
27	3.112	2.150 $\pm$ 0.005
28	3.045	2.217 $\pm$ 0.005
29	2.988	2.274 $\pm$ 0.005
30	2.952	2.310 $\pm$ 0.005
31	2.914	2.348 $\pm$ 0.005
32	2.835	2.427 $\pm$ 0.005
33	2.671	2.591 $\pm$ 0.005
34	2.528	2.734 $\pm$ 0.005
35	2.500	2.762 $\pm$ 0.005
36	2.417	2.845 $\pm$ 0.005
37	2.378	2.884 $\pm$ 0.005
38	2.363	2.899 $\pm$ 0.005
39	2.320	2.942 $\pm$ 0.005
40	2.295	2.967 $\pm$ 0.005
41	2.252	3.010 $\pm$ 0.005
42	2.214	3.048 $\pm$ 0.005
43	2.197	3.065 $\pm$ 0.005
44	2.176	3.086 $\pm$ 0.005

Level	Value	Std. Dev.
14	1.140	1.140 ± 0.140
15	1.141	1.141 ± 0.141
16	1.142	1.142 ± 0.142
17	1.143	1.143 ± 0.143
18	1.144	1.144 ± 0.144
19	1.145	1.145 ± 0.145
20	1.146	1.146 ± 0.146
21	1.147	1.147 ± 0.147
22	1.148	1.148 ± 0.148
23	1.149	1.149 ± 0.149
24	1.150	1.150 ± 0.150
25	1.151	1.151 ± 0.151
26	1.152	1.152 ± 0.152
27	1.153	1.153 ± 0.153
28	1.154	1.154 ± 0.154
29	1.155	1.155 ± 0.155
30	1.156	1.156 ± 0.156
31	1.157	1.157 ± 0.157
32	1.158	1.158 ± 0.158
33	1.159	1.159 ± 0.159
34	1.160	1.160 ± 0.160
35	1.161	1.161 ± 0.161
36	1.162	1.162 ± 0.162
37	1.163	1.163 ± 0.163
38	1.164	1.164 ± 0.164
39	1.165	1.165 ± 0.165
40	1.166	1.166 ± 0.166
41	1.167	1.167 ± 0.167
42	1.168	1.168 ± 0.168
43	1.169	1.169 ± 0.169
44	1.170	1.170 ± 0.170
45	1.171	1.171 ± 0.171
46	1.172	1.172 ± 0.172
47	1.173	1.173 ± 0.173
48	1.174	1.174 ± 0.174
49	1.175	1.175 ± 0.175
50	1.176	1.176 ± 0.176
51	1.177	1.177 ± 0.177
52	1.178	1.178 ± 0.178
53	1.179	1.179 ± 0.179
54	1.180	1.180 ± 0.180
55	1.181	1.181 ± 0.181
56	1.182	1.182 ± 0.182
57	1.183	1.183 ± 0.183
58	1.184	1.184 ± 0.184
59	1.185	1.185 ± 0.185
60	1.186	1.186 ± 0.186
61	1.187	1.187 ± 0.187
62	1.188	1.188 ± 0.188
63	1.189	1.189 ± 0.189
64	1.190	1.190 ± 0.190
65	1.191	1.191 ± 0.191
66	1.192	1.192 ± 0.192
67	1.193	1.193 ± 0.193
68	1.194	1.194 ± 0.194
69	1.195	1.195 ± 0.195
70	1.196	1.196 ± 0.196
71	1.197	1.197 ± 0.197
72	1.198	1.198 ± 0.198
73	1.199	1.199 ± 0.199
74	1.200	1.200 ± 0.200
75	1.201	1.201 ± 0.201
76	1.202	1.202 ± 0.202
77	1.203	1.203 ± 0.203
78	1.204	1.204 ± 0.204
79	1.205	1.205 ± 0.205
80	1.206	1.206 ± 0.206
81	1.207	1.207 ± 0.207
82	1.208	1.208 ± 0.208
83	1.209	1.209 ± 0.209
84	1.210	1.210 ± 0.210
85	1.211	1.211 ± 0.211
86	1.212	1.212 ± 0.212
87	1.213	1.213 ± 0.213
88	1.214	1.214 ± 0.214
89	1.215	1.215 ± 0.215
90	1.216	1.216 ± 0.216
91	1.217	1.217 ± 0.217
92	1.218	1.218 ± 0.218
93	1.219	1.219 ± 0.219
94	1.220	1.220 ± 0.220
95	1.221	1.221 ± 0.221
96	1.222	1.222 ± 0.222
97	1.223	1.223 ± 0.223
98	1.224	1.224 ± 0.224
99	1.225	1.225 ± 0.225
100	1.226	1.226 ± 0.226

<u>Level</u>	<u>Q-Value</u>	<u>Ex (Mev)</u>
45	2.147	3.115 $\pm$ 0.005
46	2.077	3.185 $\pm$ 0.005
47	2.047	3.215 $\pm$ 0.005
48	2.024	3.238 $\pm$ 0.005
49	1.978	3.284 $\pm$ 0.005
50	1.948	3.314 $\pm$ 0.005
51	1.923	3.339 $\pm$ 0.005
52	1.895	3.367 $\pm$ 0.005
53	1.843	3.419 $\pm$ 0.006
54	(1.798)	(3.464 $\pm$ 0.006)
55	1.764	3.498 $\pm$ 0.006
56	1.698	3.564 $\pm$ 0.006
57	1.671	3.591 $\pm$ 0.006
58	1.609	3.653 $\pm$ 0.006
59	1.580	3.682 $\pm$ 0.006

The excitation energy was found by subtracting the average Q-value of a level from the Q-value of the ground level. The average thus obtained was compared with the excitation energy determined for the individual exposures and agreement was again good.

The determination of energy levels was ended after fifty-nine levels had been measured. At levels above fifty-nine, the resolution of peaks is much poorer because of a larger background and closer spacing of proton groups. The beginning of this background may be



Level	Energy (eV)	Energy (eV)
12	1.111	$1.112 \pm 0.001$
13	1.117	$1.118 \pm 0.001$
14	1.123	$1.124 \pm 0.001$
15	1.129	$1.130 \pm 0.001$
16	1.135	$1.136 \pm 0.001$
17	1.141	$1.142 \pm 0.001$
18	1.147	$1.148 \pm 0.001$
19	1.153	$1.154 \pm 0.001$
20	1.159	$1.160 \pm 0.001$
21	1.165	$1.166 \pm 0.001$
22	1.171	$1.172 \pm 0.001$
23	1.177	$1.178 \pm 0.001$
24	1.183	$1.184 \pm 0.001$
25	1.189	$1.190 \pm 0.001$
26	1.195	$1.196 \pm 0.001$
27	1.201	$1.202 \pm 0.001$
28	1.207	$1.208 \pm 0.001$
29	1.213	$1.214 \pm 0.001$

The transition energy was found by subtracting the average value of a level from the value of the next level. The values thus obtained are compared with the calculated energy differences for the individual systems and systems are also found. The determination of energy levels was aided after information levels had been measured. At levels above 110 eV, the transition of peaks is much poorer because of a larger background and slight bending of proton groups. The bending of this background may be

seen in Figure 5 to the left of a radius of curvature of 48 cm. Figure 5 presents only that part of the data from the 30-degree exposure which was analyzed. It is noted that in the plot of the peaks in Figure 5, several peaks have half-widths greater than normal or display structure in the peak. Some of the effects noticed may be due to (d,p) reactions of the contaminant elements present, but several peaks display this at all angles of observation. In the latter cases, it is possible that the levels are closely spaced doublets, and the energy given is possibly in error because of this effect. More discussion of the effects of closely spaced doublets will be given in the discussion of the angular distribution curves. The peaks which are suspected of being doublets are numbers 2, 4, 10, 19, and 25. Level number 19 is particularly suspected of being a doublet, since pronounced double structure is shown at several angles.

It is interesting to compare the present results with the work of Foglesong and Foxwell<sup>2</sup> and with Bartholomew and Kinsey<sup>3</sup>. This comparison is presented in Table VI, listing both Q-values and excitation energies. It will be noted that the present work shows some fifty-nine levels in the region of excitation through 3.682 Mev, compared with the twenty-nine levels found by Foglesong and Foxwell. The agreement of the Q-value for the ground level in this investigation with that which is obtained from the work of Bartholomew and Kinsey is excellent. The Q-value of the ground level reported by Foglesong and Foxwell is 23 kev above that of Bartholomew and Kinsey and is 21 kev above that of the present investigation. This difference may have

mean in Figure 2 is the half of a number of numbers of 10 or  
Figure 2 presents only part of the data from the 10-1000000  
points which was analyzed. It is noted that in the case of the points  
in Figure 2, several peaks have been indicated. These are shown by  
display curves in the text. Some of the points indicated are  
due to (1,2) transitions of the mechanism elements involved, but are  
not peaks. They are at all angles of observation. In the latter  
case, it is possible that the levels are closely spaced doublets,  
and the energy levels are possibly in error because of this effect.  
The dimension of the effect of closely spaced doublets will be  
given in the discussion of the angular distribution curves. The  
peaks which are suggested of being doublets are numbers 9, 10, 11,  
and 12. Level number 13 is particularly suggested of being a doublet,  
also. The angular distribution curves are shown at several angles.  
It is interesting to compare the present results in the case  
of hydrogen and deuterium, and also tritium and helium. The  
comparison is presented in Table II, listing both 0-1000000 and 10-  
10000000. It will be noted that the present results show  
fifty-nine levels in the region of excitation between 1.000 and 1.001,  
which are the twenty-nine levels found by Johnson and Powell. The  
agreement of the values for the ground level in this investigation  
with that which is obtained from the work of Johnson and Powell  
is excellent. The values of the ground level reported by Johnson  
and Powell is 13.74 eV for the 10-10000000 and 13.74 eV for  
the 0-10000000 of the present investigation. The difference may have



been caused by an effect noted by Strait et al<sup>26</sup> who observed that at high field strengths the iron of the magnet (the 180-degree annular magnet then used) was close to saturation and that the saturation did apparently cause appreciable errors in the energy measurements. The error in energy was of the order of 0.2 percent at values of B around 14,000 gauss. In the work of Foglesong and Foxwell, this represents an error of about 20 kev for a proton corresponding to the ground level and thus is very close to the observed difference. It should be possible to introduce a correction term in the form of a power series of the emergent particle energy<sup>23</sup>. This correction would be zero at or above the field strength used for calibration with polonium alpha particles. A careful scrutiny of the Q-values of the present work and those of Foglesong and Foxwell shows that there is a correlation between the two which qualitatively agrees with the above argument. The values of Foglesong and Foxwell are generally higher through level number nine and from ten on agree within the limits of error except for number 48. If the difference in the Q-values for the ground level is subtracted from the excitation energy of the excited levels above nine, close agreement is again noticed. It should be noted that the present work covers part of a region which was obscured in the work of Foglesong and Foxwell. No level was found to correspond with a level at Q of 2.659 Mev.



been caused by an error in the value of  $\epsilon$  in the conversion from  
at this level (the 100-1000)  
another magnet (the 100-1000) was done to determine and that the value  
relation did previously cause considerable errors in the energy measure-  
ments. The error in energy was of the order of 0.5 percent at values  
of a second 10,000 gauss. In the work of Fokker and Janssen, this  
remains an error of about 10 per cent for a typical observation in the  
ground level and that is very close to the observed difference. It  
would be possible in principle to determine a correction factor in the 100-1000  
power series of the magnetic field energy. This correction would  
be zero at or above the field strength used for calibration with  
positive alpha particles. A small correction at low values of the  
present work and those of Fokker and Janssen shows that there is a  
correlation between the two which qualitatively agrees with the energy  
argument. The values of Fokker and Janssen are generally lower  
than the level under discussion and this is in agreement with the  
error except for values of  $\epsilon$ . If the difference in the values for  
the ground level is subtracted from the calculated energy of the ac-  
celerated level, the agreement is again improved. It should  
be noted that the present work is based on a typical value of  $\epsilon$   
scattered in the work of Fokker and Janssen. The level was found to  
correspond with a level of 1.127 per.

TABLE VI

Comparison with Previous Results

Peak No	Present work		Foglesong + Foxwell <sup>2</sup>		Bartholomew + Kinsey <sup>3</sup>	
	Q-value (Mev)	Ex*(Mev)	Q-value (Mev)	Ex*(Mev)	Q-value (Mev)	Ex*(Mev)
Ground	5.262	0	5.283	0	5.260**	
1	5.204	0.058	5.223	0.060		
2	4.980	0.282	4.997	0.285		0.285
3	4.830	0.432	4.838	0.445		0.445
4	4.761	0.501	4.770	0.513		0.512
5	4.721	0.541	4.726	0.557		
6	4.650	0.612	4.661	0.622		0.619
7	4.524	0.738				
8	4.479	0.783	4.491	0.792		0.796
9	4.256	1.006	4.271	1.012		1.012
10	4.055	1.207	4.046	1.237		1.236
11	3.925	1.337				
12	3.885	1.377	3.889	1.394		1.376
13	3.815	1.447				
14	3.750	1.512	3.750	1.533		1.520
15	3.624	1.638	3.620	1.663		
16	3.578	1.684				
17	3.555	1.707				
18	3.514	1.748				1.760
19	3.463	1.799	3.458	1.825		
20	3.433	1.829				1.840

[illegible]

<u>Peak</u>	<u>Q-value</u>	<u>Ex*(Mev)</u>	<u>Q-value</u>	<u>Ex*(Mev)</u>	<u>Q-value</u>	<u>Ex*(Mev)</u>
21	3.412	1.850				
22	3.375	1.887				
23	3.339	1.923				
24	3.283	1.979	3.278	2.005		
25	3.231	2.031	3.218	2.065		
26	3.131	2.131	3.129	2.154		2.135
27	3.112	2.150				
28	3.045	2.217				
29	2.988	2.274	2.988	2.295		
30	2.952	2.310				2.307
31	2.914	2.348	2.913	2.370		
32	2.835	2.427				
33	2.671	2.591	2.673	2.610		2.583
			2.659	2.624		
34	2.528	2.734				
35	2.500	2.762	2.497	2.786		
36	2.417	2.845	2.413	2.870		
37	2.378	2.884				
38	2.363	2.899	2.359	2.924		2.90
39	2.320	2.942				
40	2.295	2.967				
41	2.252	3.010	2.245	3.038		
42	2.214	3.048				
43	2.197	3.065				
44	2.176	3.086	2.163	3.120		



Point	Distance	Altitude	Distance	Altitude	Distance	Altitude
11	1.100	1.100				
12	1.100	1.100				
13	1.100	1.100				
14	1.100	1.100				
15	1.100	1.100				
16	1.100	1.100				
17	1.100	1.100				
18	1.100	1.100				
19	1.100	1.100				
20	1.100	1.100				
21	1.100	1.100				
22	1.100	1.100				
23	1.100	1.100				
24	1.100	1.100				
25	1.100	1.100				
26	1.100	1.100				
27	1.100	1.100				
28	1.100	1.100				
29	1.100	1.100				
30	1.100	1.100				
31	1.100	1.100				
32	1.100	1.100				
33	1.100	1.100				
34	1.100	1.100				
35	1.100	1.100				
36	1.100	1.100				
37	1.100	1.100				
38	1.100	1.100				
39	1.100	1.100				
40	1.100	1.100				
41	1.100	1.100				
42	1.100	1.100				
43	1.100	1.100				
44	1.100	1.100				
45	1.100	1.100				
46	1.100	1.100				
47	1.100	1.100				
48	1.100	1.100				
49	1.100	1.100				
50	1.100	1.100				

Peak	Q-value	Ex*(Mev)	Q-value	Ex*(Mev)	Q-value	Ex*(Mev)
45	2.147	3.115	2.145	3.138		3.12
46	2.077	3.185	2.075	3.208		
47	2.047	3.215				
48	2.024	3.238	1.995	3.288		
49	1.978	3.284	1.979	3.304		
50	1.948	3.314				3.30
51	1.923	3.339				
52	1.895	3.367				
53	1.843	3.419				
54	(1.798)	(3.464)				3.46
55	1.764	3.498				
56	1.698	3.564				
57	1.671	3.591				
58	1.609	3.653				
59	1.580	3.682				

\*\* Obtained by subtracting the binding energy of the deuteron from their highest value gamma-ray energy.

The excitation energies reported by Bartholomew and Kinsey are found to be within the limits of error except for level number ten. This seems to confirm further the assumption that the gamma rays observed in their work originated in transitions to the ground state. Within the region obscured in the work of Foglesong and Foxwell, agreement with the 3.30-Mev and 3.46-Mev gamma rays is found to be good.

Peak	0-7500	7500-10000	10000-12500	12500-15000	15000-17500	17500-20000
12	2.117	2.112	2.110	2.118	2.115	2.115
13	2.077	2.102	2.072	2.102	2.102	2.102
14	2.067	2.112				
15	2.051	2.050	2.042	2.050	2.050	2.050
16	1.970	2.000	1.942	2.000	2.000	2.000
17	1.942	2.000				
18	1.942	2.000				
19	1.942	2.000				
20	1.942	2.000				
21	1.980	2.000				
22	2.002	2.002				
23	2.002	2.002				
24	(2.000)	(2.000)				
25	2.002	2.002				
26	1.990	2.000				
27	1.972	2.002				
28	1.962	2.002				
29	1.962	2.002				

\* Estimated by extrapolating the initial energy of the detector from their highest value given by energy.

The estimated energies reported by instruments and lines are found to be within the limits of error except for level number two. This seems to explain further the assumption that the lower rays observed in their work originated in transitions to the ground state. Within the region observed in the case of potassium and cesium, agreement with the 1.20-1.30 eV and 2.16-2.20 eV rays is found to be good.

# STRIPPING THEORY

The theory of deuteron stripping has been dealt with extensively<sup>11-14,27</sup>. Therefore only a brief discussion of the principles will be given. A beam of monoenergetic incident particles can be represented in terms of plane waves, and the angular distribution of the emergent particles can be analyzed in terms of spherical harmonics. These harmonics are characterized by definite values of orbital angular momentum with respect to the nucleus. We can let the angular momentum of the incoming deuteron be  $\overline{\ell}_d$  and its spin be  $\overline{S}_d$ . The angular momentum of the outgoing proton wave will be  $\overline{\ell}_p$  and its spin  $\overline{S}_p$ . The captured neutron will have angular momentum  $\overline{\ell}_n$  and spin  $\overline{S}_n$ . Let the target nucleus have angular momentum  $I$  and the residual nucleus have angular momentum  $J$ .

By conservation of total angular momentum, we find

$$\overline{I} + \overline{\ell}_d + \overline{S}_d = \overline{J} + \overline{\ell}_p + \overline{S}_p$$

Also, the difference in spin and angular momentum of the two nuclei is equal to that of the captured neutron:

$$\overline{J} - \overline{I} = \overline{\ell}_n + \overline{S}_n$$

Combining the above, we find:

$$\overline{\ell}_d - \overline{\ell}_p = \overline{\ell}_n + \overline{S}_n - (\overline{S}_d - \overline{S}_p).$$

NOTE: This discussion concerns only standard stripping theory and does not take into account the recently reported spin-flip stripping<sup>28</sup>.



# APPENDIX

The theory of quantum electrodynamics, as well as its extension to the theory of quantum electrodynamics with spin, is based on the assumption that the interaction of the electromagnetic field with the matter is described by the Lagrangian density

$$\mathcal{L} = \mathcal{L}_0 + \mathcal{L}_1$$

where  $\mathcal{L}_0$  is the Lagrangian density of the free electromagnetic field and  $\mathcal{L}_1$  is the Lagrangian density of the interaction of the electromagnetic field with the matter. The Lagrangian density of the free electromagnetic field is given by

$$\mathcal{L}_0 = -\frac{1}{4} F_{\mu\nu} F^{\mu\nu}$$

where  $F_{\mu\nu} = \partial_\mu A_\nu - \partial_\nu A_\mu$  is the electromagnetic field strength tensor. The Lagrangian density of the interaction of the electromagnetic field with the matter is given by

$$\mathcal{L}_1 = j_\mu A^\mu$$

where  $j_\mu$  is the four-current density. The total Lagrangian density is then given by

$$\mathcal{L} = -\frac{1}{4} F_{\mu\nu} F^{\mu\nu} + j_\mu A^\mu$$

The equations of motion for the electromagnetic field are obtained by varying the action with respect to the vector potential  $A_\mu$ . This yields the inhomogeneous Maxwell equations

$$\partial_\mu F^{\mu\nu} = j^\nu$$

where  $j^\nu$  is the four-current density. The homogeneous Maxwell equations are obtained by varying the action with respect to the field strength tensor  $F_{\mu\nu}$ . This yields the homogeneous Maxwell equations

$$\partial_\mu F_{\nu\rho} + \partial_\nu F_{\rho\mu} + \partial_\rho F_{\mu\nu} = 0$$

The solution of the inhomogeneous Maxwell equations is given by the retarded potential

$$A_\mu(x) = \int d^4x' G_{\mu\nu}(x-x') j^\nu(x')$$

where  $G_{\mu\nu}(x-x')$  is the retarded Green's function. The retarded Green's function is given by

$$G_{\mu\nu}(x-x') = \delta_{\mu\nu} D(x-x')$$

where  $D(x-x')$  is the retarded scalar Green's function. The retarded scalar Green's function is given by

$$D(x-x') = \int \frac{d^4k}{(2\pi)^4} \frac{e^{-ik \cdot (x-x')}}{k^2 + i0}$$

where  $k \cdot (x-x') = k_0(x_0-x'_0) - \mathbf{k} \cdot (\mathbf{x}-\mathbf{x}')$  is the four-vector product. The retarded scalar Green's function is a function of the invariant interval  $(x-x')^2$  and is given by

$$D(x-x') = \frac{1}{4\pi} \delta(x-x')$$

where  $\delta(x-x')$  is the Dirac delta function. The retarded scalar Green's function is a function of the invariant interval  $(x-x')^2$  and is given by

$$D(x-x') = \frac{1}{4\pi} \delta(x-x')$$

Q.E.D.

By comparison of the two Lagrangians, we find

$$\mathcal{L}_1 = \mathcal{L}_2 + \mathcal{L}_3 + \mathcal{L}_4 + \mathcal{L}_5 + \mathcal{L}_6$$

Also, the difference in the two Lagrangians is given by

which is equal to the difference between

$$\mathcal{L}_1 - \mathcal{L}_2 = \mathcal{L}_3 + \mathcal{L}_4$$

Comparing the above, we find

$$\mathcal{L}_1 - \mathcal{L}_2 = \mathcal{L}_3 + \mathcal{L}_4 = \mathcal{L}_5 + \mathcal{L}_6$$

NOTE: This discussion concerns only the case of a free field and does

not take into account the possible effects of the field on the field.

Since  $\overline{S}_d = \overline{S}_p + \overline{S}_n$ , and the spin of the proton does not change because it is not interacting with the nucleus, we find

$$\overline{l}_d - \overline{l}_p = \overline{l}_n + \Delta \overline{S}_n .$$

Thus, the values of  $\overline{l}_d - \overline{l}_p$  are restricted by the conditions on  $\overline{l}_n$ . This gives rise to a description of the angular distribution of the emergent protons as a function of discrete values of  $\overline{l}_n$ , orbital angular momentum, with which the neutron enters the nucleus. The discrete values of  $\overline{l}_n$  are characterized by varying values of angle at which there is a maximum. Our calculations were based on the work of Friedman and Tobocman<sup>14</sup>, which is derived on the basis of four simplifying assumptions:

1. The coulomb interaction can be ignored;
2. The protons have no interaction with the target nucleus;
3. The deuteron fragments can be treated as free particles;
4. The deuteron wave function can be approximated by a plane wave.

The differential cross section for a (d,p) stripping process leading to a specific bound level of the residual nucleus in the center-of-mass coordinate system may be expressed in the following elementary form for convenience in calculation:<sup>15</sup>

where  $\bar{E}_i = \bar{E}_i + \bar{E}_i$  and the sign of the system does not change

because it is not interacting with the system, so that

$$\bar{E}_i = \bar{E}_i + \bar{E}_i$$

Thus, the value of  $\bar{E}_i - \bar{E}_i$  are constant of the motion in  $\bar{E}_i$ .

This gives rise to a description of the angular distribution of the

emergent photons as a function of discrete values of  $\bar{E}_i$ , which

angular momentum, with which the system enters the medium. The

discrete values of  $\bar{E}_i$  are characterized by varying values of angle

at which there is a maximum. Our calculations were based on the

work of Fiksdal and Johnson<sup>12</sup>, which is derived on the basis of

four simplifying assumptions:

1. The optical interaction can be ignored;
2. The photon has no interaction with the  
medium;
3. The electron frequency can be treated as  
free particles;
4. The electron wave function can be approximated  
by a plane wave.

The differential cross section has a  $\langle \delta^2 \rangle$  averaging process

leading to a specific point level of the residual nucleus in the

center-of-mass coordinate system may be expressed in the following

approximate form for conversion in calculation<sup>12</sup>

$$\sigma(\theta_{\text{CMS}}) = (2J + 1) C D \sum_{\ell} \gamma_{\ell} B_{\ell}.$$

C is a constant for the level, calculated from the masses and energies of the particles in the reaction, the nuclear radius, and the angular momentum of the target nucleus. D is the deuteron factor which is determined from the approximate internal wave function of the deuteron. This is a function of angle and expresses the probability of the proton, neutron, and incident deuteron wave functions matching the correct internal wave function in the deuteron.  $\gamma_{\ell}$  is the partial reduced width for each value of  $\ell_n$  and its empirical determination will be discussed later. Finally,  $B_{\ell}$  represents a term composed of spherical Bessel and Hankel functions.



$$\pi(\frac{1}{2}, \frac{1}{2}) = (2\pi + 1) \sum_{k=0}^{\infty} \frac{1}{k!} \pi_k$$

0 is a constant for the level, calculated from the mean and variance of the population in the analysis, the analysis table, and the analysis variance of the sample analysis. 0 is the deviation factor which is determined from the asymptotic interval from the limit of the deviation. This is a function of sample size and represents the probability of the error, deviation, and analysis variance with function setting the error interval was fixed in the deviation. It is the partial product with the value of 0 and the constant. The partial product will be discussed later. Finally, 0 represents a term composed of spectral, partial and global functions.

## ANGULAR DISTRIBUTIONS

The problem of finding the cross section for the stripping reaction was attacked by use of the alpha-particle thickness gauge mentioned previously to measure the thickness of cobalt on the Formvar film. Measurements were made before and after the cobalt was evaporated onto the Formvar. The difference in the two measurements gave the thickness of the cobalt in terms of the equivalent stopping power of air, in mils, for the alpha particles of polonium. The energy loss per centimeter of path for a substance is found from<sup>24</sup>

$$\frac{dE}{dx} = \frac{4\pi e^4 z^2}{mV^2} NB,$$

where  $V$  = velocity of incident particle

$N$  = number of atoms in target per  $\text{cm}^3$

$z$  = charge of incident particle

$m$  = mass of electron

$B$ , the "atomic stopping number," is found from

$$B = Z \ln \frac{2mV^2}{I},$$

where  $Z$  = charge of target, and

$I$  = ionization potential of target.

The energy loss of the alpha particles is the same for each medium. The energy loss per centimeter of path is a constant for each medium; hence a simple constant ratio relating the energy loss in cobalt to that in air can be formed. Since the thickness of the cobalt

# ANALYSIS OF THE PROBLEM

The problem of finding the wave number for the standing wave-  
tion was attacked by use of the eigenvalue method. The eigenvalue  
problem is solved by the method of separation of variables. The  
eigenvalue problem is solved by the method of separation of variables.  
The eigenvalue problem is solved by the method of separation of variables.  
The eigenvalue problem is solved by the method of separation of variables.  
The eigenvalue problem is solved by the method of separation of variables.  
The eigenvalue problem is solved by the method of separation of variables.  
The eigenvalue problem is solved by the method of separation of variables.  
The eigenvalue problem is solved by the method of separation of variables.

$$\frac{d^2 \psi}{dx^2} + k^2 \psi = 0$$

where  $\psi$  = velocity of incident wave

$k$  = wave number of incident wave

$\psi$  = change of incident wave

$\psi$  = wave of incident

$\psi$ , the second standing wave, is found from

$$\frac{d^2 \psi}{dx^2} + k^2 \psi = 0$$

where  $\psi$  = change of wave, and

$\psi$  = reflection potential of wave.

The energy loss of the wave is found by the method of

method. The energy loss per unit length of wave is a constant for

each medium; hence a single constant value for energy loss in

media is that in air and water. The energy loss of the wave

in mils of air equivalent is known, the thickness of cobalt can be determined by multiplying the ratio of the energy losses per centimeter of path times the air equivalent thickness. For an air equivalent thickness of 13 mils, this gave about  $5.0 \times 10^{-6}$  cm for the thickness of cobalt.

The half-width of a cobalt elastically scattered deuteron peak was computed from the Q-equation using the previously determined thickness of cobalt. A comparison with the observed half-width of the deuteron elastic peak at 90 degrees showed that the cobalt layer contributed 60 to 70 percent to the observed half-width. This seems to be reasonable, taking into account the angle between the target and the incident deuteron beam.

The approximate differential cross section for the (d,p) reaction is determined from the following expression:

$$\frac{d\sigma(d,p)}{d\Omega} = \frac{N_p}{N_{Co} dx IA \Omega} \frac{\text{cm}^2}{\text{Steradian}}$$

where  $N_p$  = number of proton tracks observed in the (d,p) peak

$N_{Co}$  = number of atoms of cobalt per cubic centimeter of target

$dx$  = the effective thickness of the cobalt layer in centimeters

$IA$  = the number of incident deuterons measured by the current integrator

$\Omega$  = the solid angle subtended by the magnetic spectrograph at a distance of 52 centimeters along the plate, in steradians.



in air of equivalent thickness is known, the thickness of deposit can be determined by multiplying the ratio of the energy losses per unit distance of path in air and in equivalent thickness. For an equivalent thickness of 1.5 mls, this ratio would be  $2.0 \times 10^{-6}$  for the thickness of deposit.

The half-width of a deposit electrically measured section was was computed from the deposition ratio previously determined thickness of deposit. A comparison with the observed half-width of the detector electric peak at 90 degrees showed that the deposit layer contributed 60 to 70 percent to the observed half-width. This seems to be reasonable, taking into account the angle between the target and the incident deuteron beam.

The approximate differential cross section for the (d,p) reaction is determined from the following expression:

$$\frac{d\sigma}{d\Omega} = \frac{I_A}{I_D} \frac{dN}{d\Omega} \frac{1}{N_D} \frac{1}{N_T} \frac{1}{N_{Co}}$$

where  $I_D$  = number of proton tracks observed in the (d,p) count  
 $I_A$  = number of alpha or alpha particles observed in target  
 $d\sigma$  = the effective thickness of the deposit layer in units of  
 $I_A$  = the number of incident deuterons measured by the current  
 $d\Omega$  = the solid angle subtended by the magnetic spectrograph at  
 a distance of 50 centimeters from the target, in steradians.

It was found advantageous to convert the constant term in the above expression into a conversion term equal to

$$0.02 \frac{\text{millibarns/steradian}}{\text{proton track}} .$$

This term, multiplied by the number of proton tracks observed, gives the value of cross section used in the results.

A comparison of observed elastic scattering at 90 degrees to the calculated Rutherford scattering was made. The differential elastic cross section was determined from the above expression, using the number of deuterons observed and was found to be about

25  $\frac{\text{nb}}{\text{steradian}}$  at 90 degrees. The Rutherford cross section was computed from the following expression<sup>23</sup>

$$\frac{d\sigma_R}{d\Omega} = 5.2 \times 10^{-27} \left( \frac{Z_I Z_T}{E_I} \right)^2 \left[ 1 - \left( \frac{M_I}{M_T} \right)^2 \right]^{\frac{1}{2}} \frac{\text{cm}^2}{\text{steradian}}$$

where I and T refer to the incident and target nuclei. This gives a value of 109 millibarns per steradian at 90 degrees, about four times the observed elastic scattering.

In addition, a correction was made to all cross sections thus obtained and to each angle in order to convert from the laboratory system into the center-of-mass system for comparison with the theory. This was facilitated by figures in Enge and Graue<sup>15</sup> and amounted to a small increase in each angle and a small reduction in cross sections below 90 degrees.

It was found experimentally that the observed rate in the above reaction is a composite law equal to

$$\frac{0.05}{\text{mole liter}} \frac{\text{mole liter}}{\text{mole liter}}$$

This law, indicated by the nature of the reaction observed, gives the value of the reaction rate in the reaction.

A comparison of observed kinetic results at 30 degrees

the calculated values for the reaction was made. The difference

between the observed and calculated values was about 10 percent, being

the number of observed values and was found to be about

25 percent at 30 degrees. The observed reaction rate was

found from the following equation

$$\frac{S_{\text{obs}}}{S_{\text{calculated}}} = \frac{1}{2} \left[ 1 + \left( \frac{S_{\text{obs}}}{S_{\text{calculated}}} \right)^2 \right]^{1/2}$$

where  $S$  and  $T$  refer to the initial and final states. This gives a

value of the equilibrium constant of 30 degrees, about four times

the observed kinetic results.

In addition, a correction was made to all cross section data

obtained and to each value in order to correct from the laboratory

values into the center-of-mass system for comparison with the theory.

This was facilitated by knowing in each case the  $Q$  value and the

masses of the particles, and a small correction to cross section

below 30 degrees.



The solid angle on the photographic plate, as mentioned in Section II, is approximately  $3.4 \times 10^{-4}$  steradians at a plate distance of 52 centimeters. The relative solid angle curve of reference 17 can be used to correct for variation in solid angle as a function of distance along the plate. The data points and curves of angular distributions presented later in this section were not so corrected, but the correction term is listed in Table VII. This correction varies from 1.155 to 0.875 and has been used to obtain all the results reported in Table VII.

The paper by Enge and Graue<sup>15</sup> presents the method of numerical calculations in detail with the aid of an example. The same procedure was used in the present work with the results for the twenty-six levels being shown in Figure 6 through 31.

Prior to fitting the theoretical curve to the experimental points which represent the angular distribution of the cross section, an arbitrary isotropic background cross section was subtracted from the value at each angle<sup>27</sup>. The amount was determined by inspection of each level distribution at the angle where the curve is most nearly zero (that is, 90 to 110 degrees). The background cross sections for all reported levels are given in Table VII and are shown in Figures 32 and 33. Twenty-three levels with small cross sections could not be assigned a value of  $\ell_n$  for one of two reasons. Some of these display an isotropic distribution which may be caused by compound-nucleus formation or by a stripping reaction with an  $\ell_n > 3$



The solid angle of the anisotropic element was measured in Section II, is approximately  $2.1 \times 10^{-4}$  steradians at a distance of 25 centimeters. The relative solid angle curve of reference is not be used to correct for variation in solid angle as a function of distance along the plate. The data points and curves of angular distribution presented later in this section were not so corrected, but the correction given is listed in Table VII. This correction varies from 1.1% to 0.8% and has been used to obtain all the results reported in Table VII.

The paper by Bate and Brown<sup>12</sup> presents the method of numerical calculations in detail with the aid of an example. The same procedure was used in the present work with the results for the twenty-five levels being shown in Figure 8 through 31.

Prior to fitting the theoretical curve to the experimental points which represent the angular distribution of the cross section, an arbitrary isotropic background cross section was subtracted from the value at each angle. The amount was determined by inspection of each level distribution at the angle where the curve is most nearly zero (about  $90$  to  $110$  degrees). The background cross section for all reported levels are given in Table VII and are shown in Figure 32 and 33. Twenty-three levels with small cross sections could not be assigned a value of  $\pm$  for one of two reasons. Some of these display an isotropic distribution which may be caused by component-matrix correction or by a scattering reaction with an  $\alpha$  particle.

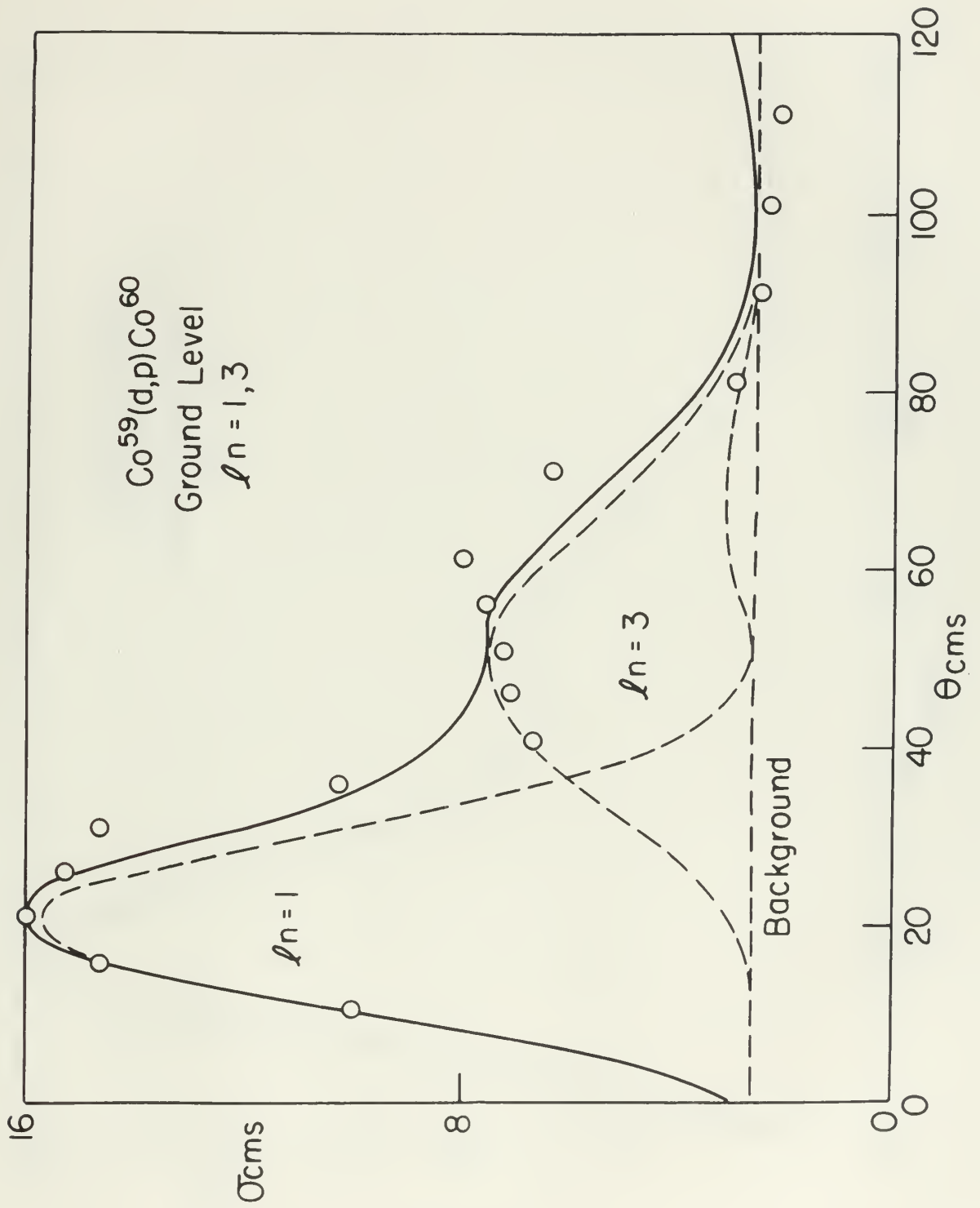


Figure 6



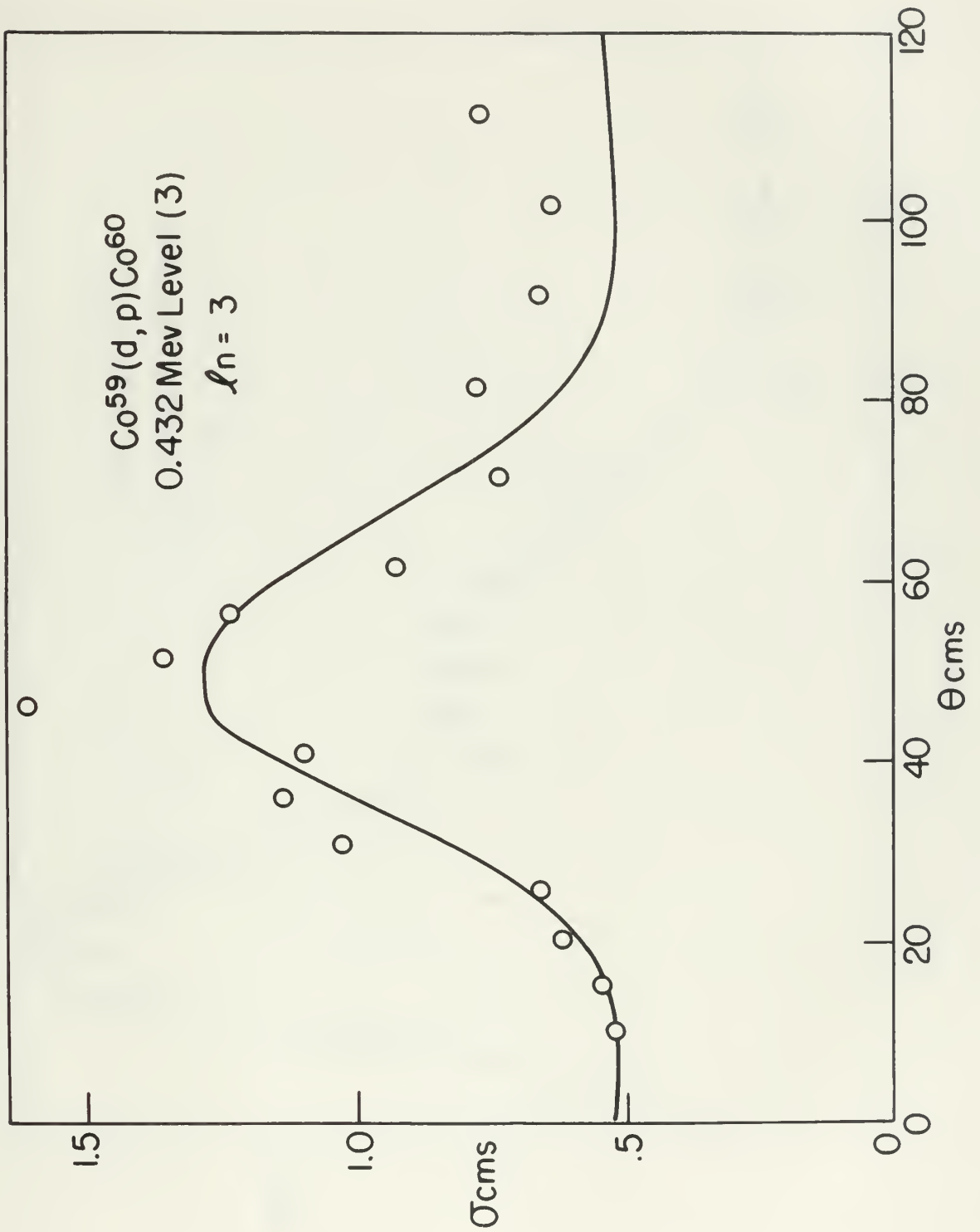


Figure 9





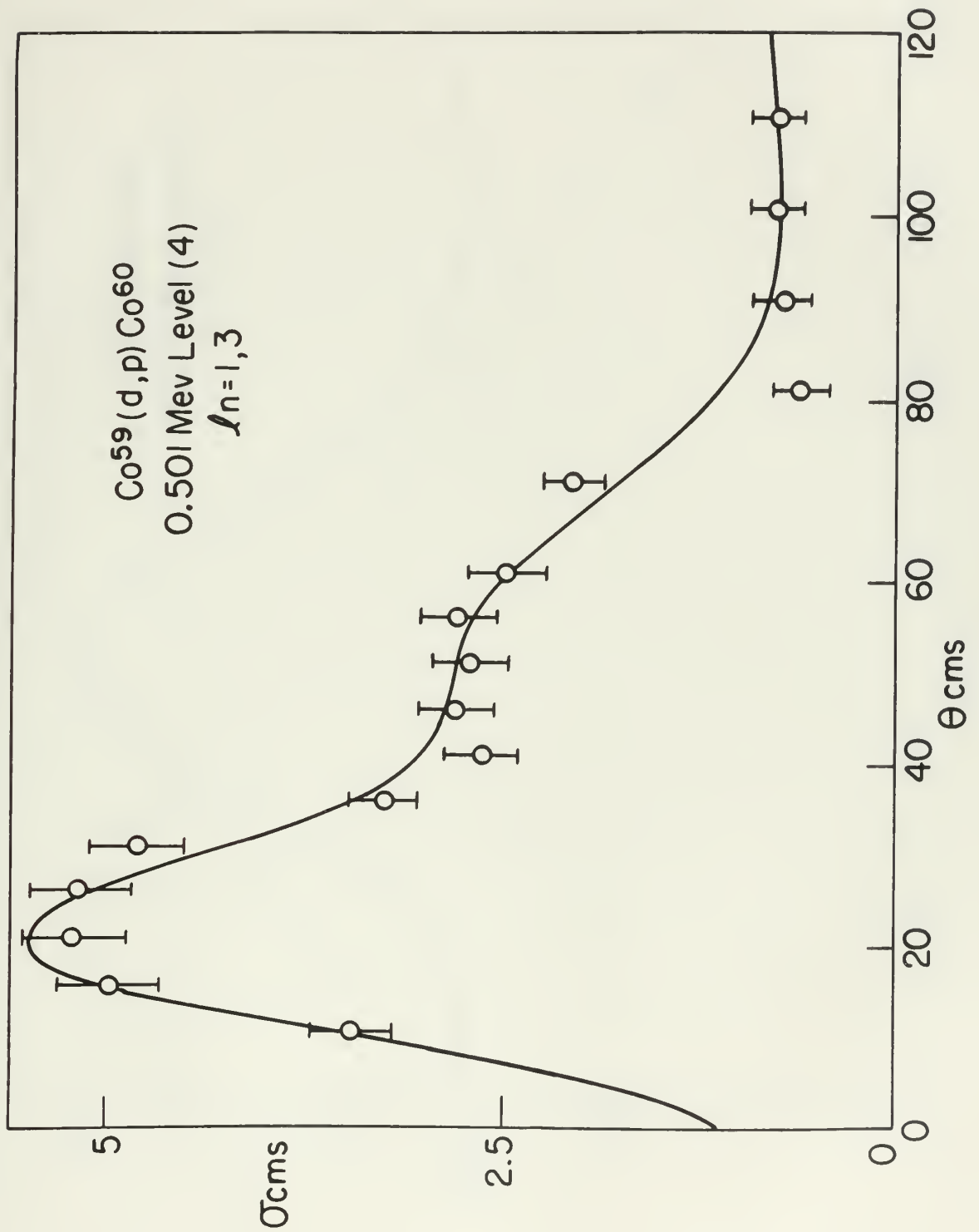


Figure 10



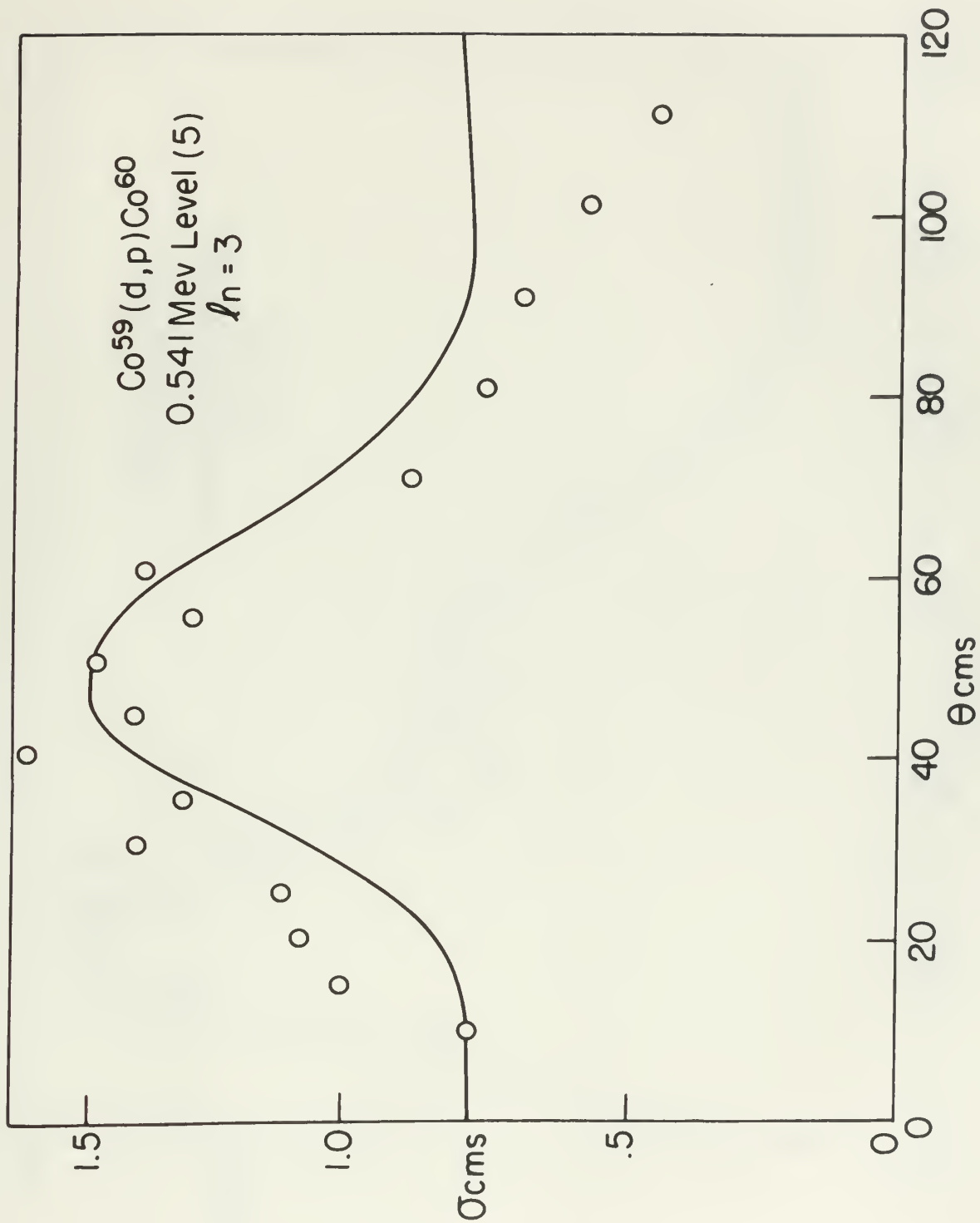


Figure 11





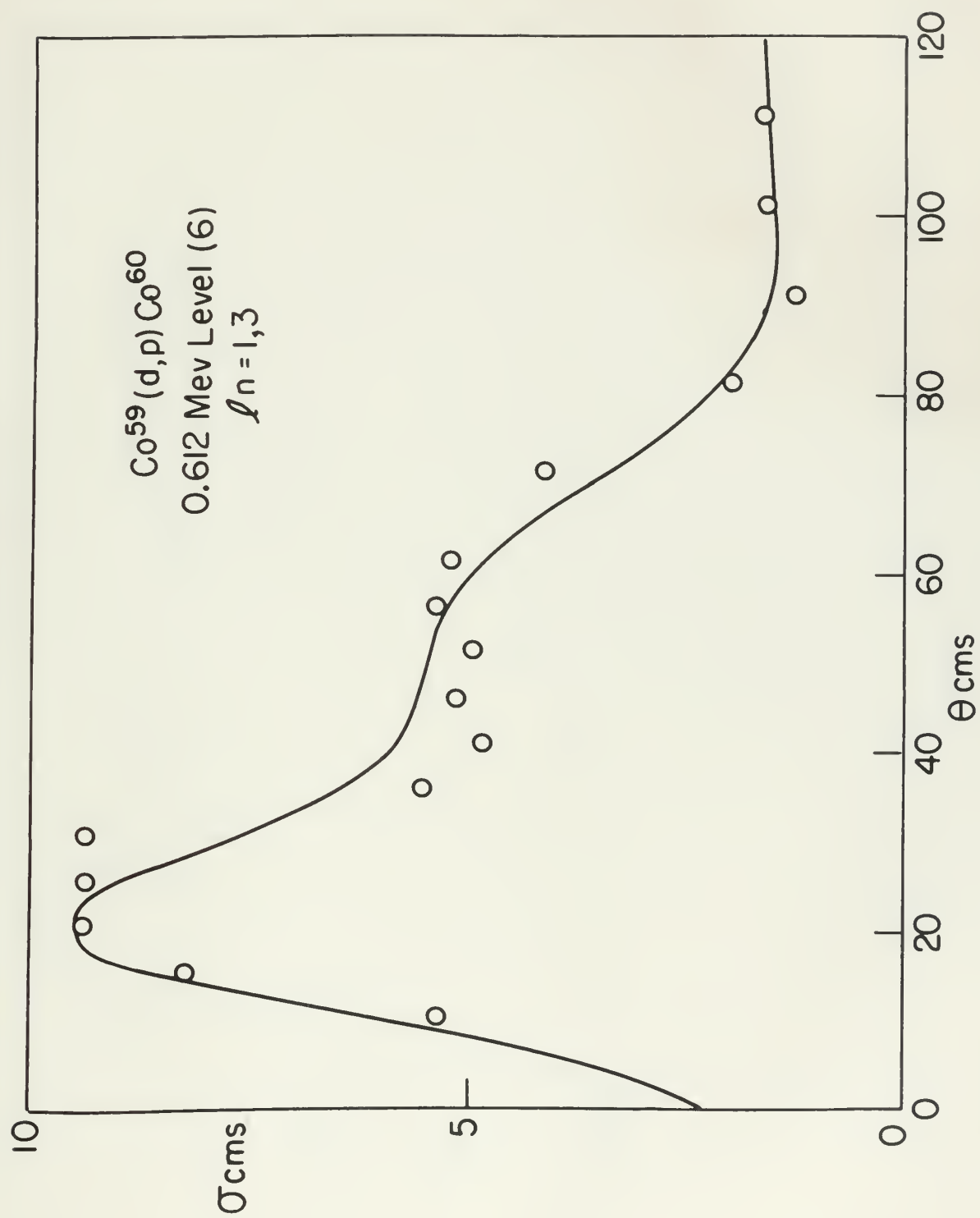


Figure 12



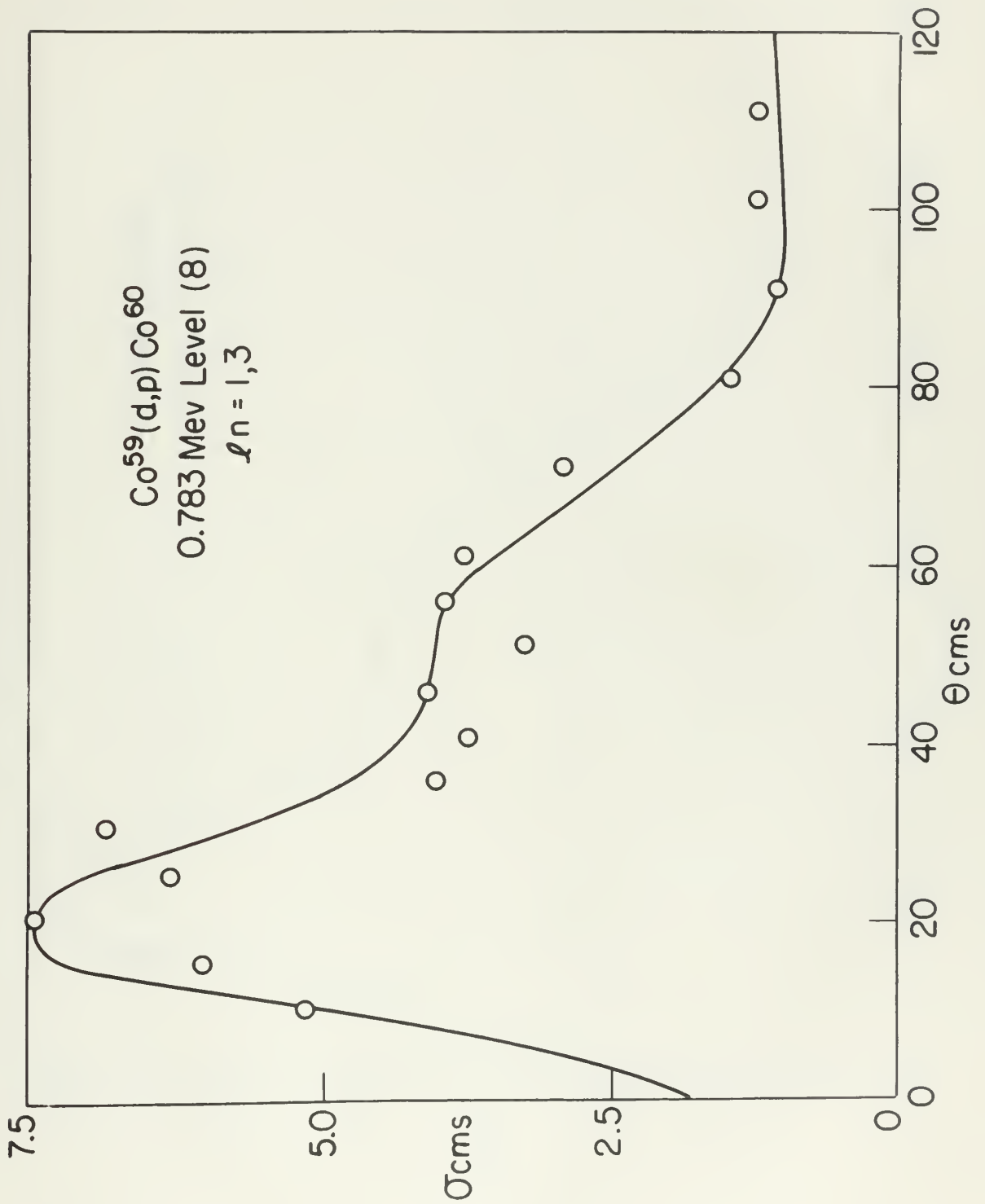


Figure 13





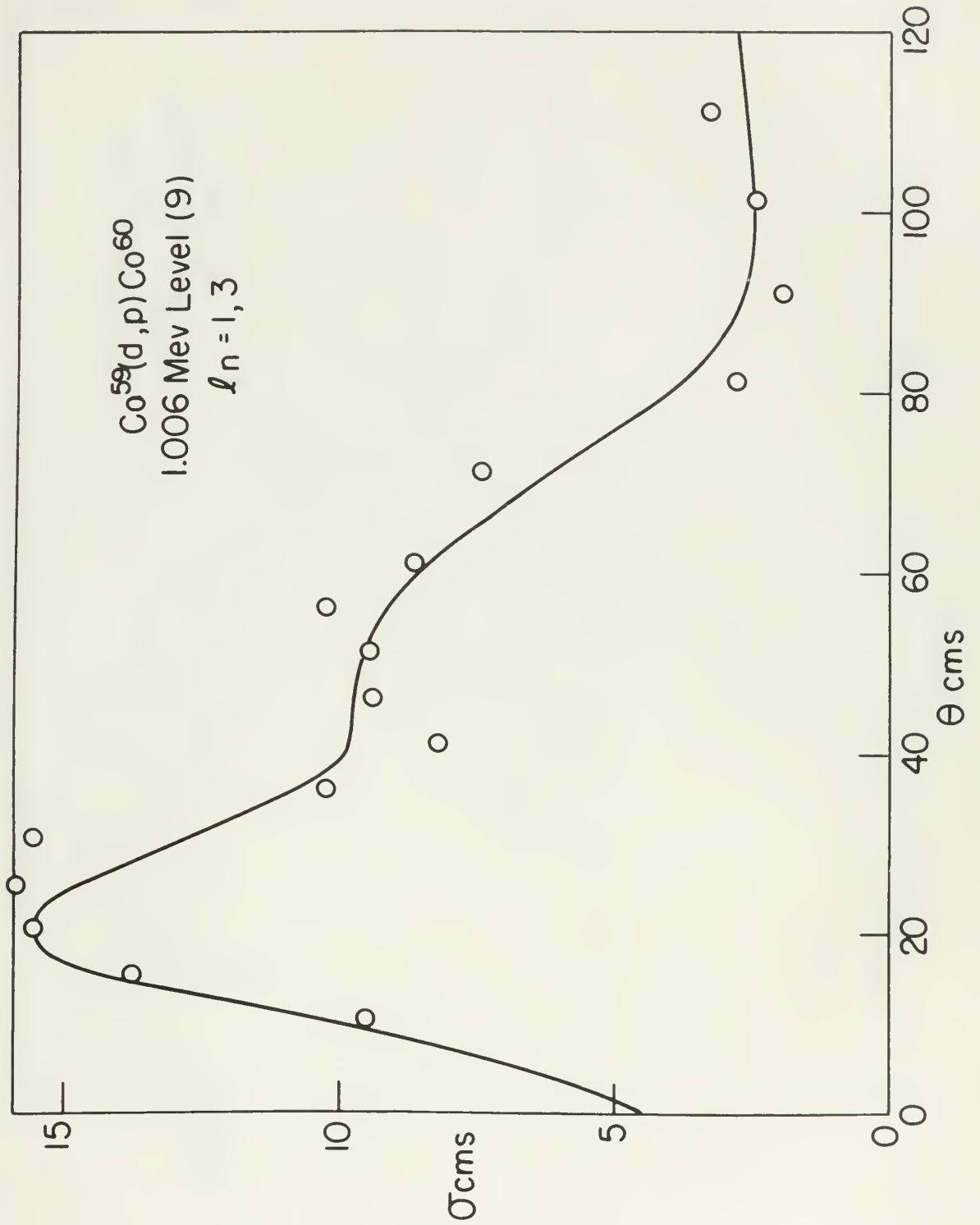


Figure 14



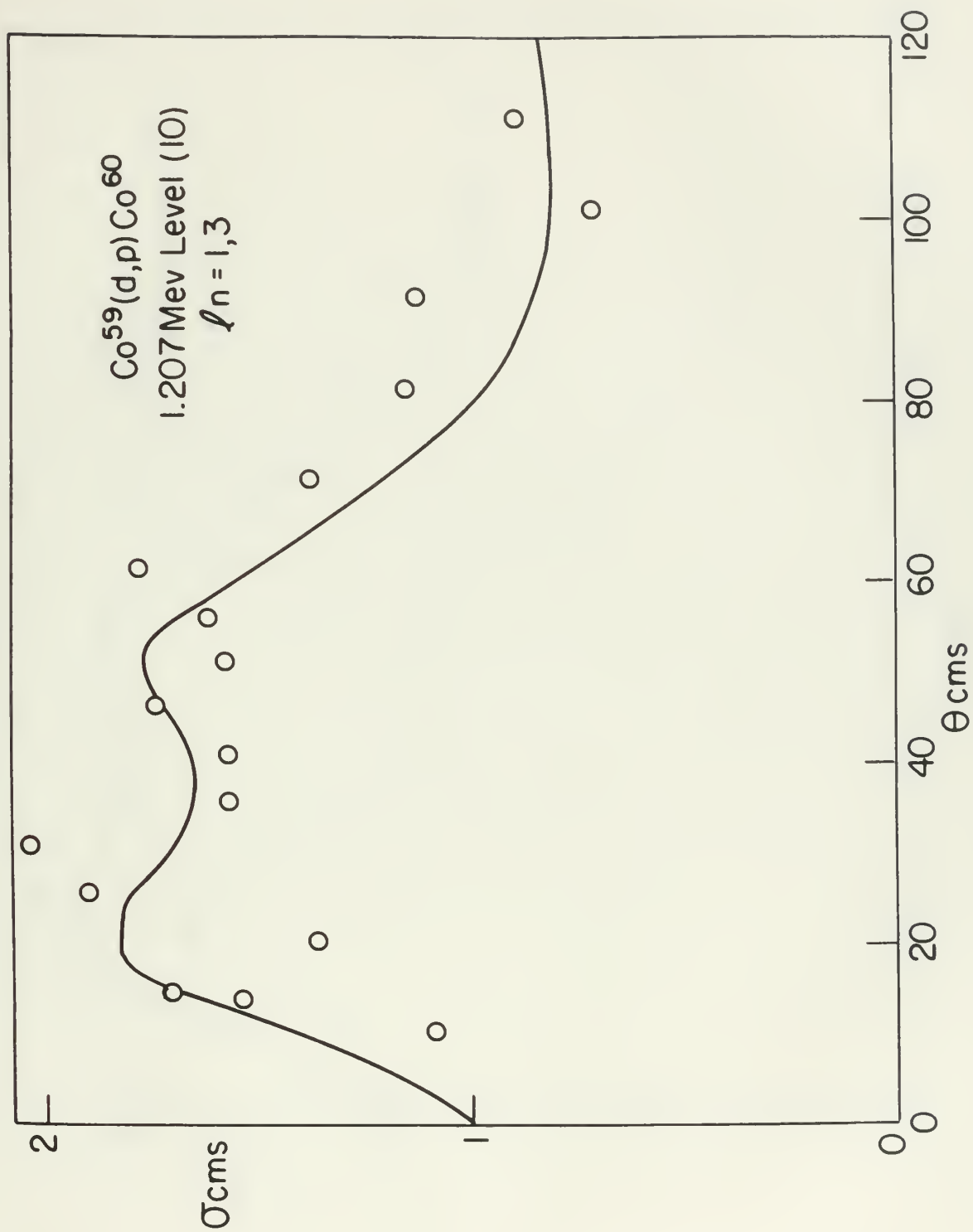


Figure 15





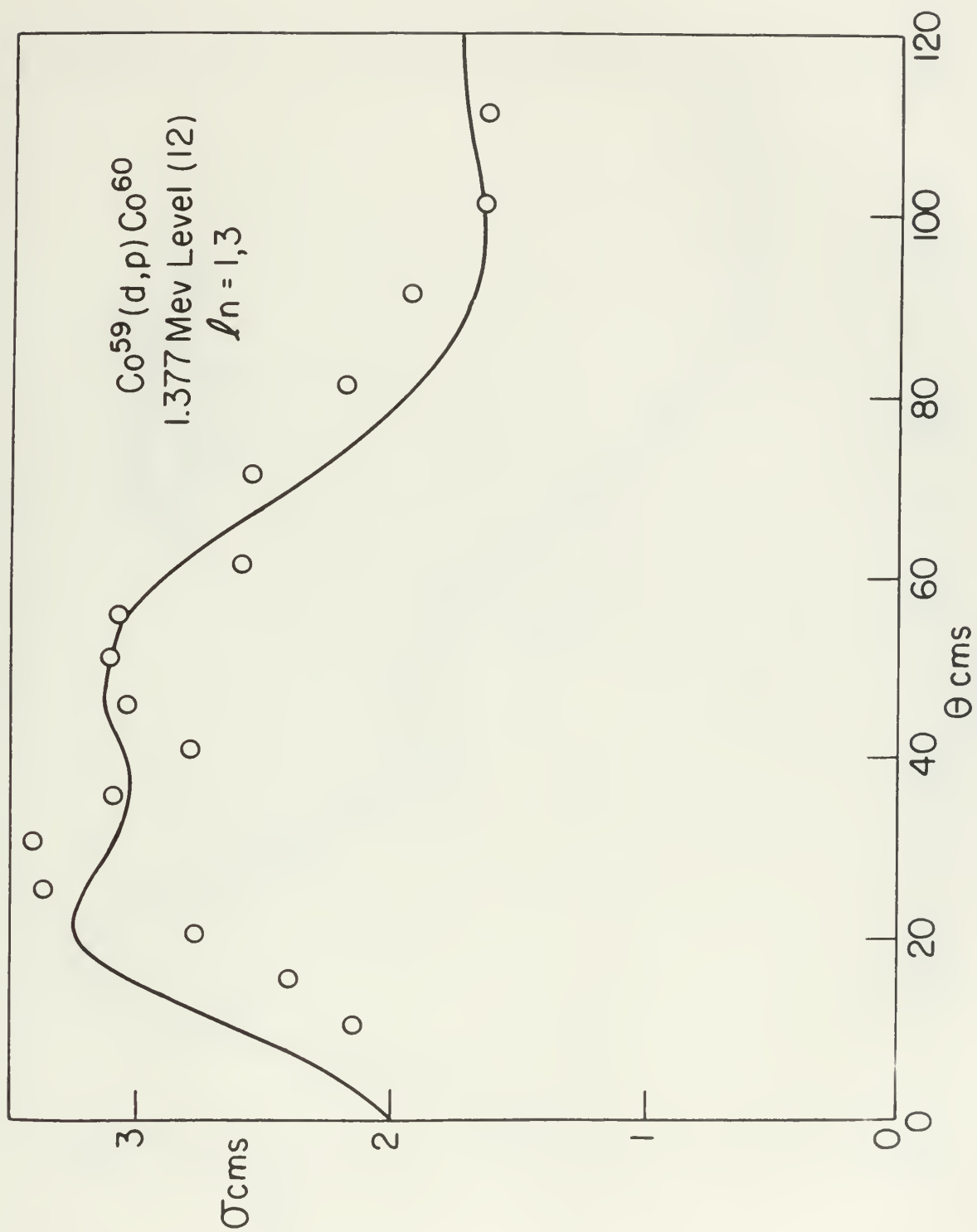


Figure 16



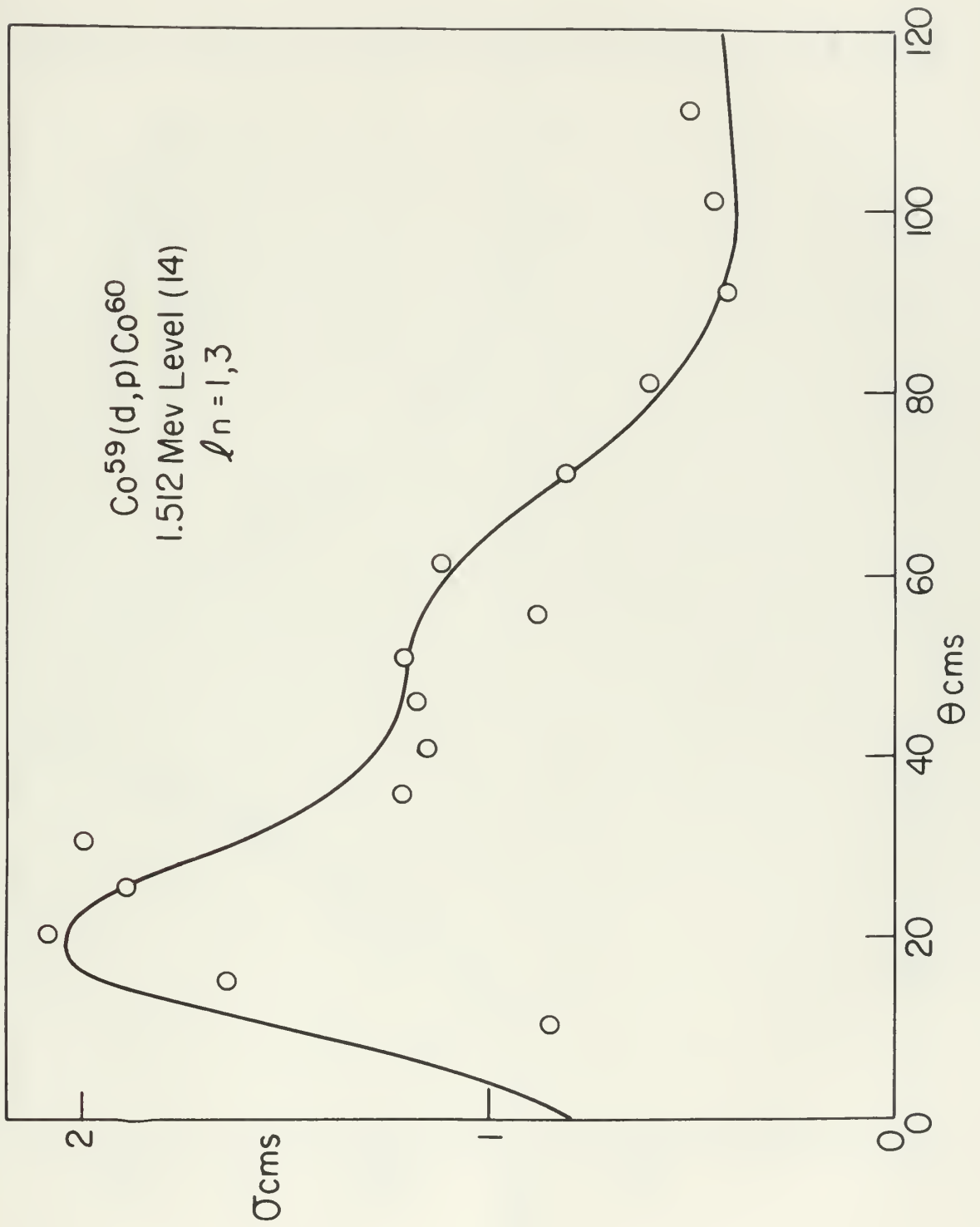


Figure 17





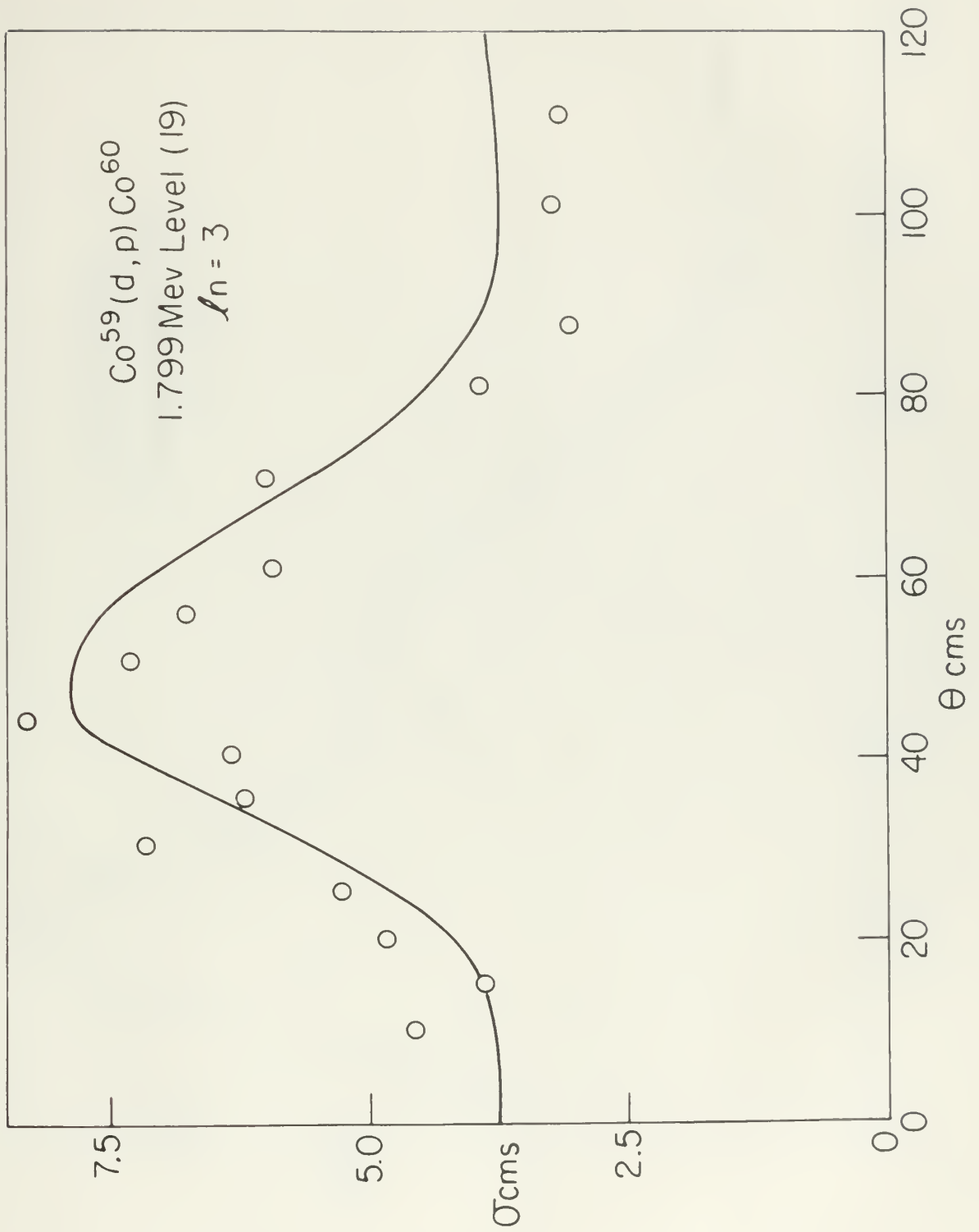


Figure 18



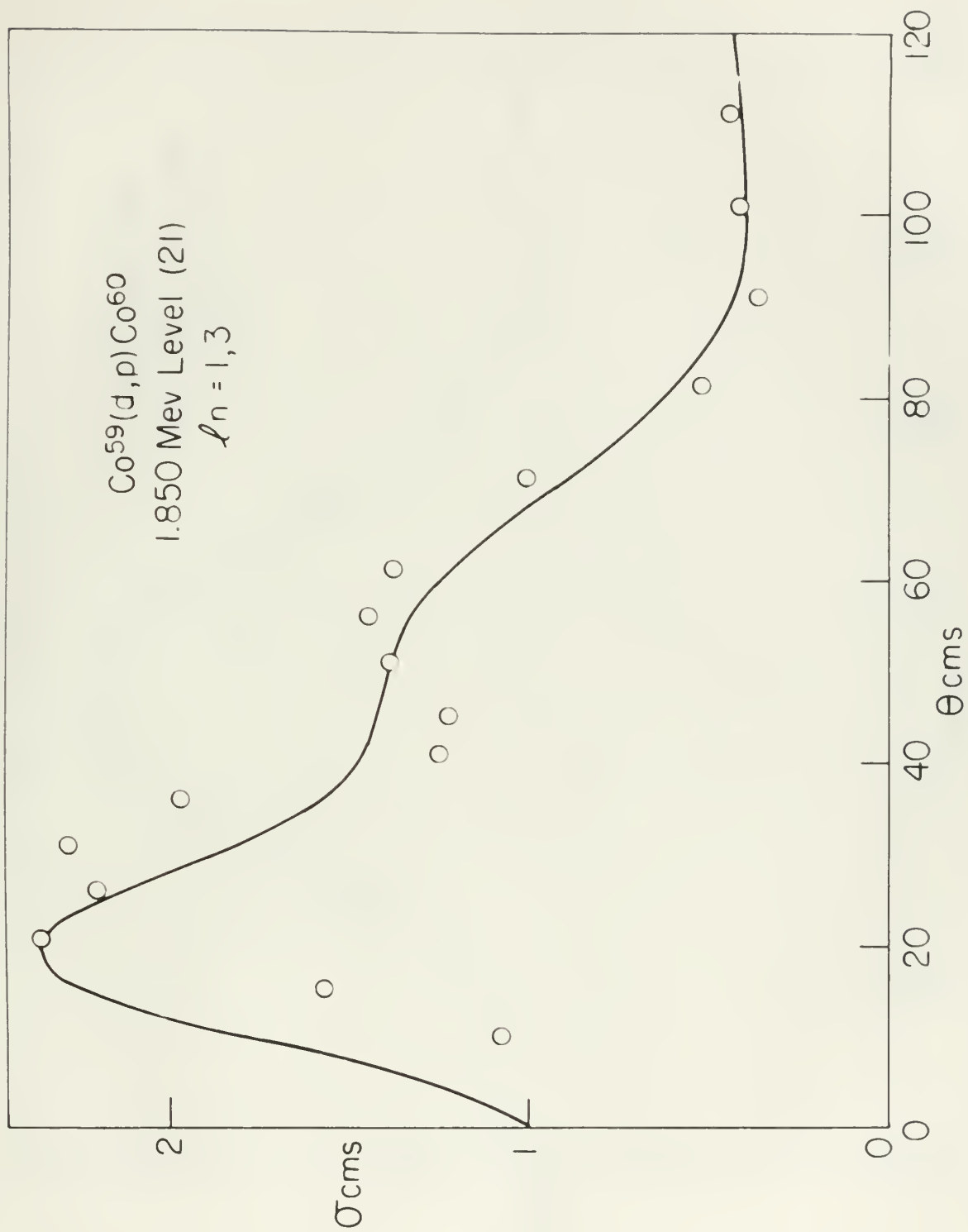


Figure 19





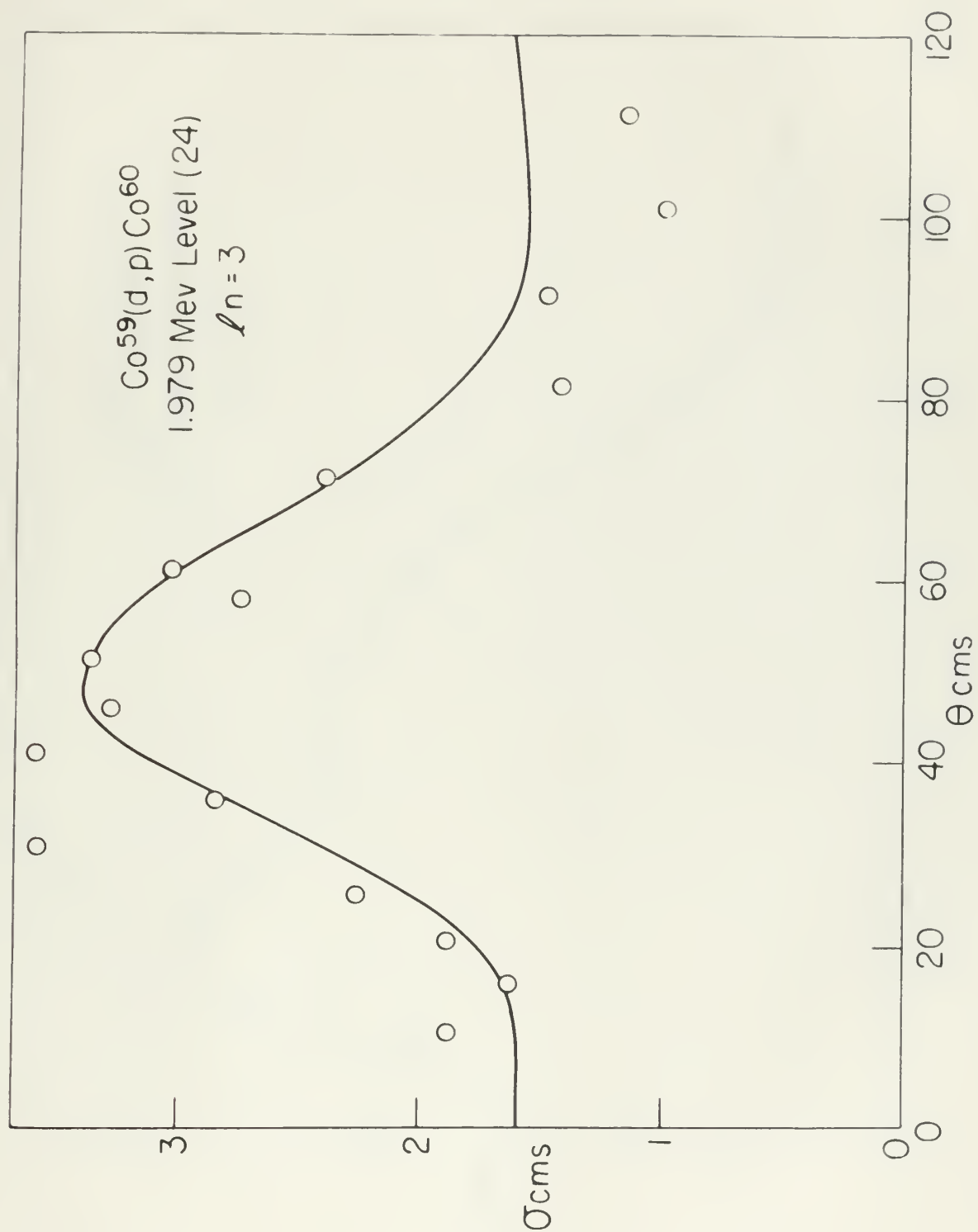


Figure 20



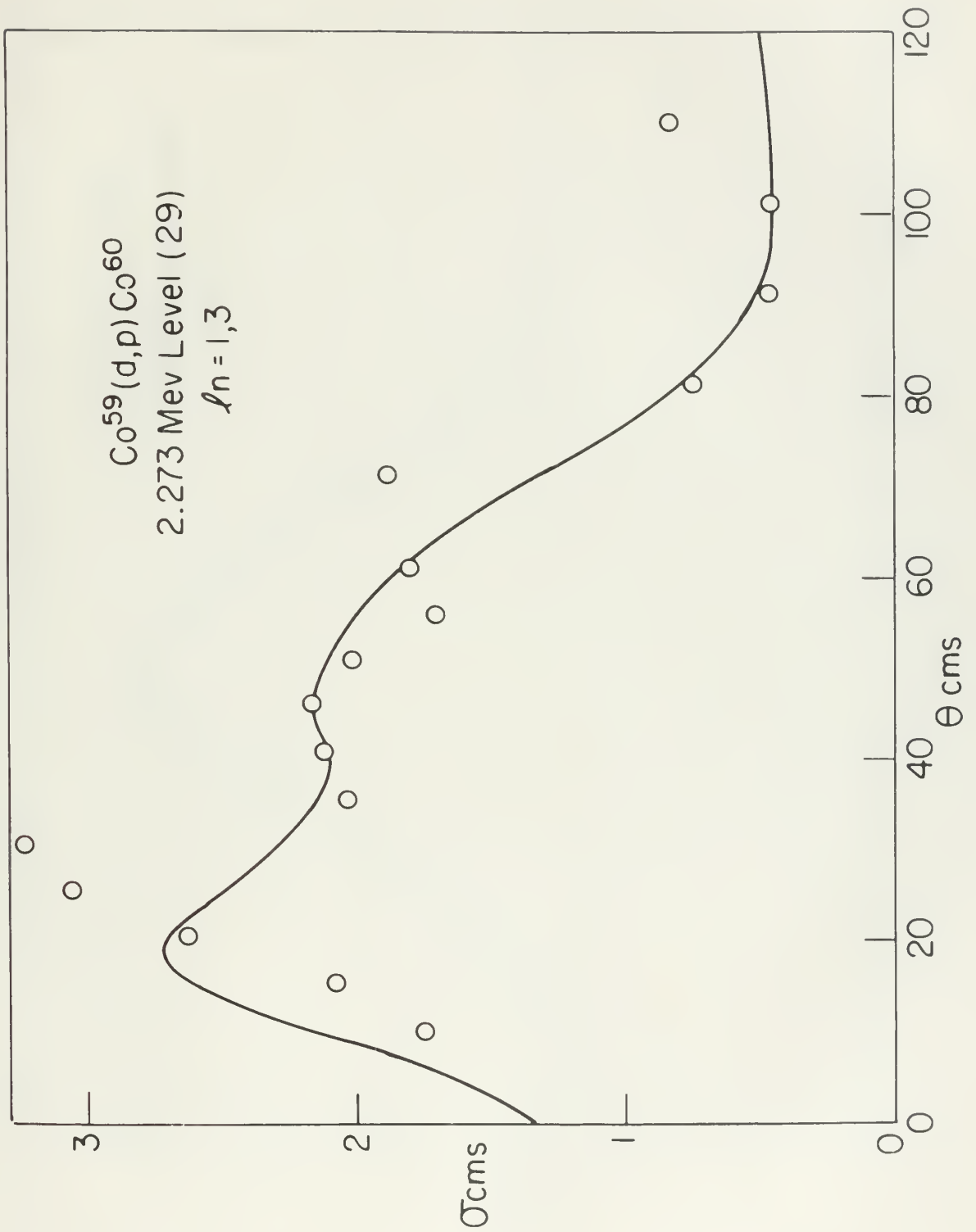


Figure 21



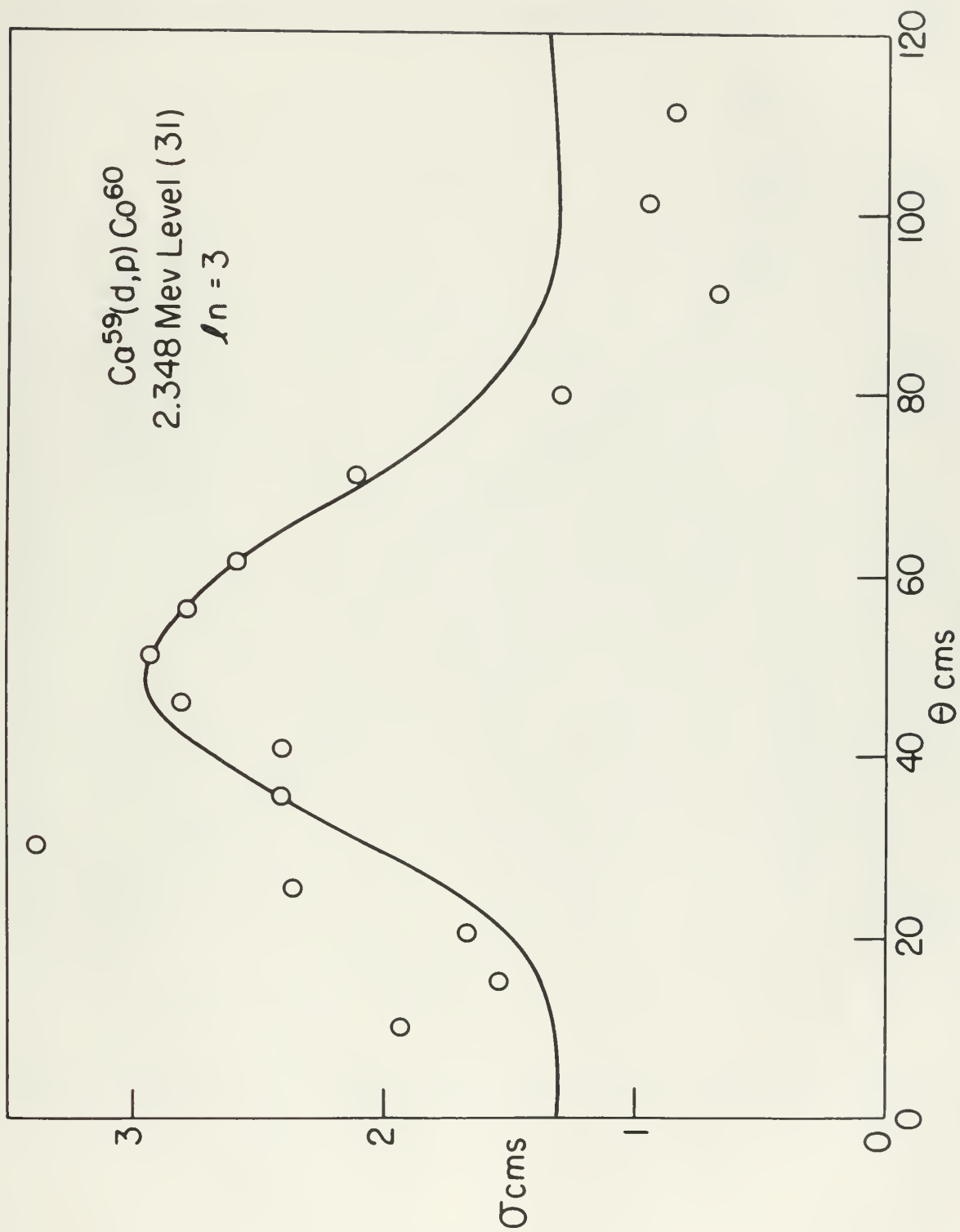


Figure 22





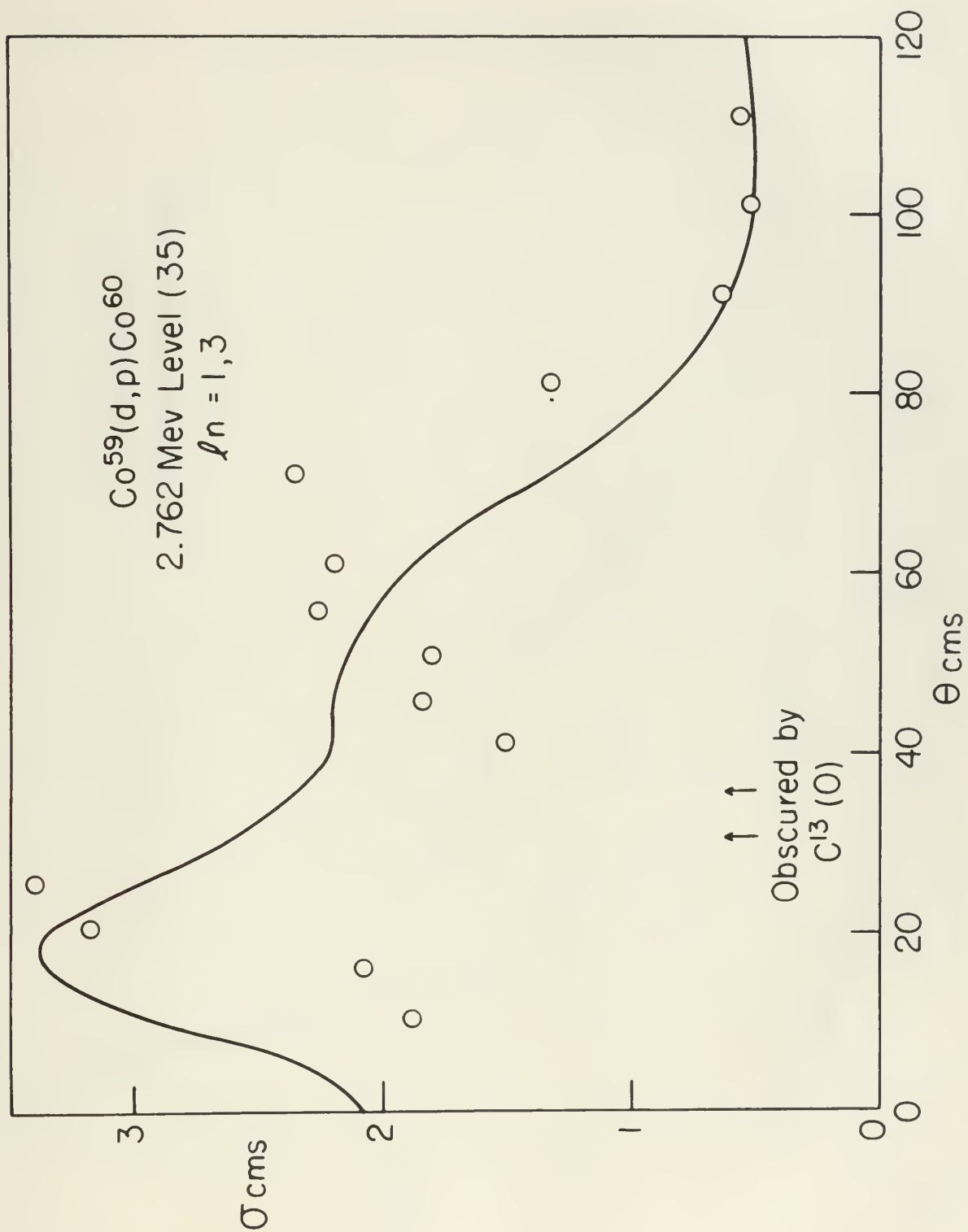


Figure 23



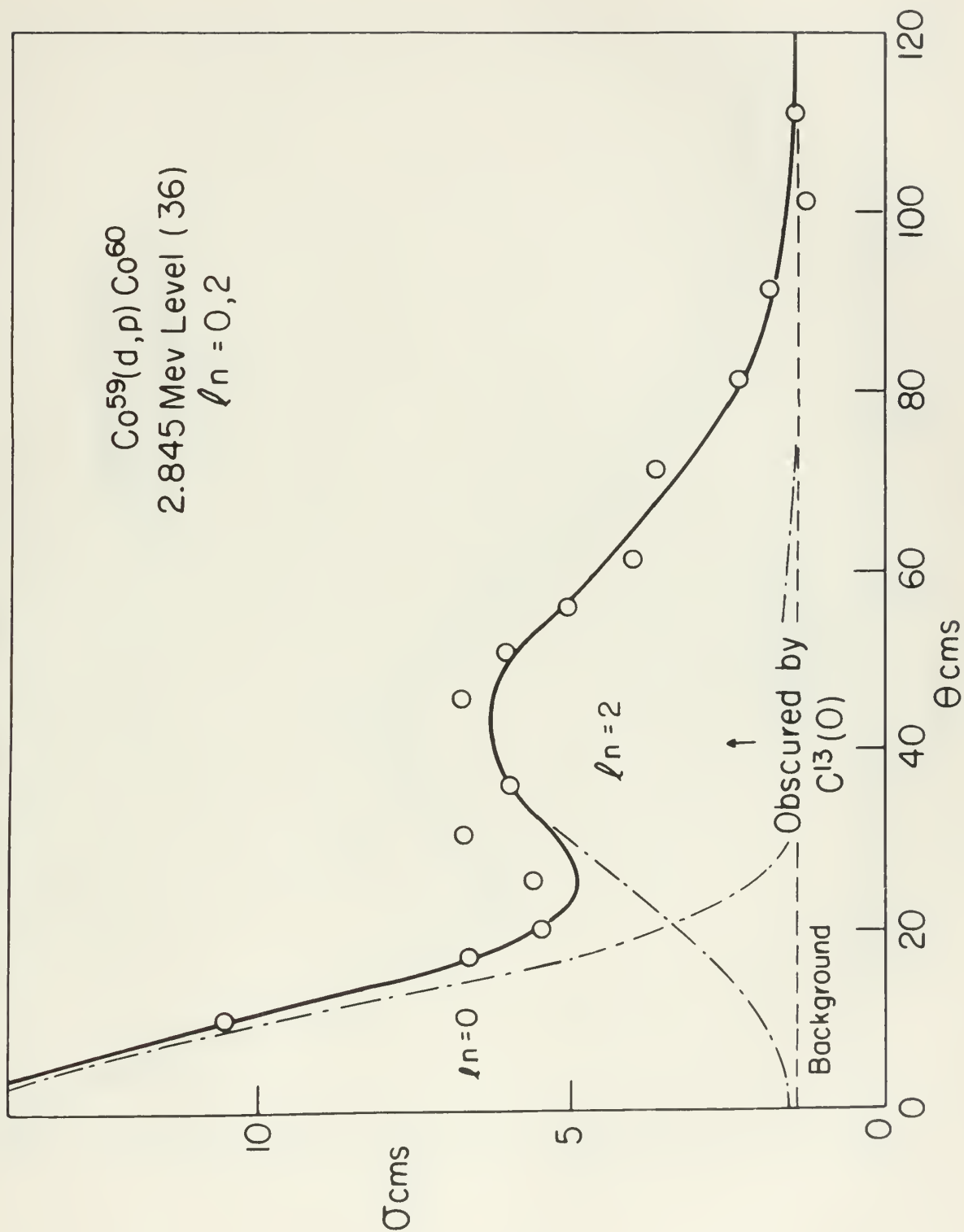


Figure 24





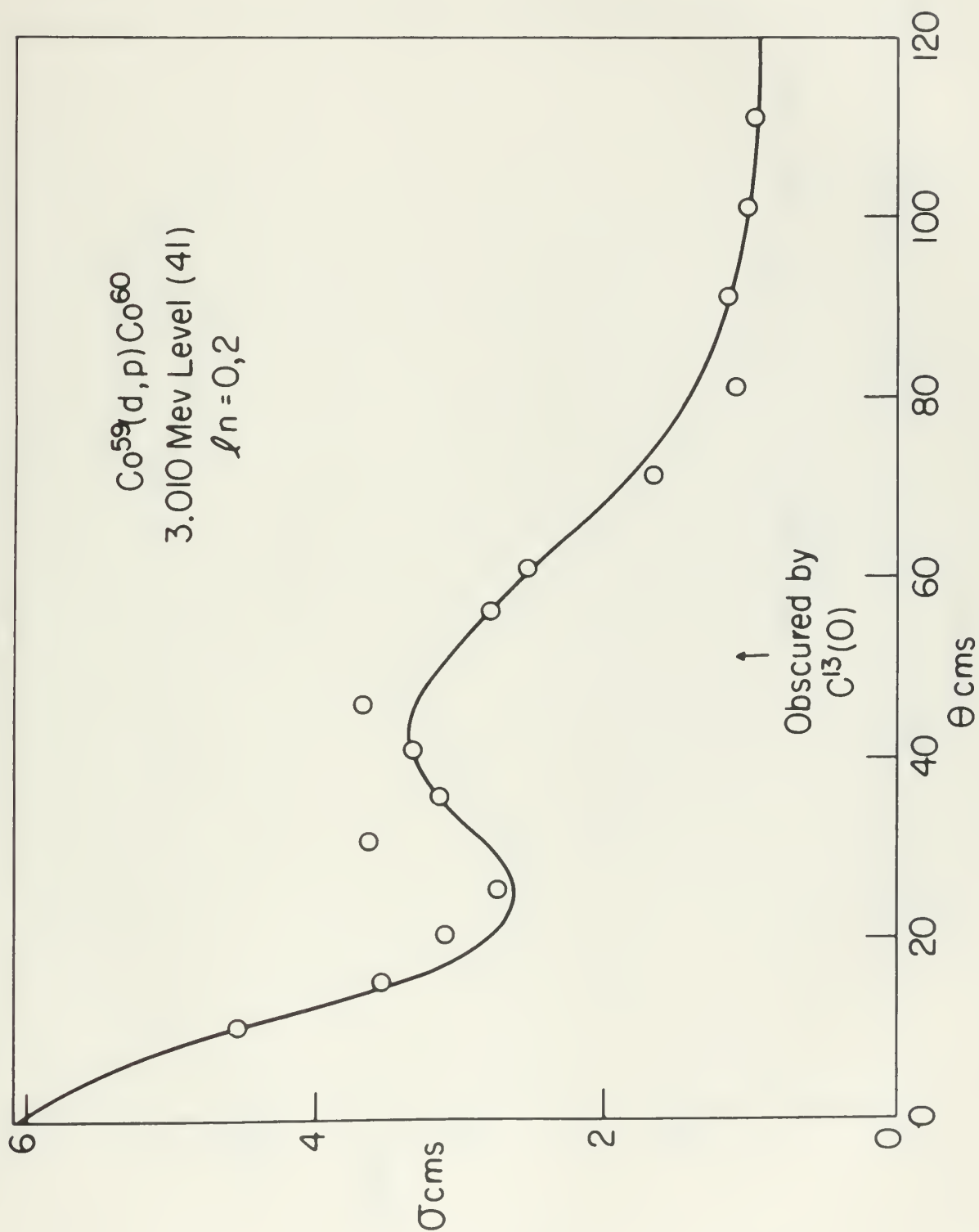


Figure 25



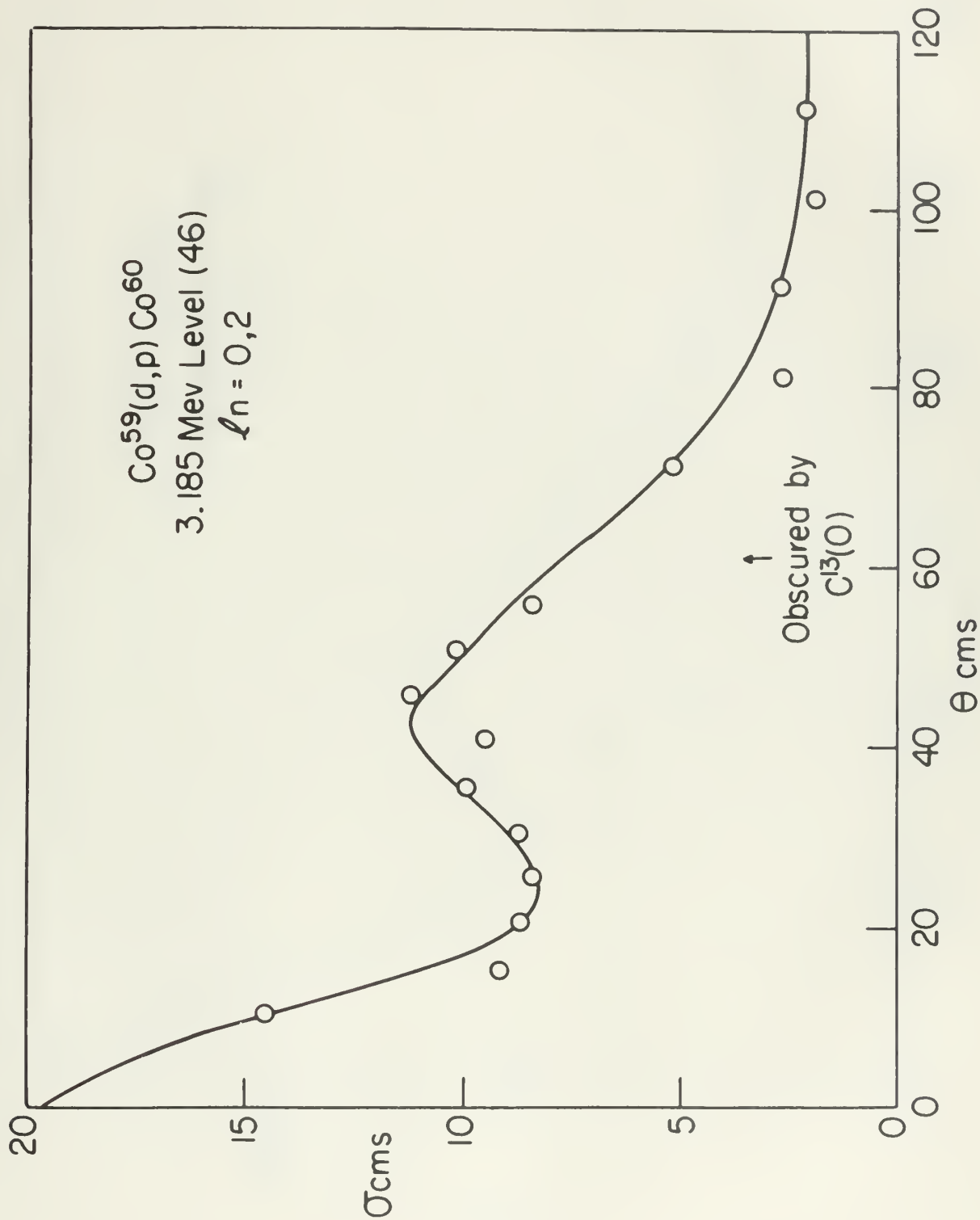


Figure 26



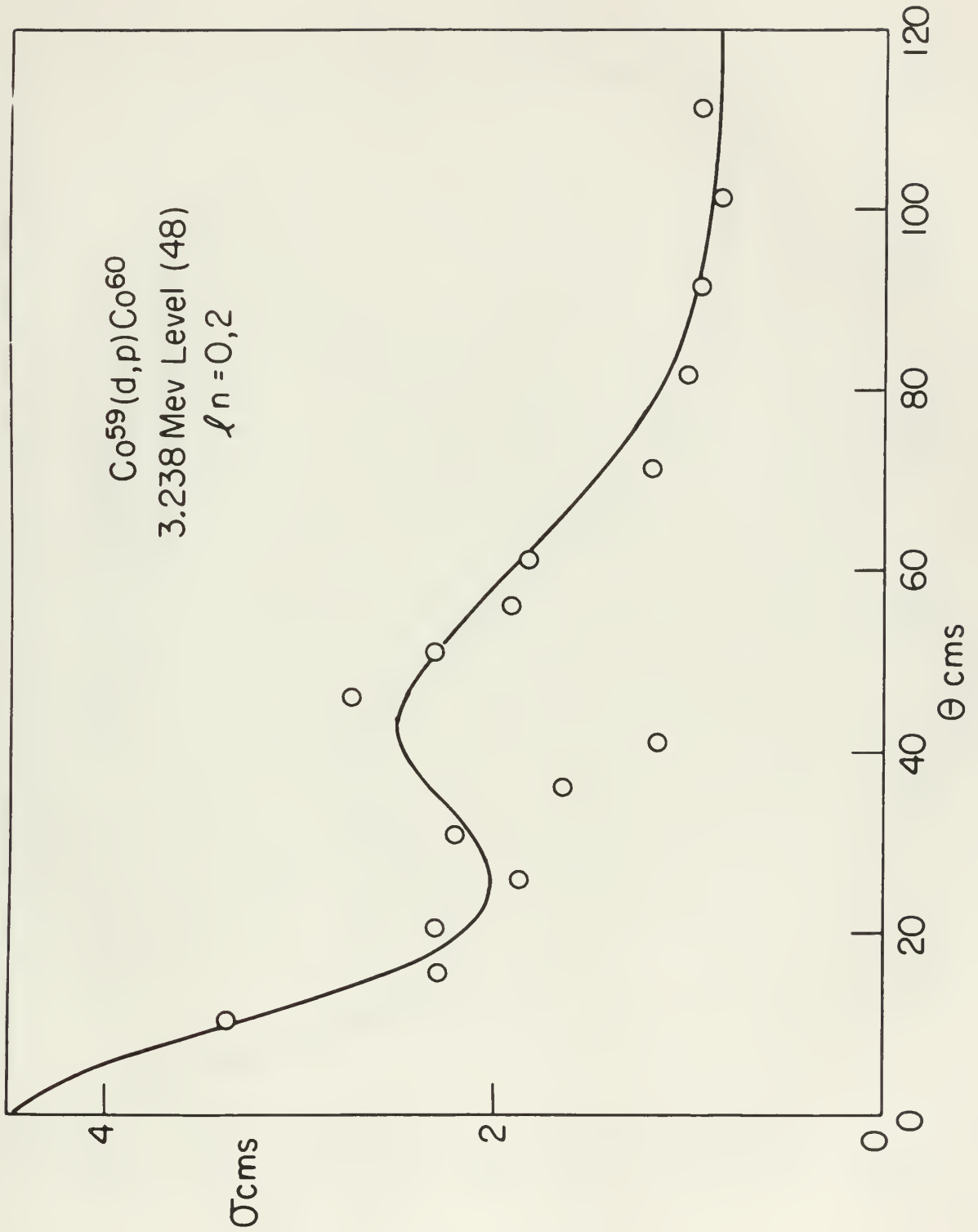


Figure 27





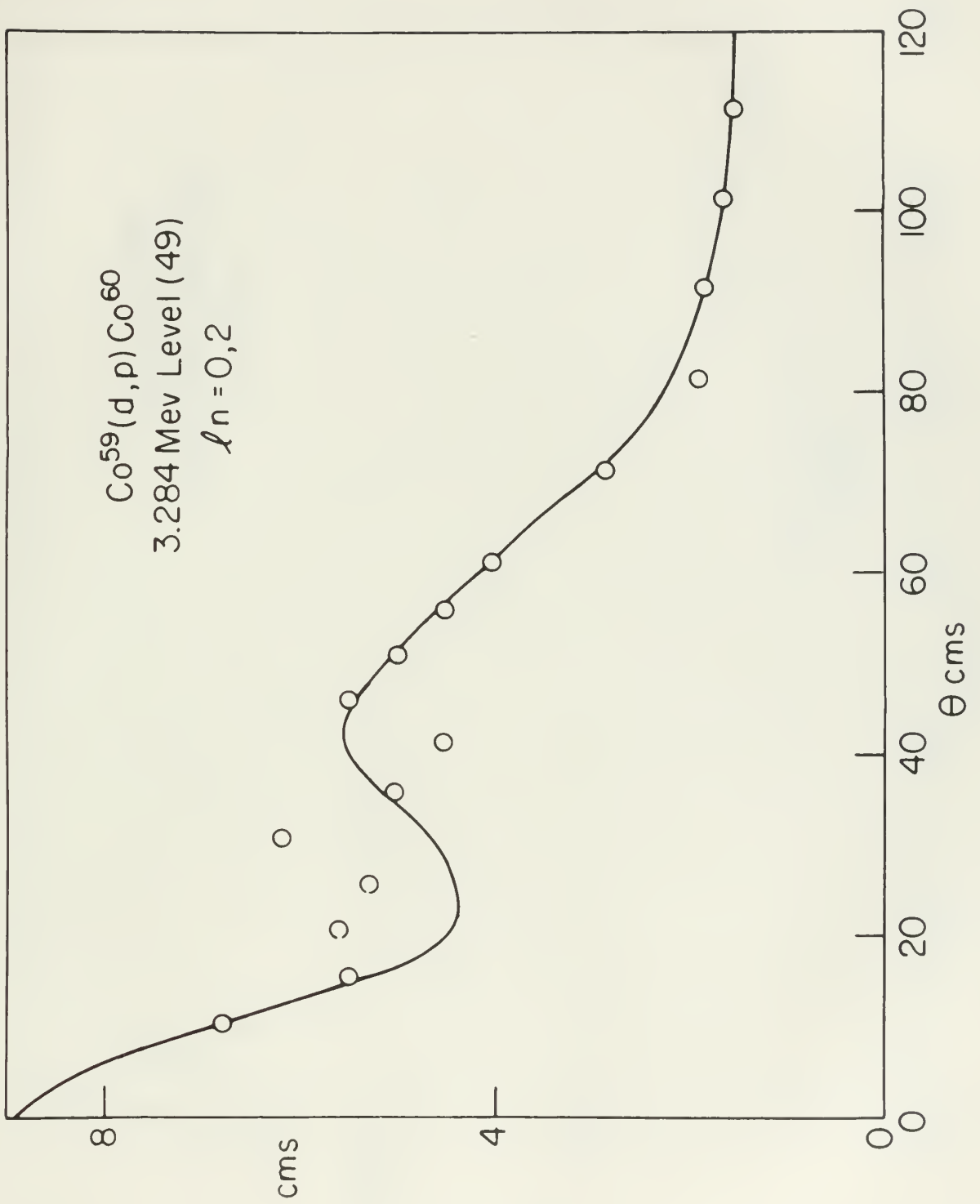


Figure 28



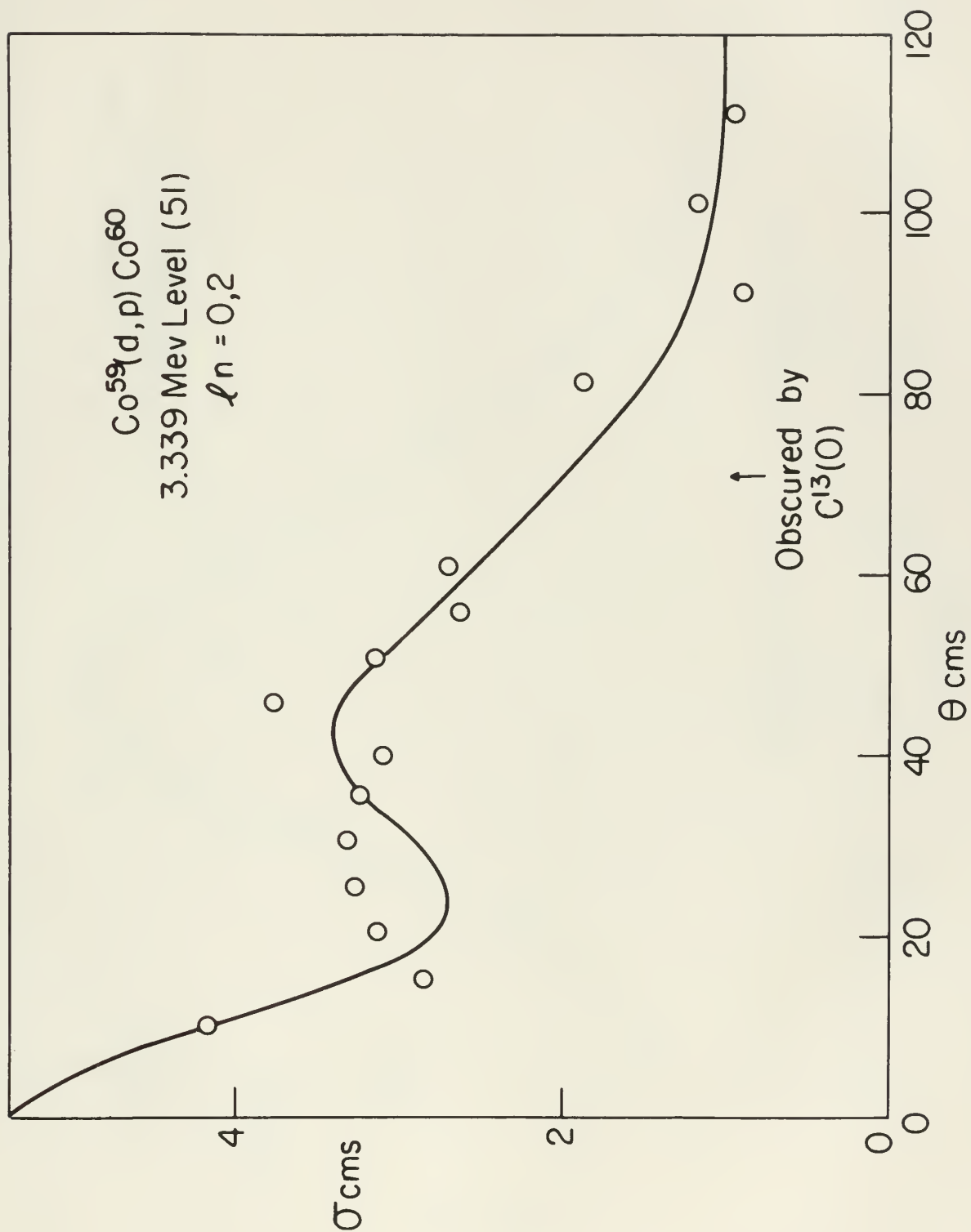


Figure 29





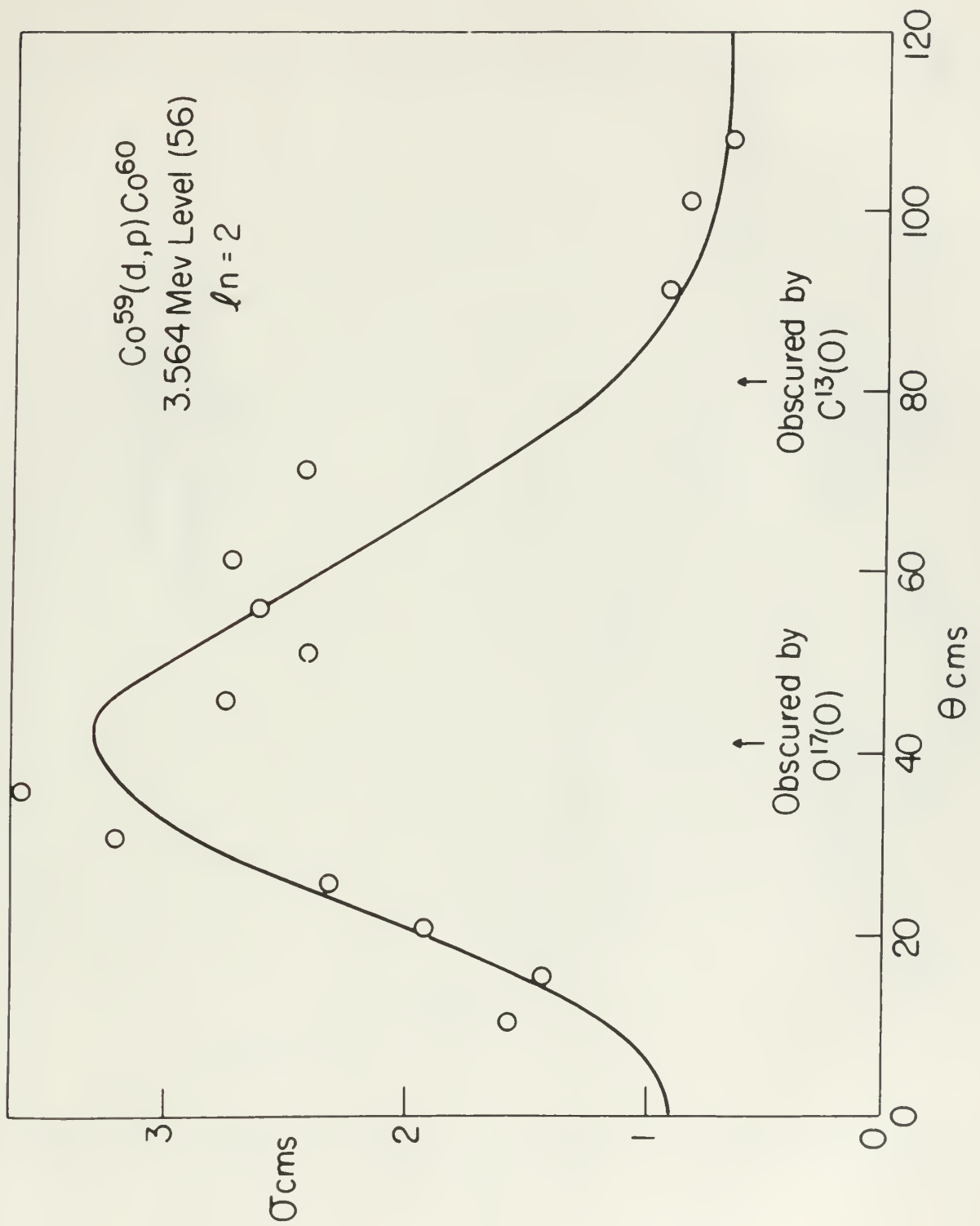


Figure 30



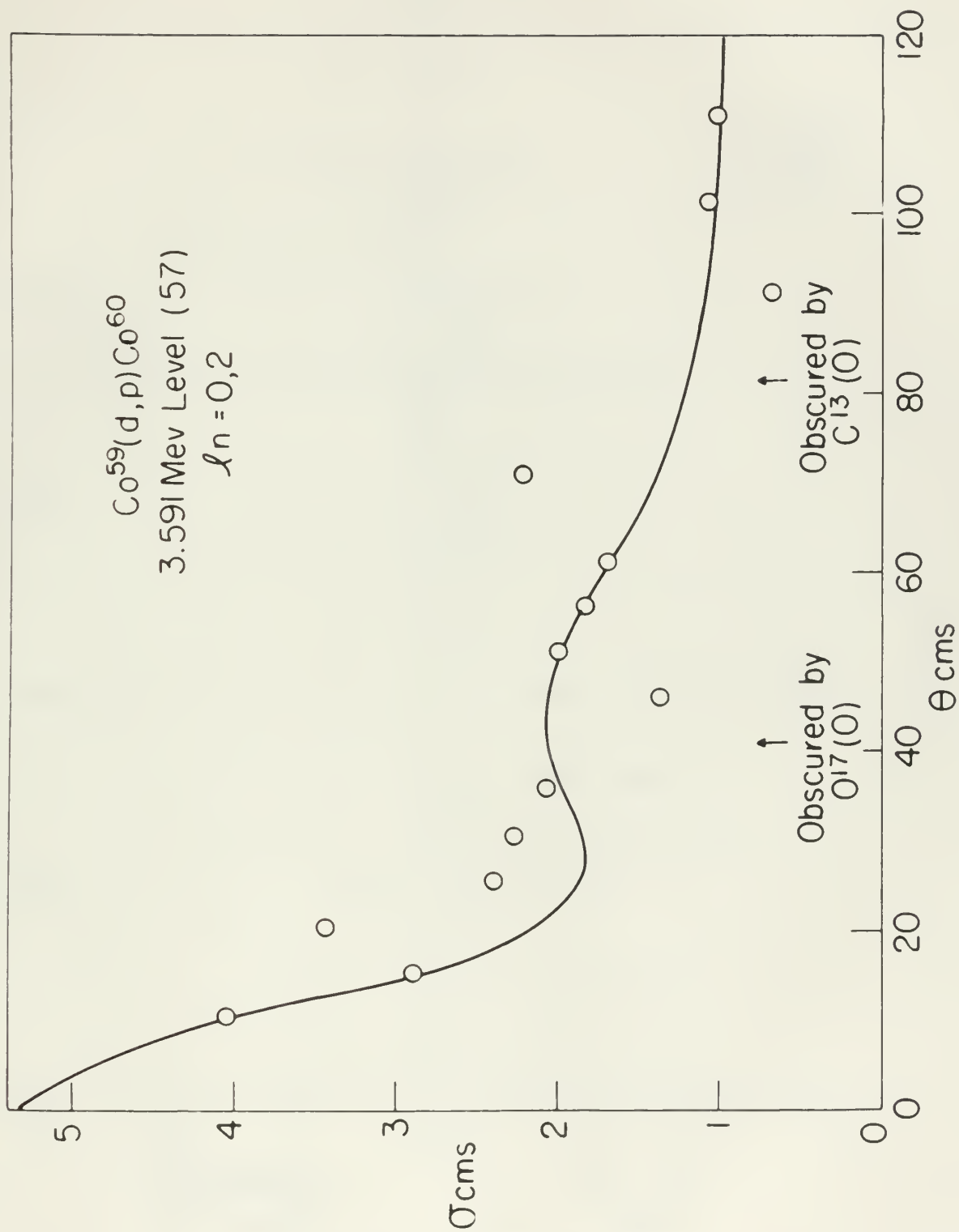
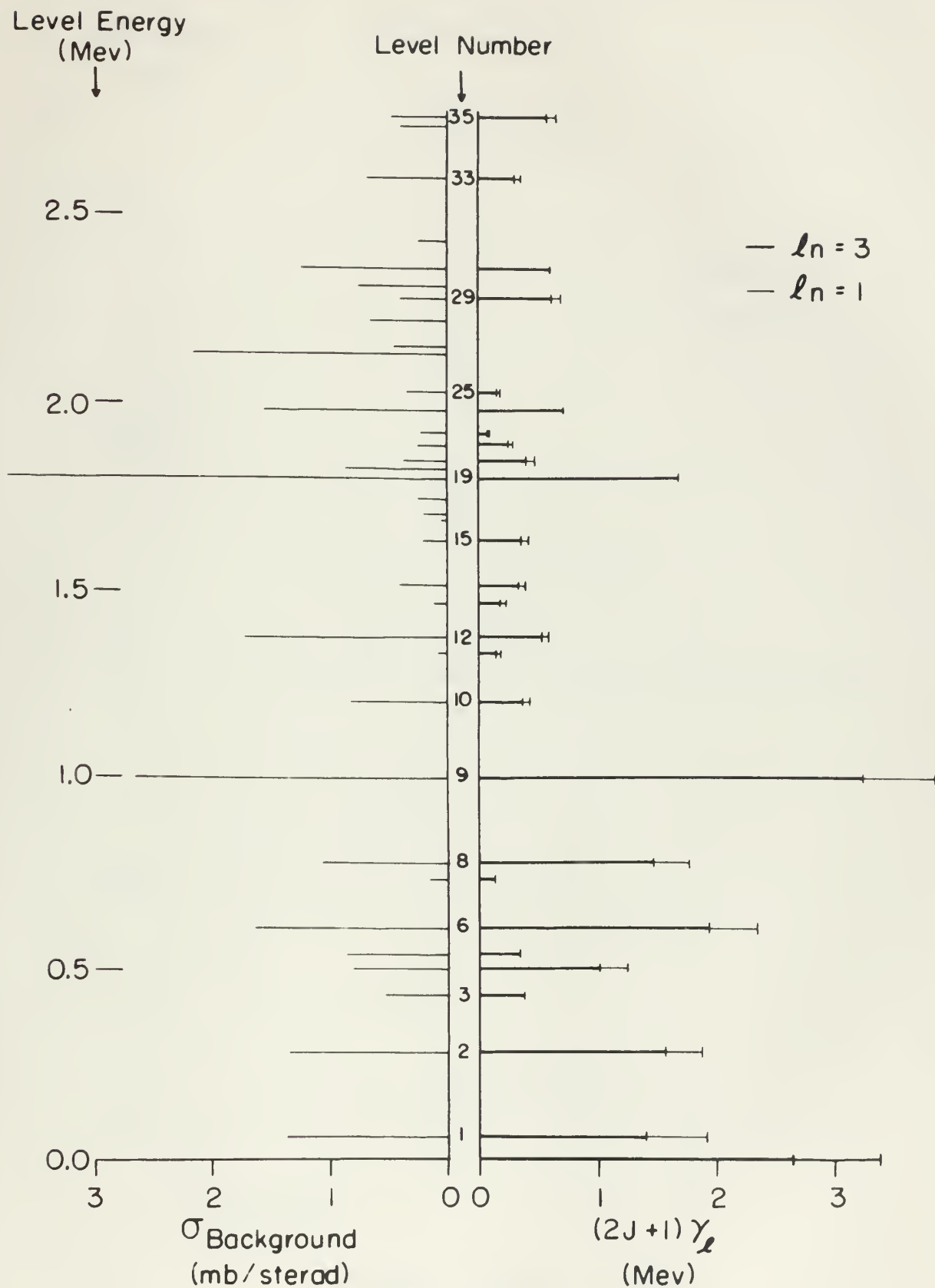


Figure 31





EXCITED LEVELS OF  $\text{Co}^{60}$

Figure 32





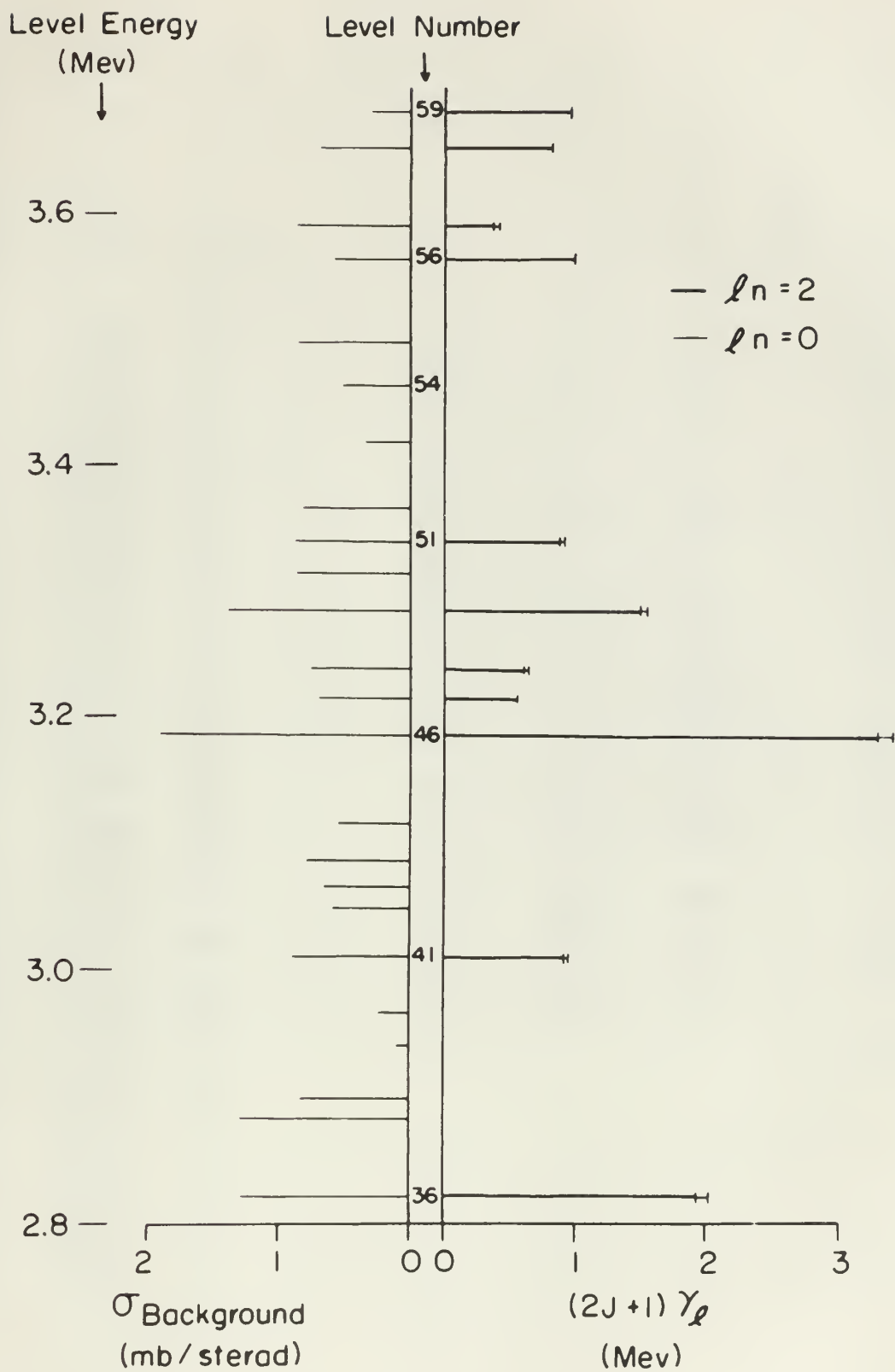


Figure 33



TABLE VII  
Summary of Calculations

<u>Level No.</u>	<u>Excit. Energy</u>	<u><math>\sigma_{\text{bkgnd}}</math></u>	<u><math>\ell_n</math></u>	<u><math>(2J+1)\gamma_3</math></u>	<u><math>(2J+1)\gamma_1</math></u>	<u><math>\gamma_1/\gamma_3</math></u>	<u>Par- ity</u>	<u>(a)</u>
0	0	3.00	1,3	2.635	0.726	0.276	+	1.155
1	0.058	1.38	1,3	1.472	0.453	0.308	+	1.15
2	0.282	1.34	1,3	1.558	0.322	0.206	+	1.12
3	0.432	0.58	3	0.382	0	0	+	1.11
4	0.501	0.83	1,3	1.021	0.230	0.225	+	1.105
5	0.541	0.88	3	0.347	0	0	+	1.105
6	0.612	1.65	1,3	1.949	0.386	0.198	+	1.10
7	0.738	0.17	1,3	0.130	0.014	0.108	+	
8	0.783	1.08	1,3	1.468	0.302	0.206	+	1.08
9	1.006	2.65	1,3	3.248	0.581	0.179	+	1.06
10	1.207	0.84	1,3	0.397	0.042	0.105	+	1.05
11	1.337	0.08	1,3	0.158	0.023	0.144	+	
12	1.377	1.71	1,3	0.643	0.062	0.097	+	1.035
13	1.447	0.12	1,3	0.190	0.028	0.148	+	

TABLE VII

Summary of Calculations

Level	Height	On	ft	(51+1)Y3	(51+1)Y1	Y1\3	Y2	(a)
0	0	3.00	1.3	5.232	0.150	0.510	+	1.122
1	0.028	1.38	1.3	1.115	0.153	0.308	+	1.12
2	0.585	1.31	1.3	1.228	0.355	0.500	+	1.15
3	0.135	0.28	3	0.385	0	0	+	1.11
4	0.201	0.13	1.3	1.051	0.530	0.522	+	1.102
5	0.211	0.15	3	0.311	0	0	+	1.102
6	0.015	1.02	1.3	1.015	0.388	0.128	+	1.10
7	0.132	0.11	1.3	0.130	0.011	0.120	+	
8	0.183	1.08	1.3	1.188	0.305	0.500	+	1.09
9	1.000	5.02	1.3	3.513	0.281	0.112	+	1.00
10	1.501	0.01	1.3	0.321	0.015	0.102	+	1.02
11	1.331	0.08	1.3	0.120	0.053	0.111	+	
12	1.311	1.11	1.3	0.013	0.003	0.031	+	1.032
13	1.111	0.15	1.3	0.120	0.055	0.110	+	



<u>Level No.</u>	<u>Energy</u>	<u><math>\sigma_{\text{bkgnd}}</math></u>	<u><math>\ell_n</math></u>	<u><math>(2J+1)\gamma_3</math></u>	<u><math>(2J+1)\gamma_1</math></u>	<u><math>\gamma_1/\gamma_3</math></u>	<u>Par- ity</u>	<u>(a)</u>
14	1.512	0.41	1,3	0.347	0.065	0.189	+	1.025
15	1.638	0.22	1,3	0.364	0.048	0.131	+	
16	1.684	0.06						
17	1.707	0.20						
18	1.748	0.27						
19	1.799	3.75	3	1.700	0	0	+	1.000
20	1.829	0.87						
21	1.850	0.40	1,3	0.407	0.073	0.178	+	0.995
22	1.887	0.26	1,3	0.259	0.034	0.131	+	
23	1.923	0.24	1,3	0.077	0.020	0.259	+	
24	1.979	1.56	3	0.726	0	0	+	0.985
25	2.031	0.35	1,3	0.170	0.032	0.190	+	
26	2.131	2.17						
27	2.150	0.48						
28	2.217	0.38						
29	2.274	0.44	1,3	0.639	0.074	0.115	+	0.970
30	2.310	0.77						
31	2.348	1.25	3	0.618	0	0	+	0.960
32	2.427	0.26						
33	2.591	0.70	1,3	0.299	0.058	0.193	+	
34	2.734	0.42						
35	2.762	0.47	1,3	0.592	0.086	0.145	+	0.935

Level No.	Interval	Co-ordinates	n	$\Sigma y(1+y)$	$\Sigma y(1+y)$	$\Sigma y^2$	Sign	(a)
14	1.215	0.41	1.3	0.341	0.002	0.182	+	1.082
15	1.434	0.55	1.3	0.364	0.009	0.171	+	
16	1.654	0.00						
17	1.701	0.50	1.3				+	
18	1.748	0.51	1.3				+	
19	1.795	2.12	3	1.100	0	0	+	1.000
20	1.852	0.41						
21	1.850	0.40	1.3	0.401	0.013	0.174	+	0.252
22	1.921	0.54	1.3	0.524	0.034	0.171	+	
23	1.983	0.54	1.3	0.611	0.050	0.252	+	
24	1.925	1.50	3	0.150	0	0	+	0.202
25	2.021	0.52	1.3	0.710	0.035	0.180	+	
26	2.127	5.11						
27	2.150	0.48	1.3				+	
28	2.211	0.58	1.3					
29	2.274	0.44	1.3	0.633	0.054	0.172	+	0.210
30	2.310	0.11						
31	2.340	1.52	3	0.618	0	0	+	0.200
32	2.451	0.50						
33	2.521	0.40	1.3	0.532	0.029	0.183	+	
34	2.534	0.45						
35	2.565	0.41	1.3	0.525	0.004	0.172	+	0.232

Level No.	Energy	$\sigma_{\text{bkgnd}}$	$\ell_n$	$(2J+1)\gamma_2$	$(2J+1)\gamma_0$	$\gamma_0/\gamma_2$	Par- ity	(a)
36	2.845	1.30	0,2	1.930	0.032	0.0425	-	0.930
37	2.834	1.30						
38	2.899	0.83						
39	2.942	0.13						
40	2.967	0.26						
41	3.010	0.90	0,2	0.917	0.032	0.0340	-	0.917
42	3.048	0.60						
43	3.065	0.66						
44	3.086	0.80						
45	3.115	0.56						
46	3.185	1.95	0,2	3.300	0.107	0.0324	-	0.905
47	3.215	0.71	2	0.570	0	0	-	
48	3.238	0.77	0,2	0.610	0.022	0.0362	-	0.903
49	3.284	1.40	0,2	1.491	0.045	0.0303	-	0.900
50	3.314	0.88						
51	3.339	0.90	0,2	0.890	0.027	0.0304	-	0.896
52	3.367	0.82						
53	3.419	0.34						
54	3.464	0.53						
55	3.498	0.89						
56	3.564	0.59	2	1.002	0	0	-	0.881
57	3.591	0.88	0,2	0.382	0.028	0.0734	-	0.880
58	3.653	0.71	2	0.836	0	0	-	
59	3.682	0.32	2	0.972	0	0	-	

(a) = solid angle correction to  $\sigma$  in Figures 6 - 31.

Year	1990	1991	1992	1993	1994	1995	1996	1997	1998	1999	2000	2001	2002	2003	2004	2005	2006	2007	2008	2009	2010	2011	2012	2013	2014	2015	2016	2017	2018	2019	2020	2021	2022	2023	2024	2025	2026	2027	2028	2029	2030	2031	2032	2033	2034	2035	2036	2037	2038	2039	2040	2041	2042	2043	2044	2045	2046	2047	2048	2049	2050	2051	2052	2053	2054	2055	2056	2057	2058	2059	2060	2061	2062	2063	2064	2065	2066	2067	2068	2069	2070	2071	2072	2073	2074	2075	2076	2077	2078	2079	2080	2081	2082	2083	2084	2085	2086	2087	2088	2089	2090	2091	2092	2093	2094	2095	2096	2097	2098	2099	2100	2101	2102	2103	2104	2105	2106	2107	2108	2109	2110	2111	2112	2113	2114	2115	2116	2117	2118	2119	2120	2121	2122	2123	2124	2125	2126	2127	2128	2129	2130	2131	2132	2133	2134	2135	2136	2137	2138	2139	2140	2141	2142	2143	2144	2145	2146	2147	2148	2149	2150	2151	2152	2153	2154	2155	2156	2157	2158	2159	2160	2161	2162	2163	2164	2165	2166	2167	2168	2169	2170	2171	2172	2173	2174	2175	2176	2177	2178	2179	2180	2181	2182	2183	2184	2185	2186	2187	2188	2189	2190	2191	2192	2193	2194	2195	2196	2197	2198	2199	2200	2201	2202	2203	2204	2205	2206	2207	2208	2209	2210	2211	2212	2213	2214	2215	2216	2217	2218	2219	2220	2221	2222	2223	2224	2225	2226	2227	2228	2229	2230	2231	2232	2233	2234	2235	2236	2237	2238	2239	2240	2241	2242	2243	2244	2245	2246	2247	2248	2249	2250	2251	2252	2253	2254	2255	2256	2257	2258	2259	2260	2261	2262	2263	2264	2265	2266	2267	2268	2269	2270	2271	2272	2273	2274	2275	2276	2277	2278	2279	2280	2281	2282	2283	2284	2285	2286	2287	2288	2289	2290	2291	2292	2293	2294	2295	2296	2297	2298	2299	2300	2301	2302	2303	2304	2305	2306	2307	2308	2309	2310	2311	2312	2313	2314	2315	2316	2317	2318	2319	2320	2321	2322	2323	2324	2325	2326	2327	2328	2329	2330	2331	2332	2333	2334	2335	2336	2337	2338	2339	2340	2341	2342	2343	2344	2345	2346	2347	2348	2349	2350	2351	2352	2353	2354	2355	2356	2357	2358	2359	2360	2361	2362	2363	2364	2365	2366	2367	2368	2369	2370	2371	2372	2373	2374	2375	2376	2377	2378	2379	2380	2381	2382	2383	2384	2385	2386	2387	2388	2389	2390	2391	2392	2393	2394	2395	2396	2397	2398	2399	2400	2401	2402	2403	2404	2405	2406	2407	2408	2409	2410	2411	2412	2413	2414	2415	2416	2417	2418	2419	2420	2421	2422	2423	2424	2425	2426	2427	2428	2429	2430	2431	2432	2433	2434	2435	2436	2437	2438	2439	2440	2441	2442	2443	2444	2445	2446	2447	2448	2449	2450	2451	2452	2453	2454	2455	2456	2457	2458	2459	2460	2461	2462	2463	2464	2465	2466	2467	2468	2469	2470	2471	2472	2473	2474	2475	2476	2477	2478	2479	2480	2481	2482	2483	2484	2485	2486	2487	2488	2489	2490	2491	2492	2493	2494	2495	2496	2497	2498	2499	2500	2501	2502	2503	2504	2505	2506	2507	2508	2509	2510	2511	2512	2513	2514	2515	2516	2517	2518	2519	2520	2521	2522	2523	2524	2525	2526	2527	2528	2529	2530	2531	2532	2533	2534	2535	2536	2537	2538	2539	2540	2541	2542	2543	2544	2545	2546	2547	2548	2549	2550	2551	2552	2553	2554	2555	2556	2557	2558	2559	2560	2561	2562	2563	2564	2565	2566	2567	2568	2569	2570	2571	2572	2573	2574	2575	2576	2577	2578	2579	2580	2581	2582	2583	2584	2585	2586	2587	2588	2589	2590	2591	2592	2593	2594	2595	2596	2597	2598	2599	2600	2601	2602	2603	2604	2605	2606	2607	2608	2609	2610	2611	2612	2613	2614	2615	2616	2617	2618	2619	2620	2621	2622	2623	2624	2625	2626	2627	2628	2629	2630	2631	2632	2633	2634	2635	2636	2637	2638	2639	2640	2641	2642	2643	2644	2645	2646	2647	2648	2649	2650	2651	2652	2653	2654	2655	2656	2657	2658	2659	2660	2661	2662	2663	2664	2665	2666	2667	2668	2669	2670	2671	2672	2673	2674	2675	2676	2677	2678	2679	2680	2681	2682	2683	2684	2685	2686	2687	2688	2689	2690	2691	2692	2693	2694	2695	2696	2697	2698	2699	2700	2701	2702	2703	2704	2705	2706	2707	2708	2709	2710	2711	2712	2713	2714	2715	2716	2717	2718	2719	2720	2721	2722	2723	2724	2725	2726	2727	2728	2729	2730	2731	2732	2733	2734	2735	2736	2737	2738	2739	2740	2741	2742	2743	2744	2745	2746	2747	2748	2749	2750	2751	2752	2753	2754	2755	2756	2757	2758	2759	2760	2761	2762	2763	2764	2765	2766	2767	2768	2769	2770	2771	2772	2773	2774	2775	2776	2777	2778	2779	2780	2781	2782	2783	2784	2785	2786	2787	2788	2789	2790	2791	2792	2793	2794	2795	2796	2797	2798	2799	2800	2801	2802	2803	2804	2805	2806	2807	2808	2809	2810	2811	2812	2813	2814	2815	2816	2817	2818	2819	2820	2821	2822	2823	2824	2825	2826	2827	2828	2829	2830	2831	2832	2833	2834	2835	2836	2837	2838	2839	2840	2841	2842	2843	2844	2845	2846	2847	2848	2849	2850	2851	2852	2853	2854	2855	2856	2857	2858	2859	2860	2861	2862	2863	2864	2865	2866	2867	2868	2869	2870	2871	2872	2873	2874	2875	2876	2877	2878	2879	2880	2881	2882	2883	2884	2885	2886	2887	2888	2889	2890	2891	2892	2893	2894	2895	2896	2897	2898	2899	2900	2901	2902	2903	2904	2905	2906	2907	2908	2909	2910	2911	2912	2913	2914	2915	2916	2917	2918	2919	2920	2921	2922	2923	2924	2925	2926	2927	2928	2929	2930	2931	2932	2933	2934	2935	2936	2937	2938	2939	2940	2941	2942	2943	2944	2945	2946	2947	2948	2949	2950	2951	2952	2953	2954	2955	2956	2957	2958	2959	2960	2961	2962	2963	2964	2965	2966	2967	2968	2969	2970	2971	2972	2973	2974	2975	2976	2977	2978	2979	2980	2981	2982	2983	2984	2985	2986	2987	2988	2989	2990	2991	2992	2993	2994	2995	2996	2997	2998	2999	3000
------	------	------	------	------	------	------	------	------	------	------	------	------	------	------	------	------	------	------	------	------	------	------	------	------	------	------	------	------	------	------	------	------	------	------	------	------	------	------	------	------	------	------	------	------	------	------	------	------	------	------	------	------	------	------	------	------	------	------	------	------	------	------	------	------	------	------	------	------	------	------	------	------	------	------	------	------	------	------	------	------	------	------	------	------	------	------	------	------	------	------	------	------	------	------	------	------	------	------	------	------	------	------	------	------	------	------	------	------	------	------	------	------	------	------	------	------	------	------	------	------	------	------	------	------	------	------	------	------	------	------	------	------	------	------	------	------	------	------	------	------	------	------	------	------	------	------	------	------	------	------	------	------	------	------	------	------	------	------	------	------	------	------	------	------	------	------	------	------	------	------	------	------	------	------	------	------	------	------	------	------	------	------	------	------	------	------	------	------	------	------	------	------	------	------	------	------	------	------	------	------	------	------	------	------	------	------	------	------	------	------	------	------	------	------	------	------	------	------	------	------	------	------	------	------	------	------	------	------	------	------	------	------	------	------	------	------	------	------	------	------	------	------	------	------	------	------	------	------	------	------	------	------	------	------	------	------	------	------	------	------	------	------	------	------	------	------	------	------	------	------	------	------	------	------	------	------	------	------	------	------	------	------	------	------	------	------	------	------	------	------	------	------	------	------	------	------	------	------	------	------	------	------	------	------	------	------	------	------	------	------	------	------	------	------	------	------	------	------	------	------	------	------	------	------	------	------	------	------	------	------	------	------	------	------	------	------	------	------	------	------	------	------	------	------	------	------	------	------	------	------	------	------	------	------	------	------	------	------	------	------	------	------	------	------	------	------	------	------	------	------	------	------	------	------	------	------	------	------	------	------	------	------	------	------	------	------	------	------	------	------	------	------	------	------	------	------	------	------	------	------	------	------	------	------	------	------	------	------	------	------	------	------	------	------	------	------	------	------	------	------	------	------	------	------	------	------	------	------	------	------	------	------	------	------	------	------	------	------	------	------	------	------	------	------	------	------	------	------	------	------	------	------	------	------	------	------	------	------	------	------	------	------	------	------	------	------	------	------	------	------	------	------	------	------	------	------	------	------	------	------	------	------	------	------	------	------	------	------	------	------	------	------	------	------	------	------	------	------	------	------	------	------	------	------	------	------	------	------	------	------	------	------	------	------	------	------	------	------	------	------	------	------	------	------	------	------	------	------	------	------	------	------	------	------	------	------	------	------	------	------	------	------	------	------	------	------	------	------	------	------	------	------	------	------	------	------	------	------	------	------	------	------	------	------	------	------	------	------	------	------	------	------	------	------	------	------	------	------	------	------	------	------	------	------	------	------	------	------	------	------	------	------	------	------	------	------	------	------	------	------	------	------	------	------	------	------	------	------	------	------	------	------	------	------	------	------	------	------	------	------	------	------	------	------	------	------	------	------	------	------	------	------	------	------	------	------	------	------	------	------	------	------	------	------	------	------	------	------	------	------	------	------	------	------	------	------	------	------	------	------	------	------	------	------	------	------	------	------	------	------	------	------	------	------	------	------	------	------	------	------	------	------	------	------	------	------	------	------	------	------	------	------	------	------	------	------	------	------	------	------	------	------	------	------	------	------	------	------	------	------	------	------	------	------	------	------	------	------	------	------	------	------	------	------	------	------	------	------	------	------	------	------	------	------	------	------	------	------	------	------	------	------	------	------	------	------	------	------	------	------	------	------	------	------	------	------	------	------	------	------	------	------	------	------	------	------	------	------	------	------	------	------	------	------	------	------	------	------	------	------	------	------	------	------	------	------	------	------	------	------	------	------	------	------	------	------	------	------	------	------	------	------	------	------	------	------	------	------	------	------	------	------	------	------	------	------	------	------	------	------	------	------	------	------	------	------	------	------	------	------	------	------	------	------	------	------	------	------	------	------	------	------	------	------	------	------	------	------	------	------	------	------	------	------	------	------	------	------	------	------	------	------	------	------	------	------	------	------	------	------	------	------	------	------	------	------	------	------	------	------	------	------	------	------	------	------	------	------	------	------	------	------	------	------	------	------	------	------	------	------	------	------	------	------	------	------	------	------	------	------	------	------	------	------	------	------	------	------	------	------	------	------	------	------	------	------	------	------	------	------	------	------	------	------	------	------	------	------	------	------	------	------	------	------	------	------	------	------	------	------	------	------	------	------	------	------	------	------	------	------	------	------	------	------	------	------	------	------	------	------	------	------	------	------	------	------	------	------	------	------	------	------	------	------	------	------	------	------	------	------	------	------	------	------	------	------	------	------	------	------	------	------	------	------	------	------	------	------	------	------	------

$\mathcal{H} = \{ \text{all } n \times n \text{ matrices} \}$



which was not resolved from the background<sup>27</sup>. Others could not be identified as stripping reactions because of large statistical or experimental fluctuations in the distributions. The background reported for these was based on a mean of the counts of all angles. This, in general, will be greater than that of a similar distribution with a stripping shape consistent enough for analysis, in which case the background is the minimum value at the higher angles.

In order to calculate the curves, a first approximation of the nuclear radius  $R$  was made by the Gamow-Critchfield formula:<sup>29</sup>

$$R \approx (1.7 + 1.22 A^{1/3}) \times 10^{-13} \text{ cm}$$

which yields  $6.5 \times 10^{-13}$  cm for  $\text{Co}^{60}$ . The value or values of  $l_n$  for each level was determined from the angle of the maxima of the distribution in accordance with the following approximate criterion derived from experience with the curves:

$l_n$	0	1	2	3
Angle (low excitation)	0°	20°	42°	49°
Angle (high excitation)	0°	17°	41°	48°

All the terms in the theoretical cross-section formula are then calculated for each angle, except the parameter  $(2J + 1)\gamma_l$ . This term is then used to normalize the curve with the correct value of  $l_n$  to the data points at their maximum and minimum. Since 10 degrees was the smallest angle at which protons could be counted, it was used as the normalization point for  $l_n = 0$ .



which was not revealed from the background. Defects could not be identified as stripping reactions because of large variations in experimental fluctuations in the distributions. The background reported for these was based on a mean of the counts at all angles. This, in general, will be greater than that of a similar distribution with a stripping shape consistent enough for analysis, in which case the background is the minimum value at the higher angles.

In order to calculate the curves, a first approximation of the nuclear radius  $R$  was made by the Gamow-Critchfield formula:<sup>29</sup>

$$R = (1.7 + 1.21 A^{1/3}) \times 10^{-13} \text{ cm}$$

which yields  $6.7 \times 10^{-13}$  cm for  $Co^{60}$ . The values of values of  $\epsilon_n$  for each level was determined from the spin of the maxima of the distribution in accordance with the following approximate criterion derived from experience with the curves:

$\epsilon_n$	0	1	2	3
Angle (for excitation)	0°	20°	40°	60°
Angle (100% excitation)	0°	15°	40°	60°

All the curves in the theoretical cross-section formula were then calculated for each angle, except the parameter  $(2\epsilon + 1)^{-1/2}$ . This term is then used to normalize the curve with the correct value of  $\epsilon_n$  to the data points at their maximum and minimum. Since 10 degrees was the smallest angle at which protons could be counted, it was used as the normalization point for  $\epsilon_n = 0$ .

The radius was then adjusted by trial and error to give the best fit to the distributions found for the levels with the largest cross sections and the lowest excitation energies at which each value of  $\ell_n$  appeared. The radius was found to be  $6.0 \times 10^{-13}$  cm for  $\ell_n = 0$  and  $\ell_n = 1$ ;  $4.0 \times 10^{-13}$  cm for  $\ell_n = 2$ ; and  $5.5 \times 10^{-13}$  cm for  $\ell_n = 3$ . For the levels with higher excitation energies, it was found that a smaller radius would give a better fit. This is particularly noticeable in levels numbered 12, 14, 21, 29, and 35 (Figures 16, 17, 19, 21, and 23, respectively). Because of the numerous and tedious trial-and-error calculations required and the lack of levels with small statistical fluctuations, no attempt was made to vary the radius with excitation energy.

A majority of levels investigated exhibited a mixture of two  $\ell$  values, either 0 and 2 or 1 and 3. In order to obtain a fit for these levels, the two curves were added together. The normalization was as described above, except that a weighting factor  $\gamma_\ell + 2/\gamma_\ell$  also must be determined algebraically. The true reduced width  $\gamma$  is a constant of the final state, but it has been placed inside the summation symbol of the cross-section equation. There it acts as a weight factor giving the relative probability of finding the neutron in one or the other of the two orbits<sup>15</sup>.

These results, which require the superposition of two curves with different  $\ell_n$  values, have been encountered before<sup>27</sup>. It was noted that some could possibly be due to the formation of a doublet level with different  $\ell_n$  values or to the overlapping of a weak group by a stronger one or to a stripping reaction with two  $\ell_n$  values.

The results were then adjusted by trial and error to give the best fit to the distributions found for the levels with the largest number of observations and the lowest excitation energies at which each value of  $\epsilon$  appeared. The results were found to be  $0.0 \times 10^{-13}$  for  $\epsilon = 0$  and  $0.1 \times 10^{-13}$  for  $\epsilon = 1$ ;  $0.0 \times 10^{-13}$  for  $\epsilon = 2$  and  $0.5 \times 10^{-13}$  for  $\epsilon = 3$ . For the levels with higher excitation energies, it was found that smaller results would give a better fit. Table 1, particularly columns 12, 13, 14, 15, 16, 17, 18, 19, and 20, summarizes the results of the numerous and tedious trial-and-error calculations required and the lack of levels with small excitation energies, no attempt was made to vary the results with excitation energy.

A majority of levels investigated exhibited a mixture of two  $\epsilon$  values, either 0 and 1 or 1 and 2. In order to obtain a fit for these levels, the two curves were added together. The normalization was as described above, except that a weighting factor  $\gamma_1 + \gamma_2$  also must be determined algebraically. The true reduced width  $\gamma$  is a constant of the final state, but it has been placed inside the summation symbol of the cross-section equation. There is now no weight factor giving two relative probabilities of finding one neutron in one or the other of the two levels  $1/2$ .

These results, which require the superposition of two curves with different  $\epsilon$  values, have been announced before<sup>27</sup>. It was noted that some could possibly be due to the formation of a doublet level with different  $\epsilon$  values as in the case of a weak group by a stronger one or to a vibrating resonance with two  $\epsilon$  values.



Also, it was noted that the experimental points which deviated from the curves had no consistent characteristics, except that points at 30 degrees were high for all but one of the twenty-six levels shown.

In Figures 6 and 24, the dashed lines show the individual curves calculated for each value of  $\ell_n$ . The solid line is the sum of the two separate curves.

It was noted that the experimental results which showed that the waves had no consistent relationship, being that some of the waves were high and some of the waves were low.

In Figure 6 and 7, the dashed lines show the individual curves calculated for each value of  $\beta$ . The solid line is the sum of the two curves.



## V. CONCLUSIONS

The present investigation of the  $\text{Co}^{59}(\text{d},\text{p})\text{Co}^{60}$  reaction, using the broad-range magnetic spectrograph, has resulted in the detection of several excited levels not previously reported. The Q-value of the ground level has been redetermined and agreement with previous  $(\text{n},\gamma)$  results is good. An explanation for the disagreement with the previous  $(\text{d},\text{p})$  determination for the ground and first nine excited levels has been offered. Comparison of the excitation energies found in this investigation with those of previous  $(\text{n},\gamma)$  values shows good agreement and serves to confirm the assumption that Bartholomew and Kinsey were measuring gamma rays to the ground level of  $\text{Co}^{60}$ , not the metastable level.

Agreement with Butler stripping theory seems adequate to assign values of  $\ell_n$  with some assurance to the ground level and to twenty-five excited levels, shown in the included curves. In addition, assignments were tentatively made to eleven weaker levels. In most of the distributions analyzed, the experimental points required the superposition of two curves calculated for different values of  $\ell_n$ . This is not surprising, because odd-odd nuclei may have quite complicated coupling of the angular momentum of the odd neutron and odd proton.

The observed values of orbital angular momentum,  $\ell_n$ , agree with the values allowed by the coupling rules for the reported spins,  $J$ , of  $5^+$  and  $2^+$  of the ground and first excited level. It must be

# V. CONCLUSIONS

The present investigation of the  $Co^{59}(d,p)Co^{58}$  reaction, using the direct-range magnetic spectrograph, has resulted in the determination of several excited levels and previously reported levels. The  $Q$ -value of the ground level has been redetermined and agreement with previous results is good. An explanation for the disagreement with the previous  $Q$ -value determination for the ground and first two excited levels has been offered. Comparison of the excitation energies found in this investigation with those of neutron ( $n,p$ ) values shows good agreement and serves to confirm the assumption that Bartholomew and Kinsey were measuring  $Q$ -values to the ground level of  $Co^{58}$ , not the metastable level.

Agreement with earlier stripping theory seems adequate to assign values of  $J^\pi$  with some assurance to the ground level and to twenty-five excited levels, shown in the included curves. In addition, assignments were tentatively made to eleven weaker levels. In most of the distributions analyzed, the experimental points required the superposition of two curves calculated for different values of  $J^\pi$ . This is not surprising, because odd-odd nuclei have quite complicated coupling of the angular momenta of the odd neutron and odd proton.

The observed values of orbital angular momentum,  $l$ , agree with the values allowed by the coupling rules for the reported spins,  $J$ , of  $2^+$  and  $2^-$  of the ground and first excited level. It must be

noted that, when several different values of  $\ell_n$  are allowed by the coupling rules, the lowest value of  $\ell_n$  can be determined, but higher values may be missed. This is explained by the behavior of the cross section for the stripping reaction, which decreases rapidly as  $\ell_n$  increases.

The J-values derived from the coupling rules, using the known value  $I = 7/2^-$  for  $\text{Co}^{59}$  and the observed  $\ell_n$ , agree with the J-values allowed by the shell model for the thirty-third neutron being accepted into a  $p_{3/2}$  state for  $\ell_n = 1$ . Agreement is also found for acceptance of the thirty-third neutron into the  $p_{1/2}$ ,  $p_{3/2}$ , or  $f_{5/2}$  states for observed  $\ell_n = 1$  or 3.

The observed values  $\ell_n = 0, 2$  are consistent with the assignment of the accepted neutron into the  $g_{9/2}$  state. With  $\ell_n = 0$ , the J-values are limited to 3 or 4 from coupling rules.

It is noted that the values of  $(2J + 1)\gamma_\ell$  are found to be larger for the  $\ell_n = 3$  or 2 when these appear in combination with an  $\ell_n = 1$  or 0, respectively.

The survey of the assignments of J-values to the ground and first excited levels was reviewed in the Introduction. Using the values for  $(2J + 1)\gamma_3$  of 2.635 and 1.472, respectively, as reported in Table VII, simple calculations were made to test these assignments. If the ground level was assumed to have  $J = 5$ , the first excited level is found to have  $(2J + 1) = 6.15$ , instead of 5 as required by the  $J = 2$  assignment. This represents an error of 23 percent. Now, if  $J = 4$  is assumed for the ground level, the  $(2J + 1)$



noted that, when several different values of  $\delta$  are allowed in the coupling rules, the lowest value of  $\delta$  can be determined, and higher values may be missed. This is explained by the behavior of the cross section for the stripping reaction, which decreases rapidly as  $\delta$  increases.

The  $\delta$ -values derived from the coupling rules, using the known value  $I = \sqrt{2}$  for  $60^\circ$  and the observed  $\delta$ , agree with the  $\delta$ -values allowed by the shell model for the first three states being assigned with a  $\sqrt{2}$  factor for  $\delta = 1$ . Agreement is also found for assignments of the first three states into the  $2\frac{1}{2}^+$ ,  $1\frac{1}{2}^+$ , or  $3\frac{1}{2}^+$  states for observed  $\delta = 1$  or  $2$ .

The observed values  $\delta = 0, 2$  are consistent with the assignment of the assigned numbers into the  $2\frac{1}{2}^+$  state, with  $\delta = 0$ , for  $\delta$ -values are limited to 1 or 2 from coupling rules.

It is noted that the values of  $(2i + 1)^2$  are found to be larger for the  $\delta = 3$  or  $2$  than those given in combination with  $\delta = 1$  or  $0$ , respectively.

The survey of the assignments of  $\delta$ -values in the ground and first excited levels was reviewed in the Introduction. Using the values for  $(2i + 1)^2$  of 2.00, 2.25, and 2.50, respectively, as reported in Table VII, simple calculations were made to test these assignments. In the ground level we assume  $i = 2$ , the first excited level is found to have  $(2i + 1)^2 = 2.25$ , instead of 2 as reported by the  $i = 2$  assignment. This represents an error of 25 percent. Now, if  $i = 1$  is assumed for the ground level, the  $(2i + 1)^2$

term for the first excited state is found to be 5.22, instead of the 3 which would correspond to  $J = 1$ . This error is about 68 per cent. Since these errors are a measure of the departure of the observed (d,p) cross sections from theory, the present work clearly supports the assignments to the ground and first excited level of  $J = 5^+$  and  $2^+$ , rather than  $4^+$  and  $1^+$ , respectively.

No conclusive assignments of  $J$ -values or of  $\gamma$ , could be made on the basis of the observed results.



on the basis of the observed results.

The conservative estimates of deviations in all 12 wells are only  $1 = 2'$  and  $1' = 1'$ , respectively.

Supporting the assignments to the ground and first excited level in states (b,c) shown resulting from theory, the present work clearly points to these states being not a mixture of the components of the  $0 = 1$  and  $1 = 1$  states.

From the first excited state it found to be  $1 = 1$ , however, of this 3 states would correspond to  $1 = 1$ . This error is about 40 per cent.

From the first excited state it found to be  $1 = 1$ , however, of this 3 states would correspond to  $1 = 1$ . This error is about 40 per cent.

## B I B L I O G R A P H Y

1. Mazari, Sperduto, and Buechner, Annual Progress Report, LNS, MIT, May 31, 1956.
2. G. M. Foglesong and D. G. Foxwell, Phys. Rev. 96, 1001, (1954).
3. G. A. Bartholomew and B. B. Kinsey, Phys. Rev. 89, 386 (1953).
4. Elementary Theory of Nuclear Shell Structure, M. G. Mayer and J. Hans D. Jensen, John Wiley + Sons, New York, 1955.
5. H. E. Walchli, ORNL Report 1469 (1953), quoted in Mayer and Jensen, reference 4.
6. Dobrowski, Jones, and Jeffries, Phys. Rev. 101, 1001 (1956).
7. Wheatley, Huiskamp, Diddens, Steenland, and Tolhoek, Physica, 21, 841 (1955).
8. G. L. Keister and F. H. Schmidt, Phys. Rev. 93, 140 (1954).
9. M. Deutsch and G. Scharff-Goldhaber, Phys. Rev. 83, 1059 (L)(1951).
10. J. L. Wolfson, Can. J. Phys. 34, 256 (1956).
11. S. T. Butler, Proc. Roy. Soc. (London) A208, 559 (1951).
12. Bhatia, Huang, Huby, and Newns, Phil. Mag. (London) Ser. 7, 43, 340 (1952).
13. P. B. Daitch and J. B. French, Phys. Rev. 87, 900 (1952).
14. F. L. Friedman and W. Tobocman, Phys. Rev. 92, 93 (1953).
15. H. A. Enge and A. Graue, Universitetet i Bergen, Arbok 1955, Nat. Vitensk. rekke, nr. 13; Rev. Sci. Instr. 27, 1078 (1956).
16. Buechner, Sperduto, Browne, and Bockelman, Phys. Rev. 91, 1502 (1953).

THE APOCALYPSE

1. J. Janssen, *Phys. Rev.* **101**, 1001 (1956).
2. J. Janssen and D. G. Semakoff, *Phys. Rev.* **101**, 1001 (1956).
3. J. Janssen and D. G. Semakoff, *Phys. Rev.* **101**, 1001 (1956).
4. Janssen, *Phys. Rev.* **101**, 1001 (1956).
5. Janssen, *Phys. Rev.* **101**, 1001 (1956).
6. Janssen, *Phys. Rev.* **101**, 1001 (1956).
7. Janssen, *Phys. Rev.* **101**, 1001 (1956).
8. Janssen, *Phys. Rev.* **101**, 1001 (1956).
9. Janssen, *Phys. Rev.* **101**, 1001 (1956).
10. Janssen, *Phys. Rev.* **101**, 1001 (1956).
11. Janssen, *Phys. Rev.* **101**, 1001 (1956).
12. Janssen, *Phys. Rev.* **101**, 1001 (1956).
13. Janssen, *Phys. Rev.* **101**, 1001 (1956).
14. Janssen, *Phys. Rev.* **101**, 1001 (1956).
15. Janssen, *Phys. Rev.* **101**, 1001 (1956).
16. Janssen, *Phys. Rev.* **101**, 1001 (1956).
17. Janssen, *Phys. Rev.* **101**, 1001 (1956).
18. Janssen, *Phys. Rev.* **101**, 1001 (1956).
19. Janssen, *Phys. Rev.* **101**, 1001 (1956).
20. Janssen, *Phys. Rev.* **101**, 1001 (1956).

17. C. P. Browne and W. W. Buechner, Rev. Sci. Instr. 27, 899 (1956).
18. Bockelman, Braams, Browne, Buechner, Sharp, and Sperduto, Phys. Rev. 107 (to be published July 1, 1957).
19. Enge, Wahlig, and Aanderaa, Rev. Sci. Instr. 28, 145 (1957).
20. H. A. Enge, Rev. Sci. Instr. 23, 599 (1952).
21. H. A. Enge, Annual Progress Report, LNS, MIT, p. 148 (May 31, 1956).
22. Buechner, Strait, Sperduto, and Malm, Phys. Rev. 76, 1543 (1949).
23. H. A. Enge, Universitetet i Bergen, Arbok 1954, Nat. Vitensk. rekke, nr. 1.
24. The Atomic Nucleus, R. D. Evans, McGraw-Hill, New York, 1955.
25. Sperduto, Buechner, Bockelman, and Browne, Phys. Rev. 96, 1316 (1954).
26. Strait, Van Patter, Buechner, and Sperduto, Phys. Rev. 81, 747 (1951).
27. Progress in Nuclear Physics, R. Huby, Section 7, edited by O. R. Frisch, Pergamon Press (London) 1953. Vol. 3.
28. D. H. Wilkinson, Phys. Rev. 105, 666 (1957).
29. Theory of Atomic Nucleus and Nuclear Energy Sources, G. Gamow and C. L. Critchfield, p. 11, Oxford University Press (Oxford) 1949.



17. G. E. Brown and W. W. Macmillan, *Rev. Sci. Instr.* 27, 634 (1956).
18. Macmillan, Brown, Macmillan, Smith, and Spedding, *ibid.*  
 Rev. 101 (to be published July 1, 1957).
19. Macmillan, Smith, and Spedding, *Rev. Sci. Instr.* 28, 115 (1957).
20. H. A. Rose, *Rev. Sci. Instr.* 23, 539 (1952).
21. H. A. Rose, *Annual Progress Report, LBS, MIT, E. 115 (Nov. 20, 1950).*
22. Macmillan, Smith, Spedding, and Rose, *Rev. Sci. Instr.* 28, 115 (1957).
23. H. A. Rose, *Unpublished Report, LBS, MIT, E. 115 (Nov. 1950).*
24. *ibid.*, 28, 115.
25. *The Atomic Bomb*, W. W. Macmillan, McGraw-Hill, New York, 1952.
26. Spedding, Macmillan, and Brown, *Phys. Rev.* 80, 1316 (1954).
27. Smith, Van Lier, Macmillan, and Spedding, *Phys. Rev.* 81, 147 (1951).
28. *Progress in Nuclear Physics*, W. W. Macmillan, Editor, Vol. 3, Pergamon Press (London) 1953.
29. D. H. Wilkinson, *Phys. Rev.* 102, 664 (1957).
30. *Theory of Atomic Nuclei and Nuclear Matter*, W. W. Macmillan and W. J. Crick, McGraw-Hill, New York, 1952.

















JA 17 58  
7 Sept. 59

BINDERY  
INTERLIB  
AEC

Thesis

J296 Jarrell

35887

Angular distribution of  
protons from the

$\text{Co}^{59}(\text{d},\text{p})\text{Co}^{60}$  reaction.

JA 17 58  
7 Sept. 59

BINDERY  
INTERLIB  
AEC

The  
J29

Thesis  
J296

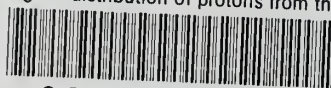
Jarrell

35887

Angular distribution of pro-  
tons from the  $\text{Co}^{59}(\text{d},\text{p})\text{Co}^{60}$   
reaction.

thesJ296

Angular distribution of protons from the



3 2768 002 10034 9

DUDLEY KNOX LIBRARY